TARGETING PROTEIN KINASE D BY NOVEL SMALL MOLECULE INHIBITORS AND RNA INTERFERENCE IN PROSTATE CANCER

by

Courtney Rebecca LaValle

Bachelor of Science, University of California, Irvine 2006

Submitted to the Graduate Faculty of

The School of Medicine in partial fulfillment

of the requirements for the degree of

Doctor of Philosophy

University of Pittsburgh

2011

UNIVERSITY OF PITTSBURGH

The School of Medicine

This dissertation was presented

by

Courtney Rebecca LaValle

It was defended on

June 24, 2011

and approved by

Chairman Guillermo G. Romero, Ph.D., Professor, Department of Pharmacology and Chemical Biology

John S. Lazo, Ph.D., Professor, Department of Pharmacology and Chemical Biology

Shivendra Singh, Ph.D., Professor, Department of Pharmacology and Chemical Biology

Peter Wipf, Ph.D., Professor, Department of Chemistry

Shi-Yuan Cheng, Ph.D., Associate Professor, Department of Pathology

Dissertation Advisor: Q. Jane Wang, Ph.D., Associate Professor, Department of Pharmacology and Chemical Biology

TARGETING PROTEIN KINASE D BY NOVEL SMALL MOLECULE INHIBITORS AND RNA INTERFERENCE IN PROSTATE CANCER

Courtney Rebecca LaValle, Ph.D.

University of Pittsburgh, 2011

Protein kinase D (PKD) has been implicated in a variety of cellular processes and pathological conditions including cancer. However, targeting PKD therapeutically and dissecting PKD-mediated cellular responses remains difficult due to lack of a potent and selective inhibitor. Here, we report the discovery of a novel class of pan-PKD inhibitors, CID755673 and its analogs. Subsequently, we use these inhibitors in conjunction with RNA interference technology to show that PKD regulates prostate cancer cell growth and motility. CID755673 was discovered in collaboration with our colleagues at the University of Pittsburgh as a compound demonstrating nanomolar potency and high selectivity for PKD inhibition. To enhance its selectivity and potency for potential *in vivo* application, several analogs of CID755673 were generated. After initial activity screening, 5 analogs having equal or greater *in vitro* potencies as CID755673 were chosen for further analysis. Our data showed that modifications to the aromatic core structure significantly increased potency while retaining high specificity for PKD. In prostate cancer cells, all compounds inhibited phorbol 12-myristate 13-acetate (PMA)-induced autophosphorylation of PKD1, with kb-NB142-70 being most active. Importantly, these inhibitors caused a dramatic arrest in cancer cell proliferation. Migration and invasion were also inhibited by this class of compounds, with varying potencies that correlated to their cellular activity, suggesting an active role for PKD in these processes. To confirm PKD involvement in prostate cancer biology, we

used short hairpin RNA (shRNA)- and small interfering RNA (siRNA)-mediated knockdown of specific PKD isoforms, demonstrating that knockdown of PKD2 and/or PKD3 significantly reduces proliferation, migration, and invasion in metastatic PC3 prostate cancer cells. We also found that inhibition of PKD expression or activity decreases secretion of several key tumor-promoting factors including matrix metalloproteinase (MMP)-9, interleukin (IL)-6, IL-8, and growth-regulated oncogene α (GROα). Finally, we demonstrated that inducible knockdown of PKD3 in both subcutaneous and orthotopic xenograft models leads to reduced prostate tumor growth. Taken together, these data provide much-needed pharmacological tools for the study of PKD function, validate PKD as a promising therapeutic target in prostate cancer treatment, and broaden our understanding of the molecular mechanisms of PKD function in prostate cancer progression.

TABLE OF CONTENTS

LIST OF TABLES

LIST OF FIGURES

PREFACE

Several sections of this dissertation have been published as peer-reviewed manuscripts during the course of my studies. These include parts of the Introduction (LaValle et al. 2010b), Materials and Methods (LaValle et al. 2010a; Sharlow et al. 2008), and Chapter 3 (Bravo-Altamirano et al. 2011; George et al. 2011; LaValle et al. 2010a; Sharlow et al. 2008). As I finish writing this work, parts of Chapters 4 and 5 are also under review for publication.

ACKNOWLEDGEMENTS

committee; this was truly an "All Star" committee, and I was delighted to participate in such insightful discussions during my committee meetings and defense.

My friends and family have been solid and strong for me, especially half-way through this venture, when the going got particularly tough. To Mom and Dad, thank you for encouraging me to keep pushing through. It is because of your constant belief in me and my abilities that I have gotten this far. I am proud to be your daughter, and I appreciate both of you more than you know. To Lindsey, thank you for always being the voice of reason and infallible logic when I needed it the most! And to Elaine, thank you for your amazing friendship and compassion.

Without a doubt, there has been no one more important to getting me through these last five years than my husband and best friend. Sean, I could not have completed this dissertation without your support and love. Through the ups and downs of grad school, you have been there for me, pushing me and believing in me, making me laugh and smile, and sharing this amazing adventure with me. Thank you for leaving sunny Southern California and braving the Pittsburgh winters with me, and for helping to make our dreams happen.

Finally, thank you to my wonderful son Connor, who has been the light of my life for the past two years. Your smiles and giggles and silliness have been joyful, especially during these last challenging years, and you have given me more hope and happiness than I ever expected.

1.0   INTRODUCTION

PKD constitutes a novel family of serine/threonine kinases and diacylglycerol (DAG) receptors that signal downstream of G protein-coupled receptors (GPCRs) and tyrosine kinase receptors. Now classified as a subfamily of the calcium/calmodulin-dependent kinase (CaMK) superfamily, the three PKD isoforms, PKD1/PKCμ (Johannes et al. 1994; Valverde et al. 1994), PKD2 (Sturany et al. 2001), and PKD3/PKCν (Hayashi et al. 1999), have emerged as key regulators of many important cellular processes. Major advances in our understanding of PKD signaling have emerged in the following fields:

1) Basic signaling mechanisms (Rozengurt et al. 2005; Waldron et al. 1999), where PKD has been identified as a protein kinase C (PKC) effector (Zugaza et al. 1996).

2) Protein trafficking (Bankaitis 2002; Cuenda and Nebreda 2009; Ghanekar and Lowe 2005), where PKD, a Golgi-resident kinase, has been shown to regulate protein transport from the Golgi to the plasma membrane (Bossard et al. 2007; Jamora et al. 1999; Liljedahl et al. 2001; Martiny-Baron et al. 1993; Yeaman et al. 2004), a significant function of PKD that underlies its critical role in multiple secretory processes including the secretion of insulin from pancreatic beta cells (Sumara et al. 2009) and cell motility (Prigozhina and Waterman-Storer 2004; Woods et al. 2004).

3) Immune system function (Matthews et al. 2006), where PKD was found to play an important role in mediating antigen-receptor signaling (Marklund et al. 2003; Matthews et al. 2006) and in regulating lymphocyte adhesion and motility (Medeiros et al. 2005).

4) Oxidative stress responses (Storz 2007; Storz et al. 2003), where PKD was shown to be activated by oxidative stress and to promote cell survival through activation of nuclear factor-kappaB (NFκB) signaling (Storz et al. 2003; Storz et al. 2005; Waldron and Rozengurt 2000).

5) Angiogenesis (Altschmied and Haendeler 2008; Ha and Jin 2009) and cardiovascular biology (Haworth and Avkiran 2001; McKinsey 2007), where PKD can mediate vascular endothelial growth factor (VEGF) signaling (Wong and Jin 2005) and promote angiogenesis in part through regulation of class IIa histone deacetylase (HDAC) activity (Ha et al. 2008a; Ha et al. 2008b; Wang et al. 2008), which plays a critical role in pathological cardiac remodeling in the heart (Fielitz et al. 2008; Vega et al. 2004).

6) Drug discovery (LaValle et al. 2010b), where emerging PKD inhibitors, beginning with our discovery of CID755673 (Sharlow et al. 2008), are proving to be useful in the study of PKD function and are showing promise in preclinical models of cancer (Harikumar et al. 2010; LaValle et al. 2010a) (reviews and papers from leading research groups in these areas are cited).

These functions of PKD are intimately coupled to its potential role in tumor development. Most notably, the regulation of immune system function, protein trafficking, oxidative stress, and angiogenesis are known to impact many aspects of tumor biology, which will be discussed in more detail in following sections.

1.1   STRUCTURE AND REGULATION OF PKD ENZYMES

Though the three-dimensional structure of PKD has not yet been resolved, several studies have provided insight into the structural features of the PKD enzymes. All 3 isoforms of PKD share a distinct structure that includes a catalytic domain, a pleckstrin homology (PH) domain, and an N-terminal cysteine-rich DAG/phorbol ester binding domain (the C1 domain) (Hayashi et al. 1999; Johannes et al. 1994; Sturany et al. 2001; Valverde et al. 1994). High homology between the isoforms exists, particularly in the catalytic domain and C1 domain, though there are differences in the N-terminal region and in regions flanked by the C1 and PH domains which may confer isoform-specific functions (Wang 2006). The PH domain has a negative regulatory effect on PKD catalytic activity, as deletion of this domain leads to constitutive activation of the kinase (Iglesias and Rozengurt 1998).

The regulatory mechanisms that control PKD activity have been well-documented. Studies have shown that PKD is activated through direct phosphorylation of 2 conserved serine residues in the activation loop by DAG-responsive PKC isoforms (Waldron et al. 1999; Waldron and Rozengurt 2003; Zugaza et al. 1996). Subsequent autophosphorylation then confers full, sustained activation (Jacamo et al. 2008; Matthews et al. 1999). This canonical PKC/PKD activation pathway can be further "tuned" by other factors and pathways. For example, the Src-Abl pathway has been shown to prime PKD for activation by PKCδ through tyrosine phosphorylation in the PH domain (Storz et al. 2003; Storz et al. 2004). Furthermore, it has also been demonstrated that, while initial catalytic activation of PKD requires PKC, sustained activation of PKD in response to GPCR agonists is maintained by an autophosphorylation mechanism at Ser[742] of the activation loop (Jacamo et al. 2008; Sinnett-Smith et al. 2009). As a

DAG target, PKD is also subjected to spatial regulation by DAG or phorbol esters. Binding of DAG to the C1 domain allows PKD to localize to the plasma membrane and *trans* Golgi network (TGN), mediating site-specific functions (Wang 2006). PKD also shuttles between the cytoplasm and the nucleus and can demonstrate transient nuclear accumulation upon activation or through specific signals (Rey et al. 2001; Rey et al. 2003; von Blume et al. 2007). PKD can be activated in response to a variety of stimuli, including DAG, phorbol esters, growth factors, GPCR agonists, and hormones (Guha et al. 2002; Matthews et al. 1997; Rozengurt et al. 1997; Wong and Jin 2005; Zugaza et al. 1997).

1.2   SIGNALING MECHANISMS OF PKD: RELEVANCE TO TUMOR CELL BIOLOGY

Emerging evidence links PKD to a diverse set of signal transduction pathways involved in tumor development and cancer progression (**Figure 1**). Here, we will discuss the potential roles and signaling mechanisms of PKD in cancer-associated biological responses.
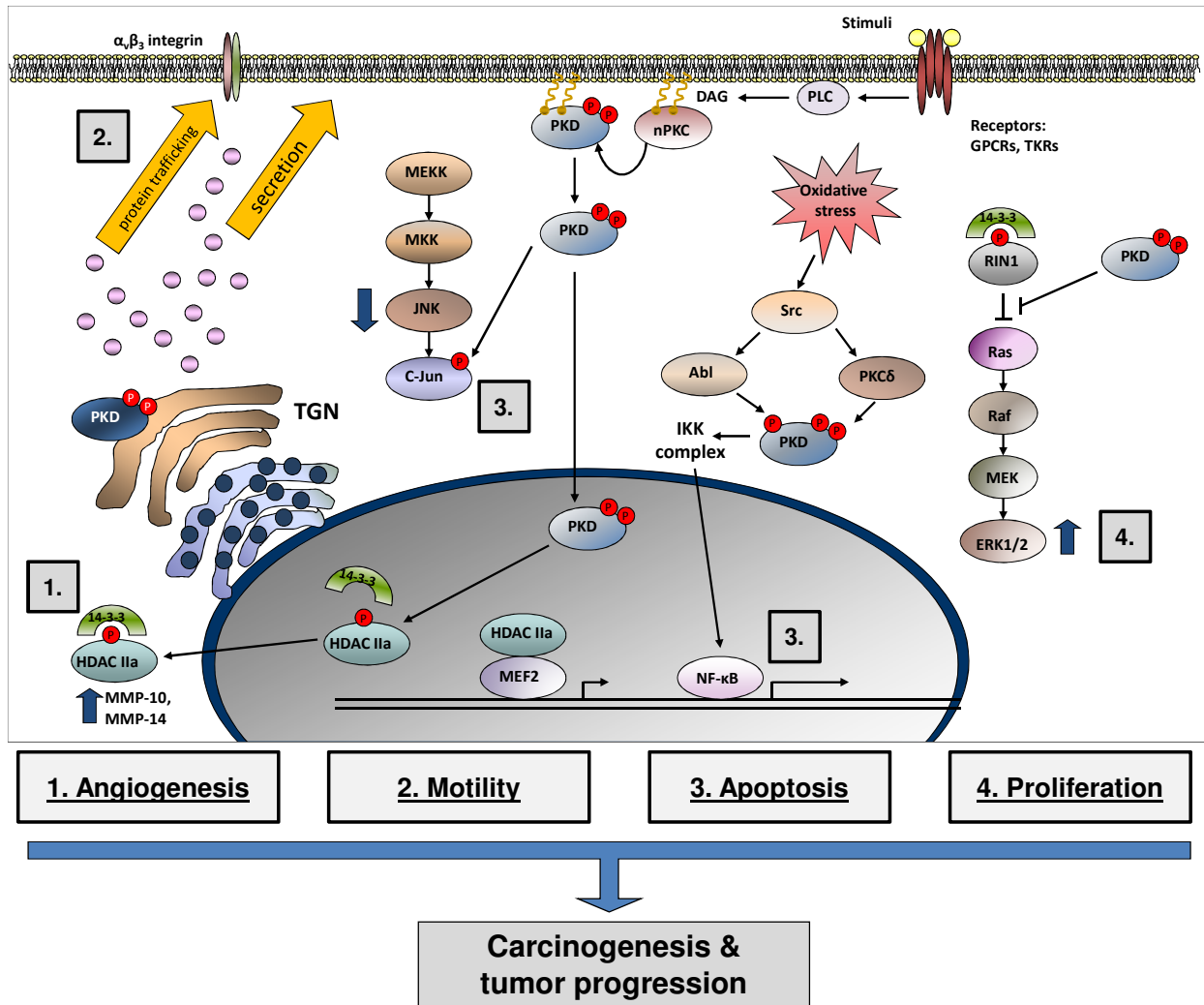
Figure 1. PKD involvement in cancer-related signal transduction pathways. PKD has been implicated in the regulation of multiple cancer-promoting pathways. PKC-mediated activation of PKD has been shown to regulate such cellular functions as proliferation, apoptosis, the epithelial to mesenchymal transition, angiogenesis, and invasion. Dysregulation of these fundamental pathways can lead to the development, progression, and metastasis of cancer.

1.2.1   Cell proliferation, survival, and apoptosis

Uncontrolled cell growth and resistance to apoptosis are among the hallmarks of cancer development. Functional studies have described PKD as a potent promoter of cell growth and

proliferation in multiple cellular systems, suggesting that PKD may possibly contribute to the cancer phenotype. For example, in Swiss 3T3 cells, overexpression of PKD has been shown to potentiate DNA synthesis in response to bombesin, vasopressin, and phorbol esters (Zhukova et al. 2001), and expression of PKD1 has been shown to correlate with levels of proliferating-cell nuclear antigen (PCNA) and proliferation state in mouse keratinocytes (Rennecke et al. 1999). Furthermore, treatment with the PKC/PKD inhibitor Gö6976 inhibits ^{3}H-thymidine incorporation in keratinocytes (Shapiro et al. 2002), supporting a role for a PKC/PKD axis in the regulation of keratinocyte proliferation. A similar role for PKD was also demonstrated in prostate and pancreatic cancer (Chen et al. 2008; Trauzold et al. 2003).

Mechanistically, PKD has been linked to several pathways known to control cell proliferation, most notably the extracellular signal-regulated kinase (ERK) signaling pathway. Inhibition of PKD expression and activity has been shown to attenuate ERK signaling, while overexpression of PKD has been shown to potentiate ERK activity in response to growth factors in multiple cell types including endothelial cells, Swiss 3T3 cells, and prostate cancer cells (Chen et al. 2008; Sinnett-Smith et al. 2004; Sinnett-Smith et al. 2007; Wong and Jin 2005). It has been proposed that PKD modulates the Ras-Raf-MEK-ERK pathway and promotes proliferation, possibly through direct phosphorylation of the Ras effector protein Ras and Rab interactor 1 (RIN1) (Van Lint et al. 2002; Wang et al. 2002). Separate studies have suggested PKD may mediate endothelial cell proliferation and growth through regulation of class IIa HDACs (Wang et al. 2008).

PKD is also implicated in the regulation of cell survival and apoptosis. Substantial work has shown that PKD promotes survival and inhibits apoptosis through modulation of the NF-κB and c-Jun N-terminal kinase (JNK) pathways (Storz 2007; Storz et al. 2005; Zhang et al. 2005).

Interestingly, in an opposing role, PKD can promote anoikis, cell death resulting from detachment from the extracellular matrix, by modulating the phosphorylation and subsequent localization of Bcl-2 inhibitor of transcription 1 (Bit1) (Biliran et al. 2008). Additionally, PKD was found to be cleaved by caspase-3 in response to certain genotoxic agents, a process that generates catalytically active PKD fragments that may play a role in sensitizing cells to the cytotoxic effects of these agents (Endo et al. 2000; Vantus et al. 2004). Furthermore, several PKD substrates including sphingosine kinase 2 (SphK2) and heat-shock protein 27 (Hsp27) have also been connected to the apoptotic response, but the functional relevance of their regulation by PKD in apoptosis remains to be determined (Ding et al. 2007; Doppler et al. 2005; Hassan et al. 2009).

1.2.2 Cell migration and invasion

PKD has been implicated in several pathways mediating cell migration, invasion, and motility – processes that are critical to cancer progression and metastasis. Consistent with its important role as a modulator of protein trafficking, PKD1 regulates fibroblast motility and Rac-1-dependent leading edge activity through modulation of anterograde membrane traffic from the TGN to the plasma membrane (Prigozhina and Waterman-Storer 2004). Furthermore, PKD directs the transport of $\alpha_v\beta_3$ integrin to focal adhesions, affecting cell migration (Woods et al. 2004). PKD-mediated phosphorylation of several proteins important to cell migration and invasion, including cortactin (De Kimpe et al. 2009), Par-1 (Watkins et al. 2008), and slingshot 1 like (SSH1L) (Eiseler et al. 2009b), has also been documented. SSH1L is a phosphatase whose activity causes reactivation of the actin-remodeling protein cofilin at the leading edge of migrating cells (Nishita et al. 2005). Pioneering work by the Storz group showed that phosphorylation of SSH1L by

PKD1 leads to its dissociation from the actin cytoskeleton and subsequent inhibition of cell motility through sustained cofilin inactivation (Eiseler et al. 2009b).

Extensive studies in breast cancer cells have also demonstrated a role for PKD1 in cell motility. As early as 1999, Mueller and colleagues described an interaction between PKD1, paxillin, and cortactin at sites of invadopodia in MDA-MB-231 breast cancer cells (Bowden et al. 1999). Invadopodia are actin-containing protrusions that extend outward into the extracellular matrix (ECM) and participate in degradation of the ECM (Stylli et al. 2008). This interaction, present in invasive breast cancer cells but not in non-invasive lines, suggests that PKD1 may regulate the function or formation of the paxillin/cortactin complex to promote invasion. Furthermore, cortactin was recently determined to be a PKD1 substrate (De Kimpe et al. 2009), albeit 10 years after these initial studies were first published. However, whether this phosphorylation event and the PKD1/cortactin/paxillin association does indeed promote invasion is still not known. Additional studies have shown that PKD and its substrates are involved in the regulation of MMP expression (Eiseler et al. 2009a; Ha et al. 2008a; Lee et al. 2008). MMPs are matrix-degrading enzymes that control cell migration and invasion and have been linked to the progression of many types of cancer (Roy et al. 2009). Future studies are needed to fully elucidate the role of PKD in these events.

1.2.3 Angiogenesis

Angiogenesis is the process through which new blood vessels are formed. In tumor development, angiogenesis is required to provide growing primary and secondary tumors with oxygen and nutrients (Hanahan and Weinberg 2000). A study in 2005 by Wong and Jin showed that PKD was activated by VEGF downstream of PKCα and regulated endothelial cell proliferation (Wong

and Jin 2005). Further studies showed that VEGF-induced endothelial cell proliferation, migration, and *in vivo* angiogenesis all required PKD activity (Qin et al. 2006). Subsequently, researchers from 2 separate groups reported that VEGF-stimulated activation of PKD leads to PKD-dependent phosphorylation of HDAC7 and increased migration in endothelial cells (Ha et al. 2008a; Wang et al. 2008). This pathway was also shown to promote several additional processes required for angiogenesis including proliferation (Wang et al. 2008), tube formation, and microvessel sprouting (Ha et al. 2008a). These studies stemmed from the seminal work by Vega *et al.* that first identified class IIa HDACs as direct substrates of PKD (Vega et al. 2004). Class IIa HDACs, including HDAC4, -5, -7, and -9, catalyze the deacetylation of lysine residues in histone amino-terminal tails and, as part of large, multiprotein transcriptional co-repressor complexes, regulate the activity of transcription factors such as myocyte enhancer factor-2 (MEF2) (Martin et al. 2007). Direct phosphorylation of class IIa HDACs by PKD leads to nuclear exclusion of these proteins and subsequent expression of MEF2 target genes, including the angiogenesis-promoting MMPs (Ha et al. 2008a; Wang et al. 2008).

1.3   PKD IN PROSTATE CANCER: EXPRESSION, ACTIVITY, AND LOCALIZATION

Prostate cancer, the second leading cause of death from cancer among men in the U.S. in 2009 (Jemal et al. 2009), is characterized by generally slow-growing tumors localized in the prostate gland, a walnut-sized structure that wraps around the urethra. Despite recent advances in early diagnosis and screening procedures, there are currently no effective therapeutic treatments once

tumors have metastasized (Shirai 2008). We still have an incomplete understanding of the molecular mechanisms that cause prostate cancer to become invasive.

1.3.1 PKD expression in prostate cancer

PKD has emerged as a major player in cell proliferation, survival, motility, and angiogenesis pathways, and it is therefore no surprise that PKD has recently received considerable attention as a potential target in the treatment of cancer. Studies assessing the expression levels of all 3 isoforms have shown that, indeed, PKD is dysregulated in several cancer types, including breast, pancreatic, gastric, and prostate cancers, and that the up- or downregulation of specific PKD isoforms may be related to tumor stage and context (**Table 1**).

Table 1. Dysregulation of PKD isoforms in human tumor samples determined by immunohistochemistry analysis

PKD Isoform	Tumor Type	Expression*	Correlation/Notes
PKD1	Breast	–	Reduced PKD1 in invasive tumors[a]
	Pancreatic	+	Increased PKD1 and activated PKD1/2 in tumors[b,c]
	Prostate	+	Increased PKD1 in tumor tissues[d]
		–	Reduced PKD1 in androgen-independent tumors[e]
	Basal Cell Carcinoma	+	Elevated and misdistributed PKD1 in the hyperproliferative human skin disorders, BCC and psoriasis[f]
	Gastric	–	Decreased PKD1 in tumors, correlated with increased PKD1 promoter methylation[g]
PKD2	Breast	no change	-
	Lymphoma	no change	PKD2 expression pattern in different lymphomas correspond to its expression in normal counterparts[h]
PKD3	Breast	no change	-
	Prostate	+	Increased PKD3 in tumor tissues[d] Increased PKD3 nuclear accumulation, correlated with pathological grade[d]

*Indicates the change in expression compared to normal tissue of the corresponding organ. (+) indicates upregulation, while (–) indicates downregulation in tumor tissues. [a](Eiseler et al. 2009a); [b](Harikumar et al. 2010); [c](Trauzold et al. 2003); [d](Chen et al. 2008); [e](Jaggi et al. 2003); [f](Ristich et al. 2006); [g](Kim et al. 2008); [h](Kovalevska et al. 2006).

Recently, evidence for the role of PKD in the progression of prostate cancer has been revealed. Studies have shown that PKD1 and PKD3 expression levels are elevated in human prostate carcinoma tissues compared to normal prostate epithelial tissue, and advanced-stage tumors were found to have increased PKD3 nuclear accumulation (Chen et al. 2008). In contrast, androgen-independent tumors showed reduced PKD1 expression (Jaggi et al. 2003). Common prostate cancer cell lines also display differential expression of the PKD isoforms. The LNCaP cell line, an androgen-sensitive and less metastatic cell line, expresses PKD1 and PKD2 only, while DU145 and PC3 cells, both androgen-insensitive and highly metastatic prostate tumor cells, express primarily PKD3, with moderate expression of PKD2 and no detectable PKD1 (Chen et al. 2008). While epigenetic silencing of PKD1 has been demonstrated in breast and gastric cancers (Eiseler et al. 2009a; Kim et al. 2008), studies have not yet investigated the mechanisms modulating the selective expression of PKD1 and PKD3 isoforms in specific prostate cancer cell lines. It is likely that there is a relationship between the androgen-independent state and PKD isoform expression, as the above mentioned studies in angroden-independent prostate cancer tissues and cell lines suggest (Chen et al. 2008; Jaggi et al. 2003). Androgen independence appears to be associated with reduced expression of PKD1 in both studies. However, whether androgen independence drives the silencing of PKD1 or lack of PKD1 contributes to the development of the androgen-independent state remains to be determined. Nonetheless, the differential expression and distribution of PKD in these cell lines and in tumor samples suggests PKD might be important for the progression of prostate cancer, and that specific PKD isoforms may mediate distinct cancer-related functions at different stages of prostate cancer progression, in a cell context-dependent manner.

1.3.2 Functional role of PKD in prostate cancer

Functional analysis of PKD has revealed distinct roles for the PKD isoforms in prostate cancer. Balaji and colleagues (Mak et al. 2008) demonstrated a tumor suppressor-like function for PKD1 in prostate cancer. PKD1 was found to negatively regulate androgen receptor (AR) function and prostate cancer cell migration and proliferation. Specifically, expression of PKD1 in DU145 cells reduced cell proliferation, while co-expression of kinase-dead PKD1 with AR attenuated the AR-mediated increase in cell-proliferation (Mak et al. 2008). Furthermore, expression of either PKD1 or the kinase-dead PKD1 mutant reduced AR-mediated transcription. Additional studies have suggested that repression of AR-dependent transcription by PKD1 may be mediated through Hsp27 (Hassan et al. 2009). They have also demonstrated that overexpression of PKD1 may promote cell aggregation, inhibit migration, and reduce cell proliferation through phosphorylation of E-cadherin and regulation of β-catenin activity, linking PKD1 to the Wnt signaling pathway (Du et al. 2009; Jaggi et al. 2008; Jaggi et al. 2005; Syed et al. 2008). These studies are suggestive of a possible role for PKD1 in suppressing the development of the androgen-independent state, common to more advanced, aggressive prostate cancer. It is possible that the silencing of PKD1 is a necessary step in the progression of metastatic prostate cancer, as has been suggested for both breast and gastric cancers (Eiseler et al. 2009a; Kim et al. 2008). Further comprehensive studies are needed to determine whether the PKD1 isoform indeed acts as a tumor-suppressor in prostate cancer.

In contrast, separate studies conducted in our laboratory have demonstrated a positive role for the PKD3 isoform in prostate cancer cell proliferation and survival (Chen et al. 2008). In androgen-independent PC3 cells, where PKD3 has high endogenous expression, reduction of PKD3 levels using siRNA caused potent inhibition of cell proliferation. Analysis of a potential

mechanism revealed that PKD3 activity stimulated prolonged activation of Akt and ERK1/2. This regulation of Akt and ERK1/2 may account for the effects on proliferation, and also may affect other steps in prostate cancer progression. Akt, commonly found to be hyperactive in prostate cancer due to a phosphatase and tensin homolog (PTEN)-null phenotype, has been implicated in angiogenesis and metastasis in addition to its fundamental roles in survival and proliferation (Nelson et al. 2007; Sarker et al. 2009). Further evidence presented later in this dissertation demonstrates that PKD3 does indeed promote proliferation, migration, and invasion in androgen-independent prostate cancer cells (see Chapters 4 and 5).

These studies not only highlight the significance of PKD signaling in prostate cancer progression, but also strongly suggest isoform-specific functions and contrasting roles for PKD1 and PKD3 in different prostate cancer cell lines and tissues. These differences can likely be explained by variations in cell type and context, with factors such as the androgen-independent state and expression profiles of various other tumor suppressors and oncogenes all contributing to the function of PKD isoforms. Further studies are needed to conclusively describe these potentially distinct and opposing roles for the PKD isoforms in prostate cancer and to determine what implications this might have in the development of PKD inhibitors for potential use as chemotherapeutic agents in the treatment of prostate cancer.

1.4   CHEMICAL INHIBITORS OF PKD: OLD AND NEW

Novel biotechnologies such as RNAi-mediated knockdown of endogenous proteins now allow the study of protein function through direct targeting of specific proteins. The limitations of these

approaches, however, are that they irreversibly deplete the entire protein and they are extremely difficult to apply *in vivo*. On the other hand, the development of chemical probes with high potency and selectivity provides the opportunity to directly and reversibly target the enzymatic activity of PKD in cells and animals. Moreover, one can titrate the level of inhibition. In the past, PKD inhibition was achieved by various general kinase inhibitors or through compounds that were primarily developed as PKC inhibitors. Recently however, novel chemical inhibitors targeting PKD in various disease states including cancer have emerged, with several new compounds being developed in the past few years (**Table 2**).

In earlier studies, several compounds capable of inhibiting PKD among a range of other kinases were reported. The pan-kinase inhibitor staurosporine and staurosporine-related compounds such as K252a have been reported to inhibit PKD in the low nanomolar range (**Figure 2**). However, these compounds lack the specificity necessary to interrogate PKD in cells (Gschwendt et al. 1996). The indolocarbazole Gö6976 inhibits PKD with an IC_{50} around 20 nM and is commonly used to inhibit PKD in various cellular contexts. However, this inhibitor is foremost a classical PKC inhibitor with single digit nanomolar IC_{50}s (Gschwendt et al. 1996; Martiny-Baron et al. 1993). Other compounds reported to inhibit PKD include the antioxidant and chemopreventive agent resveratrol. Resveratrol inhibits many proteins in addition to PKD, and high micromolar concentrations are required for inhibition of PKD (Aggarwal et al. 2004; Haworth and Avkiran 2001; Stewart et al. 2000). Despite these limitations, resveratrol has been extensively studied as a potential chemotherapeutic and chemopreventive agent, showing potent antitumor activity in multiple animal models, and it is possible that a small part of its effectiveness is indeed due to inhibition of PKD activity (Aggarwal et al. 2004). In contrast to the abovementioned agents, suramin, a hexasulfonated naphthylurea, has been shown to be a

31

novel and effective *activator* of PKD. Although suramin is a valuable tool for discriminating the activities of PKC isozymes, it too is rather unselective, thereby limiting its effectiveness as a chemical probe for the study of PKD in a relevant biological environment (Gschwendt et al. 1998). In recent years, following our discovery of the first potent and selective PKD inhibitor (Sharlow et al. 2008), there has been a surge of reports describing novel small molecules targeting PKD (Harikumar et al. 2010; LaValle et al. 2010a; Monovich et al. 2009; Raynham et al. 2008), which will be discussed in detail in Chapter 3 of this dissertation.

Table 2. *In vitro* IC_{50} values for chemical inhibitors of PKD1

Class	Structural Category	Compound	IC_{50} PKD1 (μM)	Other Biological Activities
ATP-competitive inhibitors	Staurosporine-derived	Staurosporine	0.04	Broad spectrum kinase inhibitor. Targets include PKC, PKA, CaMK II, and p60[v-src] tyrosine protein kinase.[a]
		Gö6976	0.02	Inhibits PKCα and -β1, TrkA and –B, and JAK2 and -3. Inhibits the mitotic spindle.[b]
		Gö6983	20	Broad spectrum PKC inhibitor. Cardioprotective properties.[c]
		K252a	0.007	Nonselective kinase inhibitor. Inhibits PKC, MLCK, and RTKs, among others.[d]
		GF 109203X	2	Selective inhibitor of PKCα and -β1. Anti-inflammatory effects *in vivo*.[e]
	Stilbene	Resveratrol	200	Antioxidant, antitumor, and anti-inflammatory. Inhibits a range of enzymes, including PKCs and cytochrome P450.[f]
	Bipyridyl	BPKDi	0.001	Attenuates cardiac hypertrophy.[g]
	Flavonoid	Quercetin	4	Multiple biological functions, including antitumor and pro-apoptotic agent. Inhibits PKCs, PI3K, mitochondrial ATPase, and phosphodiesterases, among others.[h]
	Aglycone	Phloretin	50	Inhibits PKCs and L-type Ca^{2+} channels. PGF2a receptor agonist.[i]
Non-ATP-competitive	Benzoxolo-azepinone	CID755673	0.182	Inhibits prostate cancer cell proliferation and motility, has mitogen-stimulating effects.[j]

[a] (Ruegg and Burgess 1989; Tamaoki et al. 1986; Yanagihara et al. 1991); [b] (Behrens et al. 1999; Grandage et al. 2006; Martiny-Baron et al. 1993; Rennecke et al. 1996; Stolz et al. 2009); [c] (Gschwendt et al. 1996; Peterman et al. 2004); [d] (Morotti et al. 2002; Ruegg and Burgess 1989); [e] (Jacobson et al. 1995; Toullec et al. 1991); [f] (Aggarwal et al. 2004; Chun et al. 1999; Haworth and Avkiran 2001); [g] (Monovich et al. 2009); [h] (Graziani et al. 1983; Gschwendt et al. 1996; Picq et al. 1989; Wei et al. 1994); [i] (Gschwendt et al. 1996; Kitanaka et al. 1993; Prevarskaya et al. 1994); [j] (Sharlow et al. 2008; Torres-Marquez et al. 2010).

A significant obstacle in the development of novel PKD inhibitors with high potency and selectivity is the current lack of information regarding the three-dimensional (3D) structure of PKD, preventing the use of structure-based drug design as a strategy for future development of PKD chemical probes. Structure-based drug design is a powerful approach that has been widely used to develop targeted therapies against many cancer targets, including BCR-ABL, phosphoinositide 3-kinase (PI3K), Hsp90, p53, and epidermal growth factor receptor (EGFR) (van Montfort and Workman 2009). The availability of structural information on PKD would greatly accelerate the optimization of current lead compounds and would potentially facilitate the targeting of specific interactions between PKD and its substrates or binding partners. Furthermore, it might provide significant insight into structural differences between the PKD isoforms that could be exploited in the development of isoform-selective inhibitors.
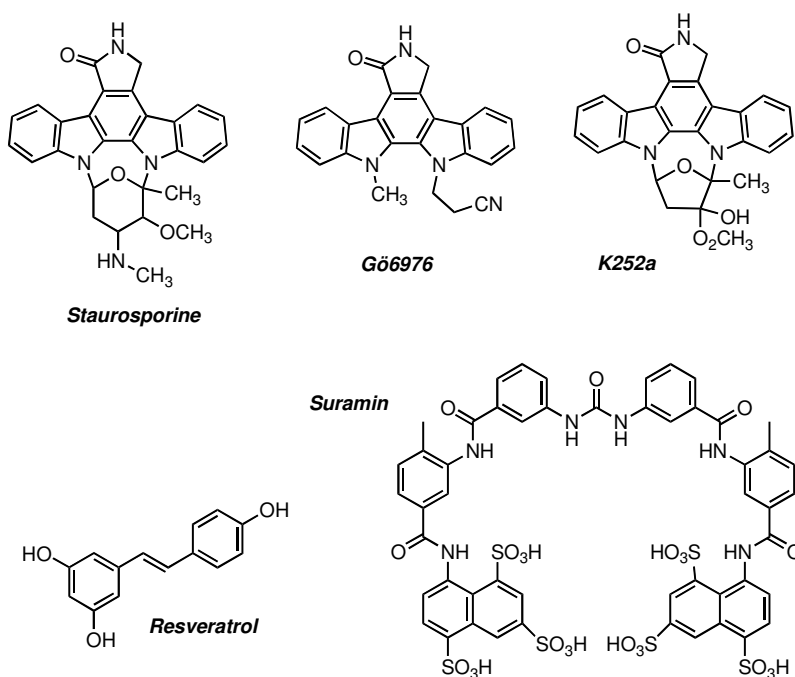
Figure 2. Chemicals commonly used to inhibit PKD. Staurosporine, Gö6976, K252a, and resveratrol inhibit PKD, but are rather unselective. They are active site inhibitors, competing with ATP. Suramin, a PKD activator, is a useful tool for differentiating PKC isoforms, but its application is similarly hampered by a lack of selectivity.

1.5   PKD AS A CHEMOTHERAPEUTIC TARGET

Extensive evidence indicates that PKD expression is deregulated in multiple cancer types and plays an active role in a variety of cancer-associated biological processes including proliferation, survival, apoptosis, migration, invasion, and angiogenesis, making PKD an attractive target for drug discovery. However, the prominent lack of animal models to support the potential role of PKD in cancer remains a significant gap in knowledge in this field. To date, there have been no reports in the literature describing whether specific targeting of PKD in animal models alters the initiation and progression of any type of cancer. Recently, tumor xenograft studies have shown that treatment with the novel PKD inhibitor CRT0066101 reduced tumor growth in both subcutaneous PANC-1 tumors and in orthotopically implanted PANC-1 tumors (Harikumar et al. 2010). However, since this compound has not yet been completely characterized with regards to specificity toward PKD, it cannot be concluded that this effect was mediated through PKD. Indeed, further studies describing the specific targeting of PKD in animal models are needed to validate PKD as a potentiat chemotherapeutic target.

A wide range of studies have characterized PKD as being a promoter of cell proliferation and survival. However, it is important to note that PKD may have cell-specific and isoform-specific functions, especially with regards to motility, and data suggests that the PKD1 isoform may even act as a tumor suppressor in certain types of cancer. In prostate cancer, where reports have indicated potential opposing roles for PKD1 and PKD3 (Chen et al. 2008; Du et al. 2009; Jaggi et al. 2003; Sharlow et al. 2008), isoform selectivity may prove to be a limiting factor in treatment efficacy.

It is important to note that while global PKD1 knockout results in embryonic lethality in mice (Fielitz et al. 2008), gene-trapping studies have revealed that mice deficient in PKD2 develop normally and are indistinguishable from their wild-type littermates (Matthews et al. 2010), and deletion of PKD3 results only in only mild abnormalities in bone development (Lexicon Genetics 2005). Conditional global knockout of any PKD isoform in adult mice has not yet been described; thus it is difficult to predict potential side effects of chemotherapeutic agents targeting PKD in adult cancer patients.

2.0   MATERIALS AND METHODS

2.1   CHEMICALS AND REAGENTS

DMSO was purchased from Sigma. CID755673 and its analogs, kb-NB142-70, kb-NB165-09, kb-NB165-31, kb-NB165-92, and kb-NB184-02, were synthesized in Dr. Peter Wipf's laboratory at the Department of Chemistry, University of Pittsburgh, according to standard organic synthesis procedures (Amir 2006; Connor et al. 1992; Connor 1989; Grimm et al. 2003; Khatana 1996; Lyubchanskaya 2002).

2.2   SYNTHESIS OF CID755673

CID755673 and its byproduct CID797718 were synthesized by Dr. Peter Wipf's laboratory at the University of Pittsburgh, according to experimental protocols published in multiple reports (Bravo-Altamirano et al. 2011; Sharlow et al. 2008).

2.3   *IN VITRO* RADIOMETRIC PKD OR CAMK KINASE ASSAY

In vitro radiometric kinase assays were conducted to determine the inhibitory activity of the novel compounds toward PKD and additional kinases. For these assays, 1 μCi [γ-^{32}P] ATP (PerkinElmer Life Sciences), 70 μM ATP, 50 ng purified recombinant human PKD1 (Biomol International, Plymouth Meeting, PA), PKD2 (SignalChem, Richmond, BC, Canada), or CAMKIIα (Enzo Life Sciences), or 75 ng PKD3 (Enzo Life Sciences), and 2.5 μg syntide-2 (Sigma) was incubated in 50 μL kinase buffer containing 50 mM Tris-HCl, pH 7.5, 4 mM MgCl$_2$, and 10 mM β-mercaptoethanol. For the CAMK assay, 0.5 mM CaCl$_2$ and 30 ng/μL calmodulin were pre-incubated for 10 min on ice, and then added to each reaction mixture. The reaction was incubated at 30°C for 10 min, and 25 μL of the reaction mixture was then spotted onto Whatman P81 filter paper (Whatman Inc., Clifton, NJ). The filter papers were washed 3 times in 0.5% phosphoric acid, air-dried, and counted using a Beckman LS6500 multipurpose scintillation counter (Beckman).

2.4.   *IN VITRO* RADIOMETRIC PKC KINASE ASSAY

In vitro kinase assays were performed to measure activity of several PKC isoforms. The kinase assays were carried out by coincubating 1 μCi of [γ-^{32}P] ATP (PerkinElmer), 20 μM ATP, 100 ng of purified rat PKCδ protein (a kind gift from Dr. Peter M. Blumberg, NCI, National Institutes of Health) or 50 ng of recombinant human PKCα (Cell Signaling Technology and

CalBiochem), PKCβI (Cell Signaling Technology), or PKCδ (Enzo Life Sciences) with 5 μg of myelin basic protein 4-14, 0.25 mg/mL bovine serum albumin, 0.1 mg/mL phosphatidylcholine/phosphatidylserine (80/20%) (1 μM), and 1 μM phorbol dibutyrate in 50 μL of kinase buffer containing 50 mM Tris-HCl, pH 7.5, 4 mM $MgCl_2$, and 10 mM β-mercaptoethanol. The reaction was incubated at 30°C for 10 min, and 25 μL of the reaction mixture was spotted onto Whatman P81 filter paper. The filter papers were then washed 3 times in 0.5% phosphoric acid, air-dried, and counted using a Beckman LS6500 multipurpose scintillation counter.

2.5   CELL LINES, CELL CULTURE, AND DEVELOPMENT OF STABLE CELL LINES

DU145, LNCaP, and CFPAC cells were maintained in RPMI 1640, PC3 cells were grown in Ham's F12 medium, and PANC1 cells were maintained in DMEM. All of the above cell lines were purchasedfrom American Type Culture Collection (ATCC), and were supplemented with 10% fetal bovine serum (FBS), 1000 U/L penicillin, and 1 mg/mL streptomycin and were incubated at 5% CO_2 and 37°C. LNCaP cells were additionally supplemented with glucose, HEPES, and sodium pyruvate. For development of the tetracycline (tet)-inducible PKD3 shRNA stable cell lines, PKD3 shRNA or a scrambled shRNA control were cloned into the pENTR/H1/TO vector according to the manufacturer's instructions (Invitrogen). PC3-TR cells (expressing the tet-repressor, a generous gift from Dr. Peter Blumberg) were then transfected with the plasmid containing either PKD3 shRNA or the scrambled shRNA control using

Lipofectamine 2000 reagent (Invitrogen). Six hours after transfection, the transfection medium was replaced with antibiotic-free growth medium. The following day, the cells were replated into selection medium containing 1 µg/mL blasticidin and 10 µg/mL Zeocin (Invitrogen). Selection medium was refreshed every 3 days for approximately 2 weeks, after which time clones were picked and tested for tet-inducible PKD3 knockdown. To induce expression of the shRNA, tet was added to the growth medium at a concentration of 1 µg/mL and refreshed every 2 days for 5 days. Cells were then collected, and PKD3 expression was analyzed by Western blotting and quantitative real-time RT-PCR (RT-qPCR).

2.6 TRANSIENT KNOCKDOWN OF PKD3 BY SIRNA

Transient silencing of PKD3 was achieved using multiple siRNAs targeting different regions of PKD3. A total of 5 siRNA sequences were used: 2 custom designed siRNAs (siPKD3-1: GCT GCT TCT CCG TGT TCA AGT CCT A; and siPKD3-2: GCA GAG TGA AAG TTC CAC ACA CAT T) and 3 commercially available PKD3 siRNAs (siPKD3-5: CAC GAT ATG TCA GTA CTG CAA; siPKD3-6: CGG GAG AGT GTT ACC ATT GAA; and siPKD3-10: CAG ACT TGG CTT GAC CTT AGA; purchased from Qiagen). Transient transfection of PC3 or DU145 cells was achieved using DharmaFECT reagent according to the manufacturer's instructions (Invitrogen), typically with 40-60 nM final siRNA concentration, and cells were used for subsequent experiments 48 h following transfection.

2.7   WESTERN BLOTTING ANALYSIS

Western blot analysis was carried out to analyze expression of various proteins. Cells were collected in lysis buffer containing 50 mM Tris-HCl, pH 7.4, 150 mM NaCl, 1.5 mM MgCl$_2$, 10% glycerol, 1% Triton X-100, 5 mM EDTA, 20 µM Leupeptin, 1 mM phenylmethylsulfonyl fluoride (PMSF), 1 mM NaVO$_3$, and 10 mM NaF, and incubated on ice for 30 min with occasional vortexing. Protein concentration was determined using the BCA Protein Concentration Assay kit (Pierce). Equal amounts of protein were subjected to SDS-PAGE and subsequent electrotransfer to nitrocellulose membranes. Membranes were pre-blocked in 5% nonfat milk in Tris-buffered saline with 0.01% Tween-20 (TBS-T) and then incubated with primary antibodies in either 5% nonfat milk or 5% BSA overnight at 4°C. Primary antibodies against PKD3 (1:1000 dilution; Cell Signaling Technology), PKD2 (1:1000 dilution, Abcam), p-S916-PKD1 (1:500 dilution, Millipore), p-S742-PKCµ/PKD (1:1000 dilution, Biosource), GAPDH (1:3000 dilution), or tubulin (1:3000 dilution, Santa Cruz Biotechnology) were used. Membranes were washed in TBS-T and then incubated for 1 h at room temperature with secondary anti-rabbit or anti-mouse antibodies conjugated to horseradish peroxidase (HRP, Bio-Rad). Detection of specific protein bands was facilitated by the enhanced chemiluminescence (ECL) Western blotting detection system (Amersham Biosciences).

2.8   MTT ASSAY

PC3 cells were seeded into 96-well plates (3000 cells/well) and allowed to attach overnight. Cells were then incubated in media containing 0.3-100 μM inhibitors for 72 h. 3-(4,5-Dimethylthiazol-2-yl)-2,5-diphenyltetrazolium bromide methyl thiazolyl tetrazolium (MTT) solution was prepared at 2 mg/mL concentration in PBS, sterilized by filtering through a 0.2 μm filter, and wrapped in foil to protect from light. Fifty microliters of MTT solution was added to each well and incubated for 4 h at 37°C. Then, media was removed and 200 μL DMSO was added to each well. The plate was mixed for 5 min and the optical density was determined at 570 nm on a Victor 3 Multilabel plate reader (Perkin Elmer).

2.9   CELL PROLIFERATION ASSAY

Proliferation of PC3, DU145, LNCaP, PANC1, or CFPAC cells in the presence of various concentrations of PKD inhibitors (or DMSO as a vehicle control), or of PC3-TR cells or stable clones (shScr, shPKD3-1 C7, shPKD3-1 C26, shPKD3-1 C2-1, or shPKD3-1 C2-3) in the presence or absence of tet, was measured by counting the number of viable cells upon trypan blue staining for 6 consecutive days. For the PC3-TR and stable cell lines, cells were pretreated with or without tet (1 µg/mL) for 5 days, and then replated at 5000 cells/well density in 24-well plates. Growth media containing inhibitors or tet for all cells was refreshed every 2 days.

2.10   CELL CYCLE ANALYSIS

Cell cycle analysis was performed to determine cell cycle distribution under various conditions, and was conducted as previously reported (LaValle et al. 2010a; Sharlow et al. 2008). PC3 cells were treated with indicated compounds at various concentrations for 2-6 days, and then fixed in 70% ice-cold ethanol overnight and labeled with propidium iodide. The labeled cells were analyzed using a FACScan Benchtop Cytometer (BD Biosciences).

2.11   WOUND HEALING ASSAY

Wound-induced migration was measured using the "wound healing" or "scratch" assay (LaValle et al. 2010a; Sharlow et al. 2008). In this assay, PC3, DU145, CFPAC, or PANC1 cells, or the stable clones shScr, shPKD3-1 C7, or shPKD3-1 C26 were grown to confluence in 6-well plates. Stable clones were pretreated with tet for 5 days prior to the experiment to induce PKD3 knockdown. Migration was initiated by scraping the monolayer with a pipette tip, creating a "wound." The indicated concentration of compound or the inducing agent, tet, was added to the media, and the wound was imaged immediately under an inverted phase-contrast microscope with 10X objective. After the indicated times, cells were fixed in methanol and stained with 1% crystal violet, and a final image was taken. The wound gap was measured, and the percentage wound healing was calculated. The average percent wound healing was determined based on either at least 9 measurements of the length of the wound gap or at least 3 measurements of the wound area. For the wound healing assay using conditioned medium, shScr or shPKD3-1 C7

cells were treated with tet for 5 days and then replated to normalize the cell number into serum-free medium. After 48 h, the serum-free conditioned medium was collected, centrifuged briefly to remove floating cells, and an equal volume from each cell line was applied to confluent PC3 cells. The wound healing assay was then performed as above.

2.12   MATRIGEL INVASION ASSAY

DU145, PC3, or CFPAC cells (5.0-8.0 x 10^4 cells/mL) in RPMI containing 0.1% fetal bovine serum (FBS) were seeded into the top chamber of BioCoat control inserts (pore size 8 μm) or BioCoat Matrigel invasion inserts with Matrigel-coated filters (BD Pharmingen). To stimulate invasion, media in the lower chamber of the insert contained 20% FBS. Inhibitors or tet were added at the indicated concentrations to both the upper and lower chambers, and cells were incubated for 22 h at 37°C with 5% CO_2. After incubation, noninvasive cells were removed using a cotton swab, and invasive cells were first fixed in 100% methanol and then stained with 1% crystal violet. After staining, cells were counted under a microscope (200x magnification). The percentage invasion was determined by cell counts in at least 5 fields of the number of cells that invaded the Matrigel matrix relative to the number of cells that migrated through the control insert. For experiments on the stable tet-inducible cell lines shScr or shPKD3-1 C7, cells were first pretreated with or without tetracycline for 5 days to induce PKD3 knockdown and then subjected to the Matrigel invasion assay as described above. For transient knockdown of PKD2 and/or PKD3, PC3 cells were transfected with specific siRNAs using DharmaFECT reagent

(Dharmacon, Thermo Fisher Scientific). Forty-eight hours following transfection, cells were subjected to the invasion assay.

2.13   QUANTITATIVE REAL-TIME RT-PCR

Total RNA was isolated from shScr, shPKD3-1 C2-1, and shPKD3-1 C2-3 PC3-TR cells using RNeasy Mini Kit (Qiagen, Valencia, CA). Reverse-transcription was performed using the iScript cDNA synthesis kit (Bio-Rad, Hercules, CA), typically on 1 µg total RNA, according to the manufacturer's instructions. RT-qPCR was then performed on a CFX96 Real-time Detection System with the C1000 Thermal Cycler (Bio-Rad), using SsoFast EvaGreen master mix (Bio-Rad) in a 10 µL total reaction volume. Primer pairs, used at 500 nM final concentration, were designed based on guidelines provided by Bio-Rad, and their specificity was confirmed by BLAST search. Sequences of the primer pairs used were as follows: GAPDH, GCA AAT TCC ATG GCA CCG T (forward) and TCG CCC CAC TTG ATT TTG G (reverse); PKD3, CAT GTC CAC CAG GAA CCA AG (forward) and GAC GGG TGT AAG AGT GAA CAG C (reverse); MMP-9, GAC GCA GAC ATC GTC ATC CAG TTT (forward) and GCC GCG CCA TCT GCG TTT (reverse); MMP-14, CGC TAC GCC ATC CAG GGT CTC AAA (forward) and CGG TCA TCA TCG GGC AGC ACA AAA (reverse); IL-6, ACA TCC TCG ACG GCA TCT CAG (forward) and AAT CTG AGG TGC CCA TGC TAC (reverse); IL-8, TTT GCC AAG GAG TGC TAA AGA (forward) and GCA TCT GGC AAC CCT ACA ACA (reverse); GROα/CXCL-1, CCA AAG TGT GAA CGT GAA GTC C (forward) and GGA TGC AGG ATT GAG GCA AG (reverse). The PCR protocol included 1 cycle at 95°C for 30 s, then 40 cycles of

a 95°C for 5 s step followed by 5 s at either 62°C or 65°C, depending on the optimal annealing temperature for each primer set, which had been determined experimentally. Melt curves were conducted to assure specificity of the primer sets as well as absence of primer-dimers. PCR efficiencies for the primer sets were determined by creating a standard curve using dilutions of the cDNA, as suggested by the manufacturer's protocol. PCR efficiencies were within the acceptable range (90-115%) for all primer sets. Relative transcript abundance was calculated by BioRad CFX96 Manager software using the ΔΔCt method with GAPDH as the reference gene.

2.14   ZYMOGRAPHY

Levels of latent and active MMP-2 and MMP-9 in conditioned medium were determined using gelatin zymography (Kleiner and Stetler-Stevenson 1994; Troeberg and Nagase 2004). Briefly, serum-free conditioned medium was collected for 48 h from PC3 cells undergoing various treatment conditions. If necessary, the conditioned medium was concentrated up to 10-fold using Amicon Ultra-0.5 mL Centrifugal Filters (Millipore, Billerica, MA). Non-reducing sample buffer (5X) containing 400 mM Tris-HCl, 5% SDS, 20% glycerol, and bromophenol blue was added to the conditioned medium, and the samples were run at a constant 180 V on a 10% polyacrylamide gel co-polymerized with 0.1% gelatin (Sigma-Aldrich, St. Louis, MO) until the dye front reached the bottom of the gel. Purified recombinant MMP-9 and MMP-2 (R&D Systems, Minneapolis, MN) were run alongside the samples to serve as standards. Gels were then washed once with 2.5% Triton X-100 and incubated 1 h at room temperature in fresh 2.5% Triton X-100 to remove SDS from the gel. To facilitate activation of MMPs within the gel, gels were then incubated in

buffer containing 50 mM Tris-HCl, pH 7.5, 200 mM NaCl, 5 mM $CaCl_2$, and 0.02% Brij-35 for

18 h at 37°C with gentle rotation. After overnight incubation, gels were stained with 0.5%

Coomassie Brilliant Blue R250 for 3 h and destained 3 h using destain solution (30% methanol,

10% acetic acid) with 3 changes or until clear bands were easily visible on the dark background.

2.15   MEMBRANE-BASED CYTOKINE ANTIBODY ARRAY

Analysis of cytokine secretion into conditioned medium was performed using the Human

Cytokine Array I (RayBiotech, Norcross, GA), according to the manufacturer's instructions.

Briefly, serum-free conditioned medium from untreated and tet-treated shScr and shPKD3-1 C7

cells was collected as described above. Antibody array membranes were placed in an 8-chamber

plate and pre-blocked at room temperature for 1 h using 2 mL of blocking buffer. Conditioned

medium samples were then applied and incubated overnight at 4°C. Membranes were washed 3

times for 5 min each wash in wash buffer I, followed by 1 x 5 min wash in wash buffer II. The

membranes were then incubated for 2 h at room temperature with biotin-conjugated antibody

mix. Washing was repeated as before, and the arrays were then incubated with HRP-conjugated

strepavidin for 1 h at room temperature. The membranes were washed again as before, and then

spots were visualized using the ECL Western blotting detection system (Amersham

Biosciences).

2.16   ENZYME-LINKED IMMUNOSORBENT ASSAY (ELISA)

Quantitative measurement of cytokines secreted into the conditioned medium was detected using ELISA kits (RayBiotech, Norcross, GA). Serum-free conditioned medium was collected from various cells for 48 h as described above and ELISA analysis was carried out following the manufacturer's protocol. Standard curves were determined using known amounts of recombinant IL-6, IL-8, or GROα protein, and the level of each cytokine in the collected conditioned medium was extrapolated based on the standard curve. Sensitivities of the assays were approximately 3.0 pg/mL, 1.0 pg/mL, and 50 pg/mL for IL-6, IL-8, and GROα/CXCL-1, respectively. For the ELISA using tumor lysates, frozen tumors were sliced into small pieces and tumor cells were homogenized for 1 min in lysis buffer containing 50 mM Tris-HCl, pH 7.4, 150 mM NaCl, 1.5 mM $MgCl_2$, 10% glycerol, 5 mM EDTA, 20 µM Leupeptin, 1 mM PMSF, 1 mM $NaVO_3$, and 10 mM NaF. After homogenization, 1% Triton X-100 was added, and cells were incubated on ice with vortexing for 1 h. Lysates were then centrifuged at top speed for 15 min to remove debris, and protein concentration was determined using the BCA Protein Concentration Assay kit (Pierce). Equal amounts of protein were subjected to ELISA according to the manufacturer's instructions.

2.17   SUBCUTANEOUS XENOGRAFT MOUSE MODEL

Tumor cells (shScr, shPKD3-1 C7, or shPKD3-1 C26 clones) were resuspended in growth medium and mixed with BD Matrigel Basement Membrane Matrix (BD Biosciences) at a final

cell concentration of $4x10^6$ cells per 0.1 mL. Cells were injected subcutaneously into the right flank of 6- to 8-week-old male athymic nude mice (Charles River Laboratories, Wilmington, MA). Five days after inoculation, palpable tumors had established in 42/44 mice (95.5%). Of the 2 mice in which tumors did not take, 1 had been inoculated with shScr cells, and 1 had been inoculated with shPKD3-1 C7 cells. Both of these mice were monitored for the entirety of the study, and tumors failed to establish over the 25-day period. Thus, these mice were excluded from analysis. Half of the mice in each group were then treated with 1 mg/mL doxycycline (dox), a tetracycline analog, via drinking water (this resulted in 4 groups: shScr No Dox, shScr + Dox, shPKD3-1 C7 No Dox, shPKD3-1 C7 + Dox; n = 10-11 mice per group). No other additives (i.e., sucrose) were necessary and dox-treated mice drank at similar rates to untreated mice. Additionally, no dox-associated weight loss was observed, as has been reported by some groups (Cawthorne et al. 2007). Dox-containing water was changed every 2 days. Tumor volume was measured with a caliper 3 times per week and was calculated as V $(mm^3) = (L \times W^2) / 2$, where L = the largest diameter and W = the shortest diameter perpendicular to L. Twenty-five days after inoculation, mice were euthanized by CO_2 inhalation, and tumors were excised for analysis. Mice were housed in pathogen-free conditions, and all animal studies were conducted in accordance with an IACUC-approved protocol at the University of Pittsburgh.

2.18   ORTHOTOPIC XENOGRAFT MOUSE MODEL

Training in this orthotopic prostate xenograft model was completed in the laboratory of Dr. Julie Eiseman. In this experiment, tumor cells were injected directly into the prostates of male nude

mice in order to measure growth and metastasis and mimic a more physiological state in the microenvironment of the prostate. Tumor cells (shScr or shPKD3-1 C7 clones) were resuspended in growth medium and mixed with BD Matrigel Basement Membrane Matrix to achieve a final concentration of 5 x 10^5 cells per 10 µL. Male athymic nude mice age 8-weeks (Charles River Laboratories, Wilmington, MA) were given the analgesic buprenorphine at 0.1 mg/kg subcutaneously 12 h prior to surgery and again just before the procedure. Mice were anesthetized using 60 mg/kg pentobarbital were considered ready for the surgical procedure when they did not respond to toe-pinch. All procedures were completed under sterile conditions, and tools were resterilized between mice using an Inotech Steri 350 glass bead sterilizer (Inotech). For the surgery, a 1-cm incision was made through the skin and peritoneum across the lower abdomen, exposing the abdominal cavity. The bladder was exposed, and the prostate, located at the base of the bladder, was identified. Ten microliters of the cell-Matrigel solution was then injected directly into the left dorsolateral lobe (n = 3-4 mice per group). The bladder was replaced into the abdominal cavity, and the incision was closed using coated vicryl sutures (Ethicon) in the peritoneum and 7.5 mm Michel wound clips (Roboz Surgical Instrument Co., Gaithersburg, MD) in the skin. Post-operatively, mice were monitored 2-3 times per day for signs of pain and were treated with buprenorphine subcutaneously every 12 h for 3 days to minimize pain. After this period, mice were monitored for signs of pain or other complications daily and weighed 3 times per week. Two weeks following surgery, most mice had tumors which could be carefully palpated through the abdomen. At this point, dox was added to the drinking water at 1 mg/mL concentration. Dox-containing water was changed every 2 days. Thirty-one days after inoculation, when extreme weight loss was observed in some mice, all mice were euthanized by CO_2 inhalation, and necropsies were performed. The primary prostate tumor was removed and

weighed, and any observable metastases were also excised. All animal studies were conducted in accordance with an IACUC-approved protocol at the University of Pittsburgh.

2.19   STATISTICAL ANALYSIS

All statistical analyses were completed using Graph Pad Prism V software. The student's t-test was used to determine the statistical significance of differences seen in Western blotting, RT-qPCR, cell proliferation, wound healing, invasion, and ELISA assays. For the animal studies, the Mann-Whitney-Wilcoxon test was used. A p-value of < 0.05 was considered statistically significant.

3.0 DEVELOPMENT AND CHARACTERIZATION OF NOVEL SMALL MOLECULE INHIBITORS OF PROTEIN KINASE D

3.1 INTRODUCTION

The PKD family is a novel family of serine/threonine kinases and diacylglycerol (DAG) receptors. Three isoforms of PKD have been identified: PKD1 (formerly PKCµ), PKD2, and PKD3 (PKCv) (Hayashi et al. 1999; Johannes et al. 1994; Sturany et al. 2001; Valverde et al. 1994). All isoforms contain a catalytic domain, a cysteine-rich DAG-binding domain (C1), and a pleckstrin homology (PH) domain that negatively regulates PKD activity (Iglesias and Rozengurt 1998). DAG regulates both the localization of PKD through binding to its C1 domain (Valverde et al. 1994) and the activity of PKD through regulating PKC-dependent phosphorylation of PKD on serines 738 and 742 ($Ser^{738/742}$) in the activation loop (Waldron et al. 2001; Waldron and Rozengurt 2003). Rapid, early activation of PKD by PKC then leads to autophosphorylation of PKD on serine 916 (Ser^{916}) and subsequent full activation of PKD (Matthews et al. 1999). Interestingly, evidence has suggested that while Ser^{742} transphosphorylation by PKC is required for early activation of PKD, Ser^{742} is also a site of autophosphorylation, and that autophosphorylation at this site is required for maintaining prolonged PKD activation (Jacamo et al. 2008).

Since its discovery, PKD has been implicated in various cellular functions significant to tumor development including proliferation, survival, apoptosis, angiogenesis, and motility. For example, PKD activation in response to vascular endothelial-derived growth factor (VEGF) or bombesin leads to activation of extracellular signal-regulated kinase (ERK) 1/2, regulating cell proliferation in several cell types (Sinnett-Smith et al. 2007; Wong and Jin 2005). PKD can also be activated by oxidative stress, which modulates cell survival through the NF-κB and JNK signaling pathways (Biswas et al. 2010; Hausser et al. 2005; Storz 2007; Zhang et al. 2005). Furthermore, PKD has been implicated in the regulation of the epithelial to mesenchymal transition in prostate cancer cells by modulation of β-catenin, and angiogenesis in vascular endothelial cells through modulating phosphorylation and nucleocytoplasmic shuttling of class IIa HDACs (Bertos et al. 2001; Du et al. 2009). Disruption of these fundamental pathways could potentially lead to the development, progression, and metastasis of cancer. For example, in recent studies, PKD expression has been shown to be dysregulated in human prostate cancer tissues (Chen et al. 2008; Jaggi et al. 2003), implicating PKD in the progression of prostate cancer. To support this, we previously reported that knockdown of PKD3, a member of the PKD family, using siRNA caused a dramatic arrest in cell proliferation in PC3 cells (Chen et al. 2008). Additional studies have shown that PKD expression is also dysregulated in pancreatic, breast, and gastric cancers, among others (LaValle et al. 2010b).

This involvement of PKD in a myriad of cancers, as well as other pathological conditions such as cardiac hypertrophy (Monovich et al. 2009; Vega et al. 2004), makes it an attractive target for drug discovery. Furthermore, besides the potential to target PKD therapeutically, the development of novel small molecule PKD inhibitors would facilitate the study of PKD biology *in vitro* and in cellular models. As discussed in Chapter 1, the study of PKD function and

signaling has greatly depended on the use of general kinase inhibitors and PKC inhibitors. Clearly, these compounds lack the necessary specificity to truly define PKD function. Moreover, since PKD signals downstream of PKC in many of its roles, it is especially important that compounds used to interrogate PKD function in cellular models show very little activity toward the PKC isoenzymes.

In this study, we report the discovery of CID755673 and its analogs as novel PKD inhibitors. With the aim of developing novel pharmacological tools to study PKD function and target PKD therapeutically, we conducted assays to evaluate the potency, mechanisms, and biological activities of this novel class of compounds. The analogs were synthesized in the laboratory of Dr. Peter Wipf, with modifications to both their core structures and side chains according to a thorough SAR analysis (Bravo-Altamirano et al. 2011; George et al. 2011). We show that CID755673 has potent PKD inhibitory effects, and several of the novel analogs exhibit increased potency toward PKD inhibition both *in vitro* and in cells. Additionally, CID755673 and its analogs cause potent growth arrest, moderate cell death, and inhibition of migration and invasion in prostate and pancreatic cancer cells, supporting their potential for *in vivo* applications.

3.2   RESULTS

3.2.1 The discovery of CID755673, a novel PKD inhibitor

3.2.1.1 CID755673 inhibits PKD *in vitro*

In 2008, our collaborators, Drs. John S. Lazo and Elizabeth R. Sharlow, at the University of Pittsburgh Drug Discovery Institute developed an immobilized metal affinity for phosphochemical (IMAP)-based fluorescence polarization (FP) high throughput screening (HTS) assay and identified the compound CID755673 as a potential hit (**Figure 3**). In this HTS, the PMLSC 196,173 member library was interrogated, and CID755673 emerged as a small molecule that produced >50% inhibition of PKD1 activity when screened at 10 µM (Pubchem AID 797) (Sharlow et al. 2008). Further analysis of this compound by our collaborators revealed an IC_{50} of 0.50 ± 0.03 µM for PKD1 in the IMAP-FP PKD assay, while the compound appeared to lack activity toward PLK1, CAK, or protein kinase B (AKT/PKB) (Sharlow et al. 2008). Upon interrogation of the PubMed database, they found that CID755673 appeared to show exquisite specificity for PKD and was not biologically active in more than 200 other assays (Sharlow et al. 2008).
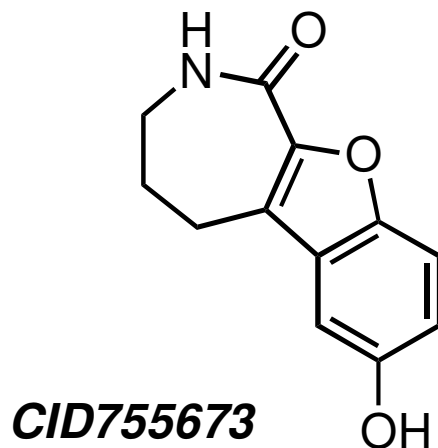
Figure 3. Chemical structure of the selective PKD inhibitor CID755673. This compound is a pan-PKD inhibitor with an IC_{50} for PKD1 inhibition of 182 nM.

Following the identification of CID755673 as a potential hit in this IMAP-based HTS performed by our colleagues, we tested the compound in a traditional *in vitro* radiometric kinase activity assay to confirm its inhibition of PKD1 and determine its IC_{50} for PKD1 inhibition. In this assay, recombinant PKD1 was incubated with the substrate peptide syntide-2, ATP, and CID755673 (ranging from 1 to 10,000 nM). We found that CID755673 was a potent inhibitor of PKD1, having an IC_{50} for PKD1 inhibition of 182 ± 27 nM (n = 5) in this assay (**Figure 4A**). Given the high homology of the PKD isoforms, we also investigated whether CID755673 may inhibit PKD2 and PKD3 in similar *in vitro* radiometric kinase activity assays. Indeed, we found that CID755673 inhibited both PKD2 and PKD3 with IC_{50}s comparable to that for PKD1 inhibition (**Figure 4B-C**). No selectivity for any isoform by CID755673 was noted.
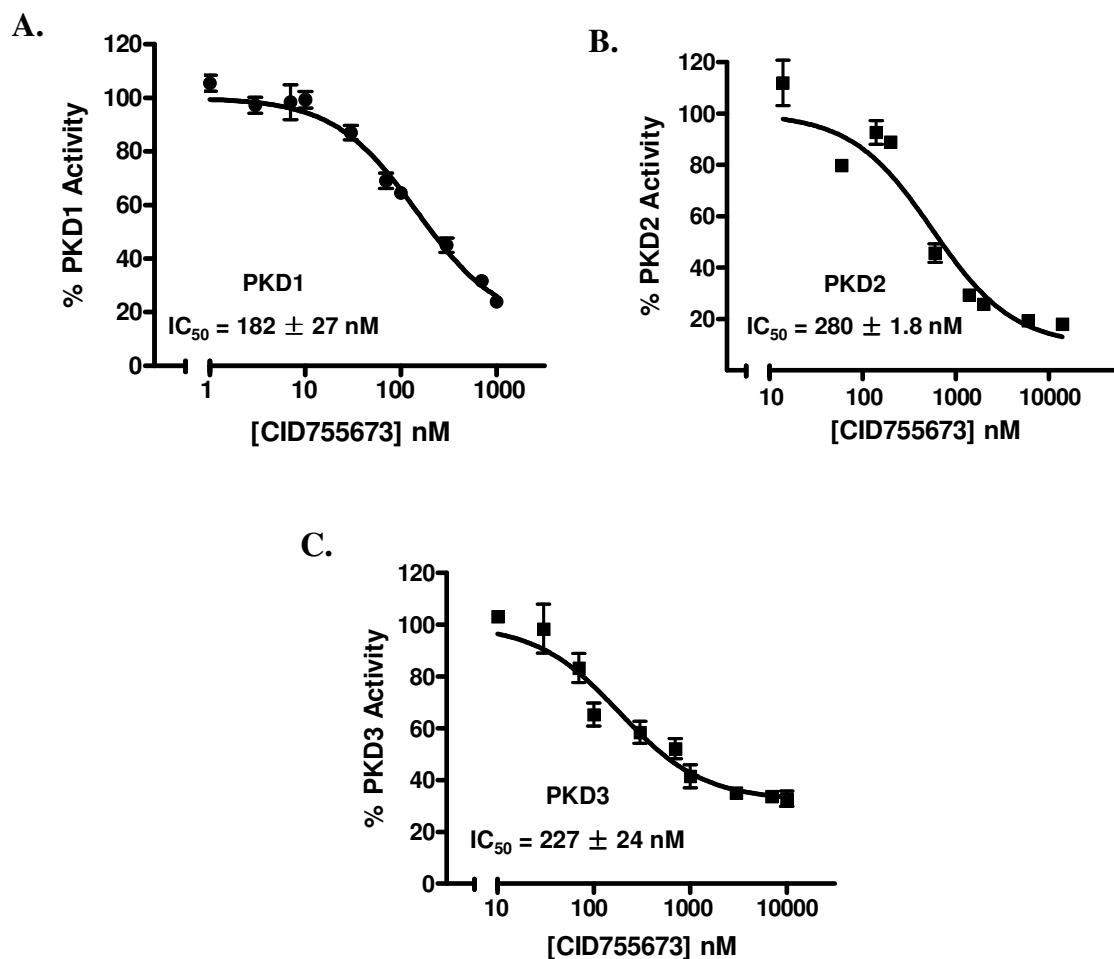
Figure 4. *In vitro* **inhibitory activity of CID755673 toward the PKD isoforms.** The kinase activities of PKD1 (A), PKD2 (B), and PKD3 (C) were assayed in the presence of 10 different concentrations of CID755673 by a radiometric kinase activity assay. The IC_{50} values were calculated, and the graphs show the mean ± S.E. IC_{50}s determined from at least 3 independent experiments with triplicate determinations at each concentration. The data were plotted as a function of CID755673 concentration, and a representative graph is shown for each kinase.

3.2.1.2 Inhibition of PKD1 by CID755673 in LNCaP cells

The initial rapid activation of PKD1 in response to GPCR agonists and phorbol esters is mediated through phosphorylation of the activation loop serines (Ser[738] and Ser[742]) by PKC and subsequent autophosphorylation at Ser[916] (Iglesias and Rozengurt 1998; Matthews et al. 1999; Waldron and Rozengurt 2003). Maintenance of PKD1 activation in response to prolonged stimulation requires autophosphorylation at Ser[742] (Jacamo et al. 2008). The phosphorylation state of these critical serine residues has been shown to correlate well with PKD activity (Matthews et al. 1999). In LNCaP cells, where PKD1 is the predominant isoform (Chen et al. 2008), PKD activity can be stimulated by addition of phorbol 12-myristate 13-acetate (PMA). Thus, we determined whether pretreatment with CID755673 could inhibit PMA-induced phosphorylation of PKD1 at the autophosphorylation site Ser[916] and the trans- and autophosphorylation site Ser[742] in LNCaP cells. Cells were pretreated with various concentrations of CID755673 for 45 min, PKD activity was stimulated by PMA for 20 min, and cell lysates were analyzed by Western blotting for presence of p-Ser[916]-PKD1 and p-Ser[742]-PKD1. We found that CID755673 was indeed able to inhibit activation of PKD1 in cells in a concentration-dependent manner, with a near full blockage of autophosphorylation at Ser[916] when cells were exposed to 50 µM CID755673 (**Figure 5**). Though the compound inhibited both Ser[742] and Ser[916] phosphorylation, inhibition at Ser[916] was more dramatic. In contrast, the inactive analog CID797718 did not inhibit cellular PKD1 activity (**Figure 5**).

	Control		CID755673					CID797718				
Inhibitor (μM):	-	-	0.5	1	5	10	50	0.5	1	5	10	50
PMA (100 nM):	-	+	+	+	+	+	+	+	+	+	+	+

p-Ser^{916}-PKD1

p-Ser^{742}-PKD1
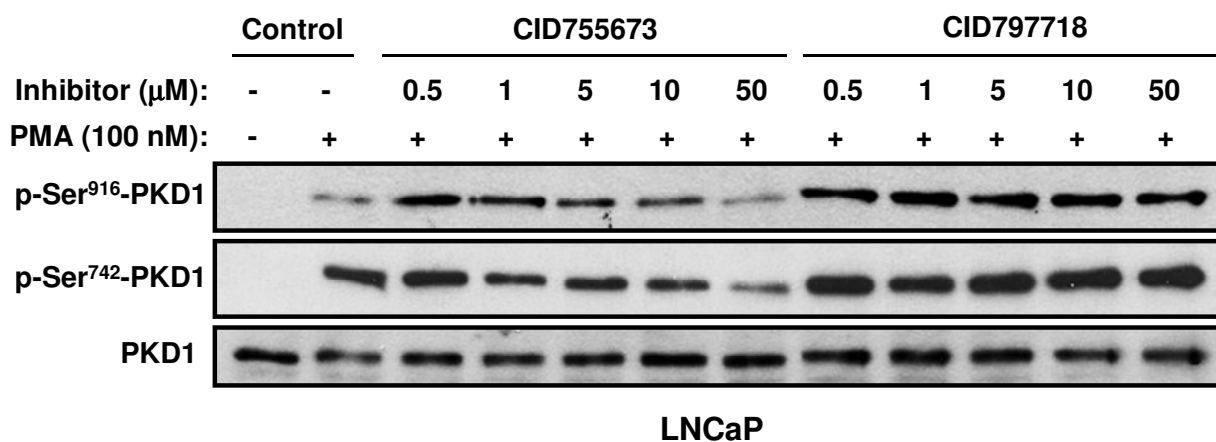
PKD1

LNCaP

Figure 5. Inhibition of endogenous PKD1 activity by CID755673 in cells. LNCaP cells were pretreated with different doses of CID755673 or CID797718 for 45 min, followed by PMA stimulation at 100 nM for 20 min. Cell lysates were subjected to immunoblotting for p-Ser^{742}-PKD1 and p-Ser^{916}-PKD1. PKD1 was blotted as loading control. Note that the low p-Ser^{916}-PKD1 signal in *lane 2* (PMA alone) was likely caused by uneven loading. The experiment was repeated 5 times, and a representative blot is shown.

3.2.1.3 Analysis of the mechanism of action of CID755673

Having confirmed that CID755673 inhibited PKD *in vitro* and in cells, we next wanted to gain insight into the mechanism of action of this compound. First, we examined the effects of increasing concentrations of ATP on inhibition of PKD1 activity by CID755673. As shown in **Figure 6A**, the compound effectively inhibited PKD1 even in the presence of up to 640 μM ATP. Varying the ATP concentration did not alter the IC$_{50}$ of CID755673 for PKD1 inhibition. An Eadie-Hofstee plot was generated by plotting the reaction velocity (*v*) versus the *v*/[ATP] ratio for each inhibitor concentration and fitting the points to linear regression lines (**Figure 6B**). In this plot, we observed that lines generated for each inhibitor concentration were parallel, indicating that addition of increasing concentrations of ATP did not alter the K_m (the slope of the

line) of the reaction. In contrast, the V_{max} (the intercept with the *y*-axis) decreased as inhibitor concentration increased. These results indicate that CID75573 is non-competitive with respect to ATP.

A.

[ATP]
- ■ 20 μM ATP, IC_{50} = 134.2 nM
- ▲ 40 μM ATP, IC_{50} = 140.3 nM
- ▼ 80 μM ATP, IC_{50} = 182.9 nM
- ◆ 160 μM ATP, IC_{50} = 187.4 nM
- ● 320 μM ATP, IC_{50} = 187.3 nM
- □ 640 μM ATP, IC_{50} = 208.5 nM

B.

[CID755673]
- ○ 0 nM
- ● 30 nM
- ▲ 100 nM
- ▼ 300 nM
- ◆ 1000 nM
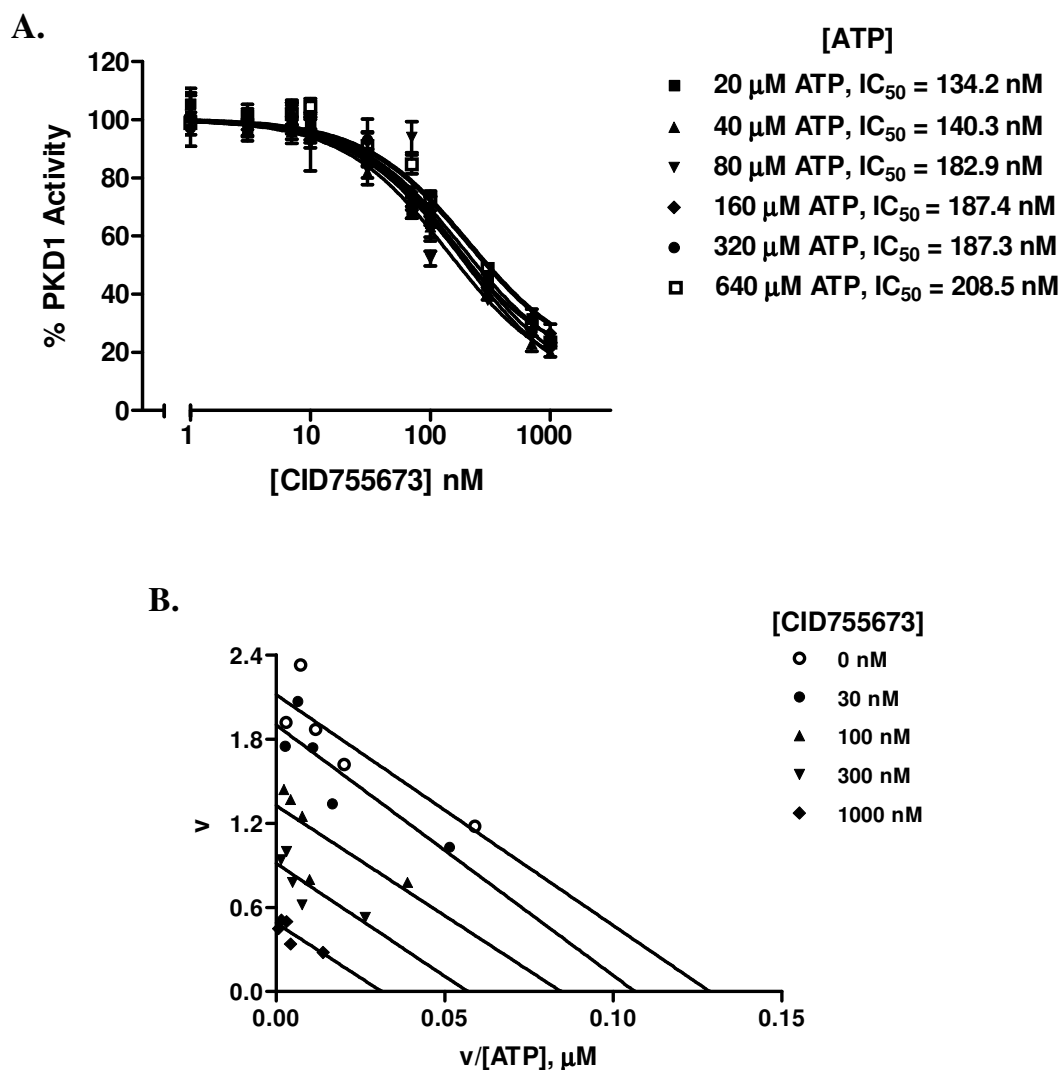
Figure 6. CID755673 is a non-ATP competitive inhibitor of PKD1. A, ATP competition analysis. PKD1 kinase activity was measured as a function of increasing concentrations of CID755673 in the presence of varying concentrations of ATP. B, Eadie-Hofstee plot analysis. The reaction velocity (*v*) was plotted as a function of the velocity *versus* ATP concentration ratio (*v*/[ATP]) for each concentration of CID755673. The points were fitted by linear regression analysis.

Next, we tested whether increasing the concentration of the peptide substrate syntide-2 could alter the inhibitory activity of CID755673. Similar to our assays with ATP competition, we found that the IC_{50} did not change significantly when the concentration of syntide-2 was varied from 6.6 µM to 106.1 µM (**Figure 7A**). Analysis using the Lineweaver-Burke plot, in which the *y*-axis is plotted as 1/*v* and the *x*-axis is 1/[substrate], demonstrated non-competitive, mixed inhibition with respect to substrate (**Figure 7B**). In mixed inhibition, the inhibitor generally binds to an allosteric site separate from the substrate binding site, and while inhibitor binding may affect substrate binding (and vice versa), the inhibitory effects cannot be overcome by increased concentrations of substrate. In this type of inhibition, inhibitor binding may alter either the K_m or V_{max}, or both (Cook and Cleland 2007). To further confirm this result, we repeated this analysis using an HDAC5 peptide substrate. We found that this peptide, a more physiologically relevant substrate as HDAC5 is phosphorylated by PKD in cells, generated similar results to that of syntide-2 when plotted in the Lineweaver-Burke plot (**Figure 7C**). Taken together, our results indicate that CID755673 is non-competitive with respsect to ATP, and appears to demonstrate non-competitive, mixed inhibition with respect to substrate, as determined using 2 different substrate peptides.

A.

% PKD1 Activity vs [CID755673] nM

[substrate]
■ 6.6 μM syntide-2, IC_{50} = 169.5 nM
▲ 13.3 μM syntide-2, IC_{50} = 213.6 nM
▼ 26.5 μM syntide-2, IC_{50} = 110.2 nM
◆ 53.1 μM syntide-2, IC_{50} = 149.3 nM
● 106.1 μM syntide-2, IC_{50} = 195.8 nM

B.

1/v vs 1/[Syntide-2] μM

■ DMSO
▲ 30 nM CID755673
▼ 100 nM CID755673
◆ 300 nM CID755673
● 1000 nM CID755673

C.

1/v vs 1/[HDAC5 Peptide] μM

■ DMSO
▲ 30 nM CID755673
▼ 300 nM CID755673
◆ 1000 nMCID755673
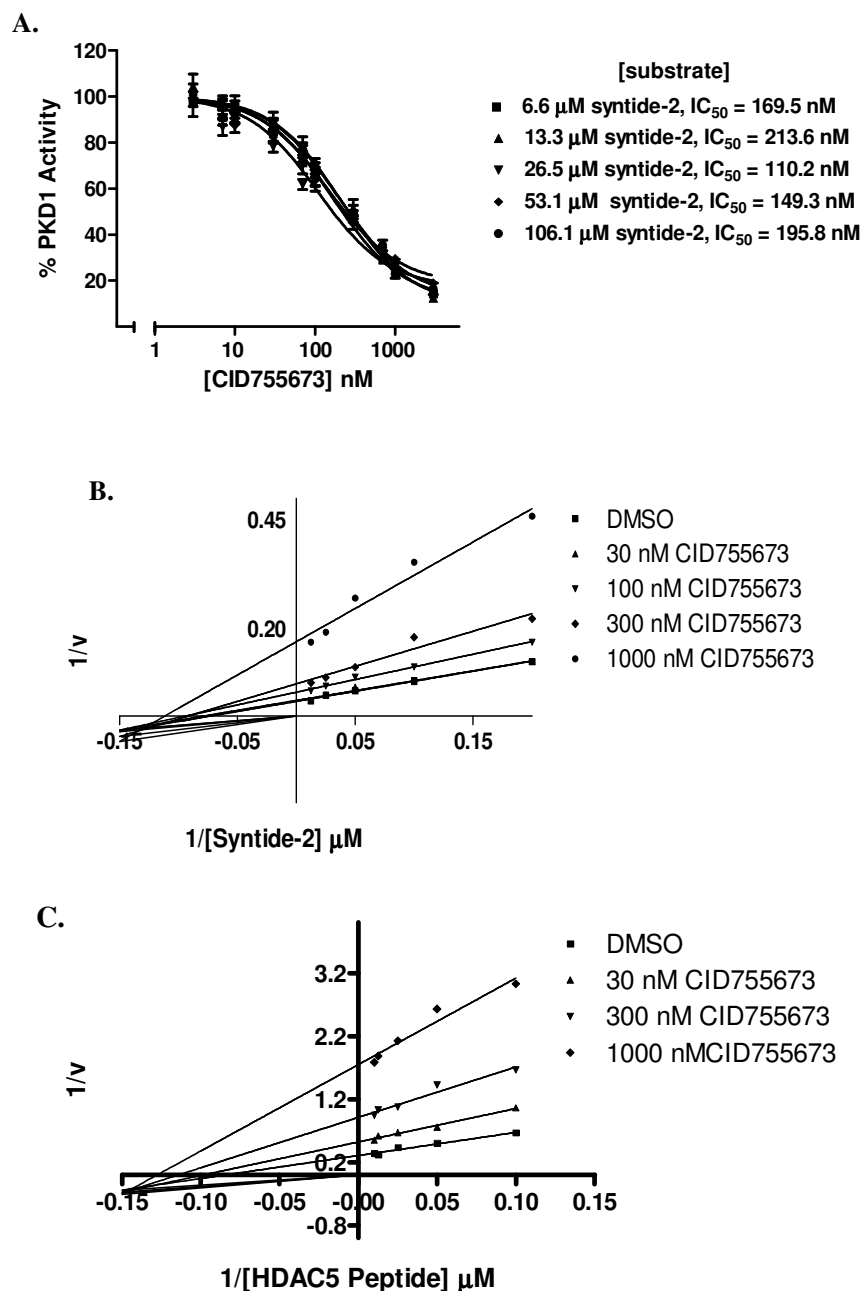
Figure 7. CID755673 shows non-competitive, mixed inhibition with respect to substrate. A, determination of IC_{50}s with varying concentrations of syntide-2. PKD1 kinase activity was measured as a function of increasing concentrations of CID755673 in the presence of varying concentrations of substrate. B-C, Lineweaver-Burke plot analysis for syntide-2 (B) or HDAC-5 peptide (C) competition assays. The reciprocal of the reaction velocity (1/v) was plotted as a function of the reciprocal of the substrate concentration for each concentration of CID755673. The points were fitted by linear regression analysis.

3.2.1.4 CID755673 does not inhibit PKC or CAMKIIα

The study of PKD function has been greatly hampered due to lack of a specific inhibitor. Compounds previously used to inhibit PKD were more general kinase inhibitors or PKC inhibitors. Since PKD is directly phosphorylated by PKC and functions downstream of PKC signaling, dissection of the biological function of PKD would be greatly aided by selective PKD inhibitors. Therefore, we tested the ability of CID755673 to inhibit several isoforms of PKC or the highly homologous CAMKIIα. Even at high concentrations, CID755673 did not show significant inhibition of PKCα, PKCβI, or PKCδ in radiometric PKC kinase activity assays (**Figure 8A-C**). As a positive control, the PKC inhibitor GF109203X potently reduced PKC activity for all isoforms tested. Similarly, CID755673 failed to inhibit CAMKIIα, reaching only 30% maximal inhibition at 100 µM concentration (**Figure 8D**). Taken together, these results suggest that CID755673 is a relatively selective PKD inhibitor and does not inhibit several related kinases.
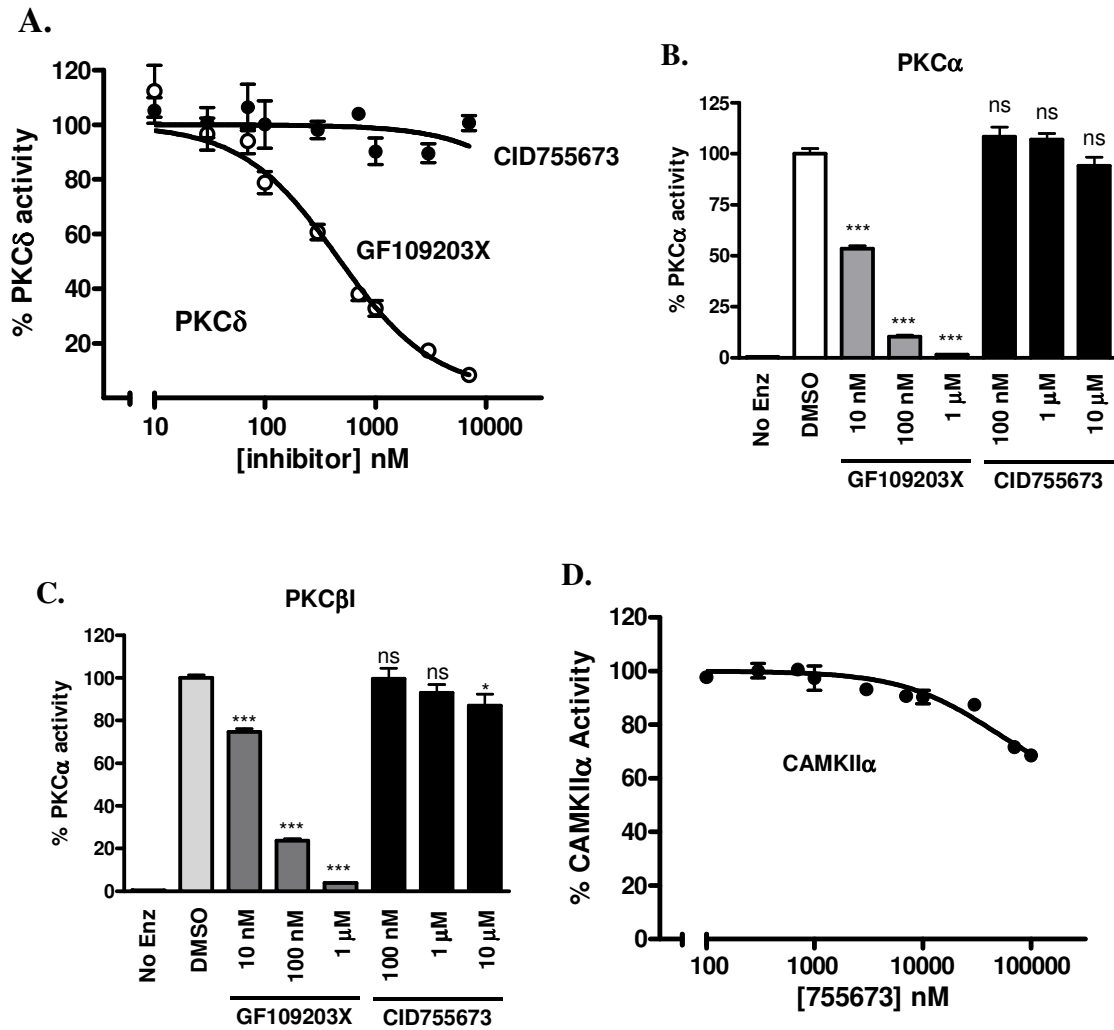
Figure 8. CID755673 does not inhibit several related kinases. A, CID755673 did not inhibit PKCδ. Inhibitory activity of CID755673 for PKCδ was measured using a radiometric kinase activity assay. Inhibition of PKCδ by GF109203X was assayed as a control. Data shows a representative graph from 3 separate experiments. B-C, CID755673 also did not inhibit PKCα (B) or PKCβI (C) when tested at 100 nM, 1 μM, or 100 μM concentration. As a control, the PKC inhibitor GF109203X potently inhibited PKCα and PKCβI activity. Data are shown as the mean ± S.E.M. of at least 2 independent experiments. ns, not statistically significant; *, $p < 0.05$; ***, $p < 0.001$. D, inhibition of CAMKIIα was measured by the radiometric CAMK kinase assay. The experiment was repeated twice, and a representative curve is shown.

3.2.1.5 CID755673 reduces tumor cell proliferation and causes cell cycle arrest

PKD is a known regulator of cell proliferation, growth, and survival (Wang 2006) and is known to be dysregulated in several types of cancer. Therefore, we evaluated the effects of CID755673 on the proliferation of prostate cancer cells. Cells were plated in 24-well plates, and cell numbers in the presence or absence of inhibitor were determined by counting the number of live cells for 6 consecutive days. CID755673 treatment caused a significant reduction in cell proliferation for PC3, DU145, and LNCaP cells over the course of the experiment (**Figure 9A-C**). In contrast, the weaker analog CID797718 showed reduced effects on PC3 cell proliferation when tested at 25 μM (**Figure 9D**). Additionally, more dramatic growth-inhibitory effects of CID755673 were observed in PC3 cells as compared with LNCaP cells, accompanying significant morphological changes from small polygonal or spindle-like shapes to large, flat, and round shapes (**Figure 10**).
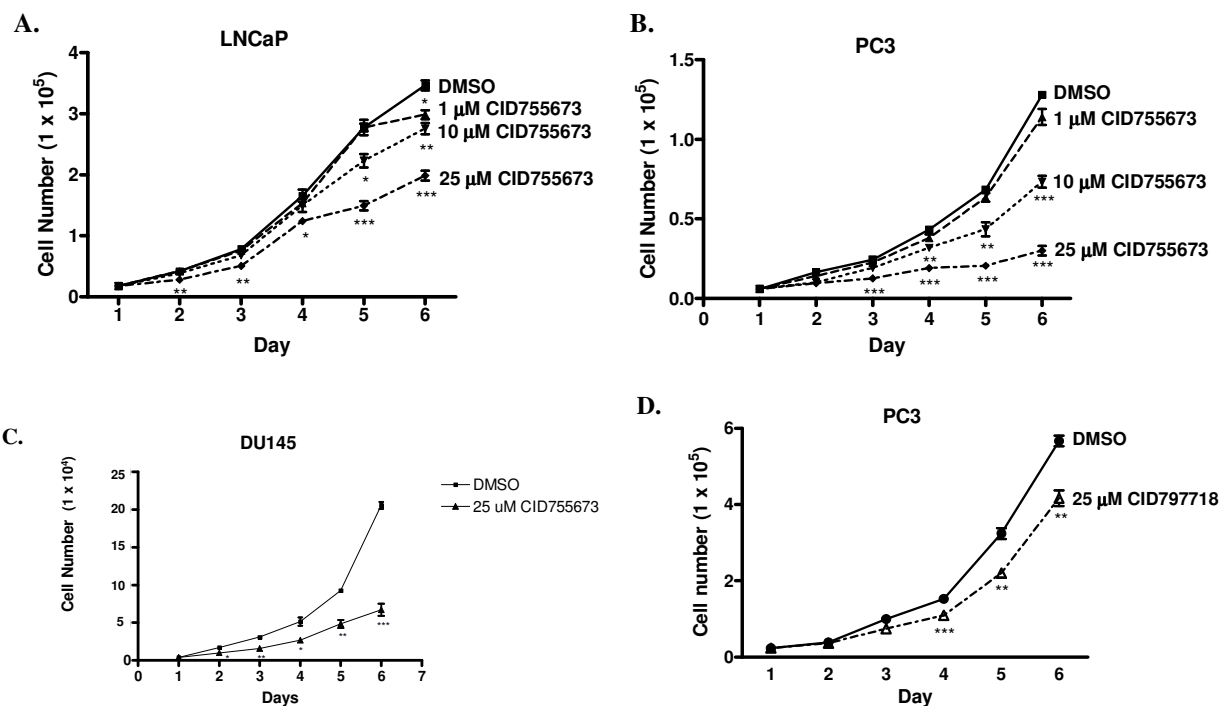
Figure 9. CID755673 inhibits prostate cancer cell proliferation. LNCaP (A), PC3 (B), or DU145 (C) cells were plated in triplicates in 24-well plates. Cells were allowed to attach overnight. A cell count at day 1 was made, and then either vehicle (DMSO) or CID755673 at the indicated concentrations was added. Cells were counted daily for a total of 6 days. Fresh media and inhibitor were added every 2 days. The means of triplicate determinations were plotted over time. The experiment was repeated at least twice, and results from a representative experiment are shown. D, the effect of the weaker analog CID797718 on PC3 cell proliferation. Results from 1 of 2 independent experiments are shown. *, $p < 0.05$; **, $p < 0.01$; ***, $p < 0.001$.
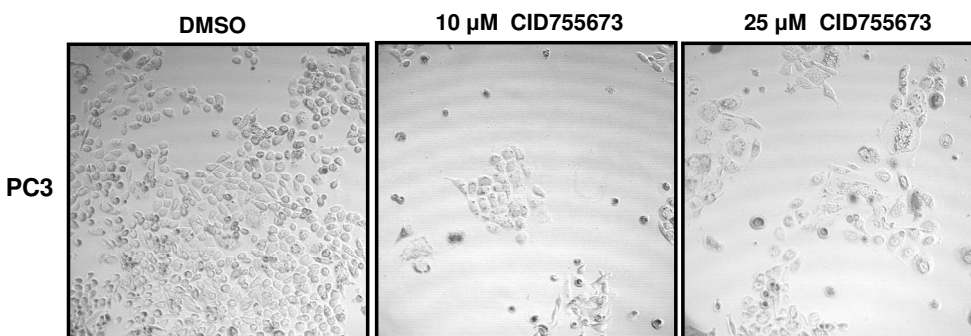
Figure 10. Morphological changes caused by CID755673 in PC3 cells. Phase-contrast images of PC3 cells after 6 days of CID755673 treatment are shown.

In order to provide more insight into the anti-proliferative effects of this compound, we analyzed the cell cycle distribution in PC3 cells treated with 10 µM or 25 µM CID755673. Cells were treated for 6 days with CID755673, and then subjected to FACS analysis as described in the "Materials and Methods." As shown in **Figure 11**, treatment with CID755673 caused significant arrest in the G_2/M phase of the cell cycle. Taken together, these data indicate that CID755673 has significant effects on the proliferation of cancer cells.
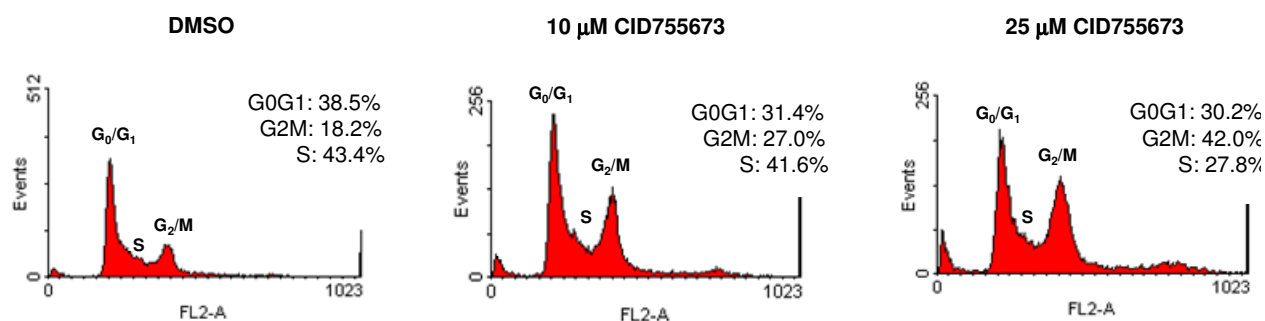
Figure 11. CID755673-induced G_2/M phase cell cycle arrest. PC3 cells were incubated with vehicle (DMSO) or varying concentrations of CID755673 for 6 days. Media with fresh inhibitors was replenished daily. Cell cycle distribution was evaluated by flow cytometry after propidium iodide labeling of fixed cells. One of at least 2 independent experiments is shown.

3.2.1.6 CID755673 inhibits tumor cell migration and invasion

Among its many functions, PKD has been implicated in modulating cell adhesion and motility (Bowden et al. 1999; Jaggi et al. 2005; Prigozhina and Waterman-Storer 2004). Therefore, we investigated the effects of CID755673 on migration and invasion in prostate and pancreatic cancer cells. To study cell migration, we used a wound healing or "scratch" assay. In this assay, cells were plated in 6-well plates and allowed to grow to confluence. Then, a "wound" was made

in the confluent monolayer using a 10 µL pipette tip. Cells were treated with various concentrations of CID755673, and wound-induced migration was measured by comparing the wound gap at time 0 versus the wound gap at various times up to 24 h. Interestingly, CID755673 was found to inhibit cell migration in PC3, DU145, and PANC1 cells when tested at various concentrations (**Figure 12A-D**). Phase contrast images of the wound in DU145 cells after 24 h treatment are shown in **Figure 12B**. In DU145 cells, wound closure was inhibited up to a maximum of 50% closure by 25 µM CID755673 while the less potent analog CID797718 did not significantly inhibit wound closure (**Figure 12E**).

To determine the effects of CID755673 on prostate cancer cell invasion, we conducted a Matrigel invasion assay in DU145 cells. Cells were seeded into Matrigel invasion or control chambers in the absence or presence of 25 µM CID755673, using 20% FBS as the chemoattractant. As shown in **Figure 13**, treatment with CID755673 caused a 3-fold reduction in invasion (invasion index = 0.32) while CID797718 had no effect. Taken together, these results indicate that the novel PKD inhibitor CID755673 suppresses prostate and pancreatic cancer cell motility.
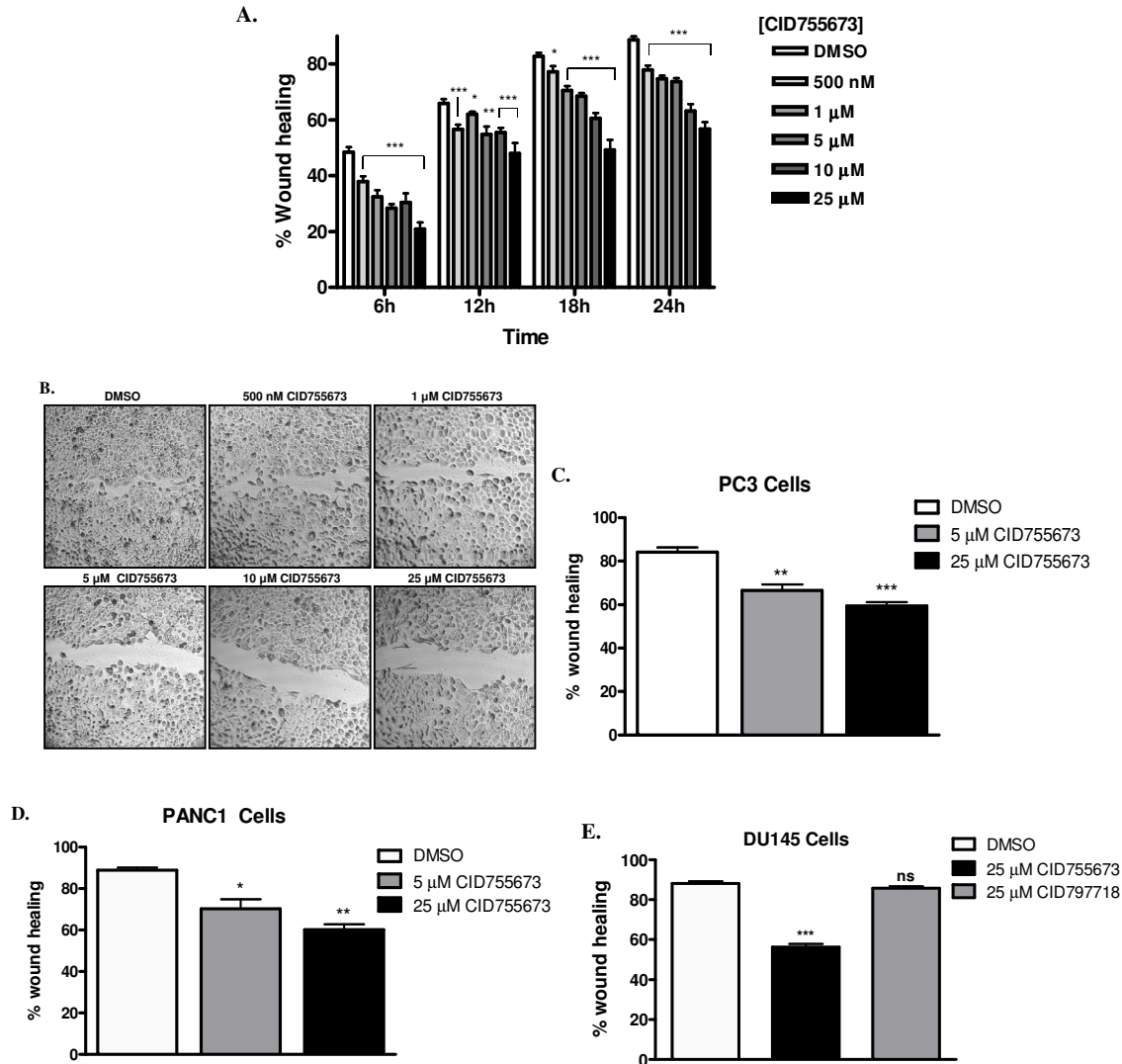
Figure 12. Effects of CID755673 on tumor cell migration. A, DU145 cells were grown to confluence in 6-well plates. The monolayer was wounded and imaged immediately (0 h). Growth media containing vehicle (DMSO) or varying concentrations of CID755673 was added. Wound closure was recorded every 6 h up to 24 h. The width of the wound is shown as the average of at least 9 determinations per time point. Percent wound healing was calculated at each time point as described under "Materials and Methods." The experiment was repeated 3 times and data are the mean ± S.E.M. of the 3 independent experiments. B, Representative images are shown. C-D, the wound healing assay in PC3 cells (C) or PANC1 (D) cells was also performed at a single time point (24 h). The experiment was repeated 3 times and data are the mean ± S.E.M. of the 3 independent experiments. E, the weaker analog CID797718 did not inhibit wound closure. The experiment was repeated twice and a representative graph is shown. ns, not statistically significant; *, $p < 0.05$; **, $p < 0.01$; ***, $p < 0.001$.

68
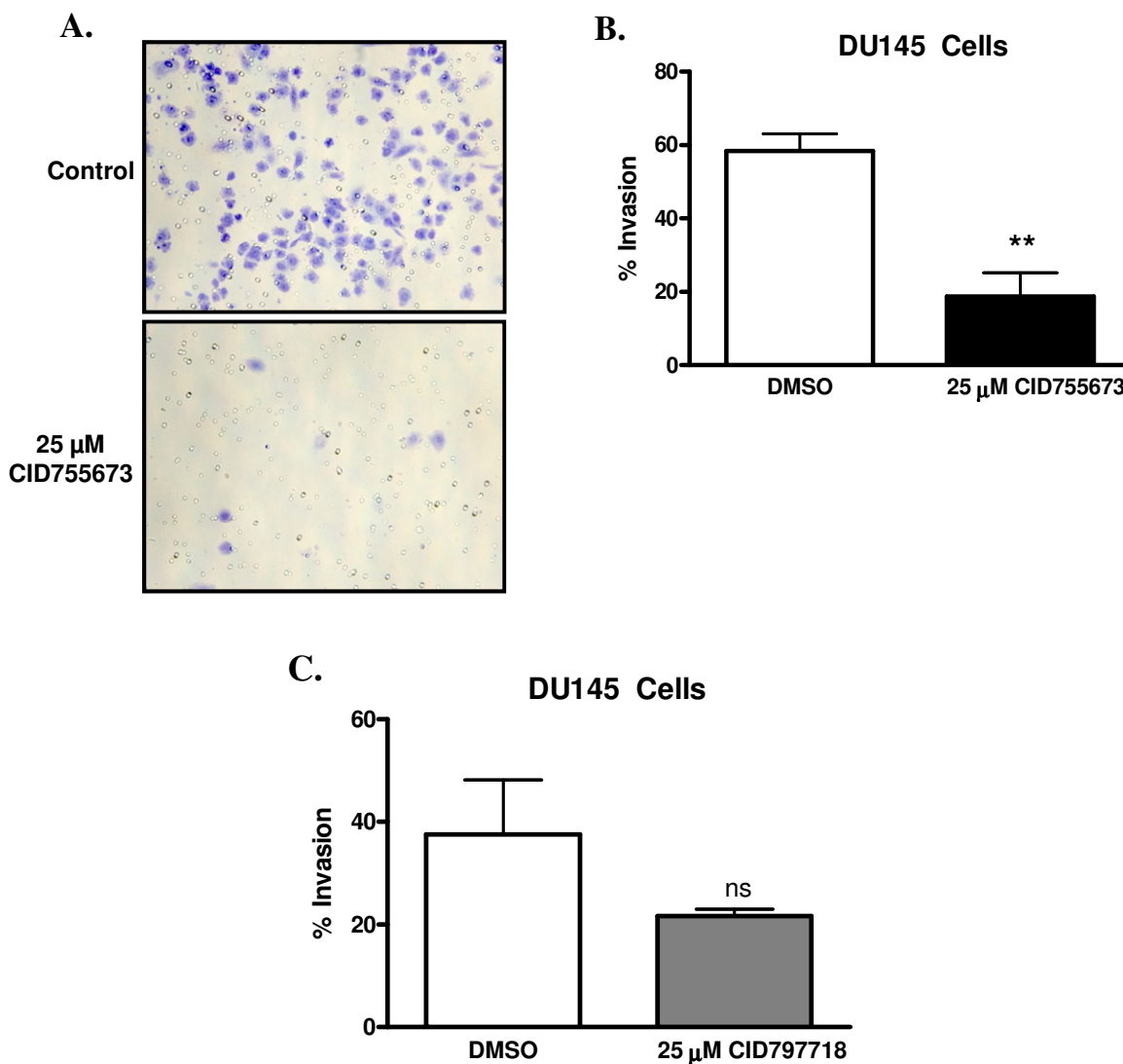
Figure 13. Effects of CID755673 on tumor cell invasion. A, tumor cell invasion was evaluated by a Matrigel invasion assay. A fixed number of DU145 cells (1.0×10^5 cells/mL) were seeded into the upper control or invasion chamber. After 22 h, non-invading cells were removed, and cells that invaded through the Matrigel were fixed, stained, and photographed under a microscope at 200x magnification. B, percent invasion is expressed as the number of cells that invaded through the Matrigel matrix relative to the number of cells that migrated through the control insert. Cell number was determined by counting total cell number in 10 random fields. The experiment was repeated twice, and a representative experiment is shown. C, the weaker analogue CID797718 did not significantly inhibit tumor cell invasion. DU145 cell invasion was measured using Matrigel invasion chambers after incubating with DMSO or 25 μM CID797718 for 22 h. ns, not statistically significant; **, $p < 0.01$.

3.2.2 Development and characterization of novel analogs of CID755673

3.2.2.1 Design of CID755673 analogs

CID755673 and CID797718, a structural analog of CID755673, were synthesized by the PMLSC

Chemistry Core. CID797718 is a byproduct of CID755673 synthesis, and has 10-fold less

inhibitory activity toward PKD than the parental compound (Sharlow et al. 2008).

The design of the CID755673 analogs was based on initial structure-activity relationship

(SAR) analysis (Bravo-Altamirano et al. 2011; George et al. 2011). We dissected the parent

compound CID755673 into 4 major structural zones in order to elucidate a fundamental SAR

(**Figure 14**). In zone I, we modified the phenolic substituent as well as the α-position on the

aromatic ring. In zone II, we substituted the oxygen ring atom with sulfur and nitrogen. In zone

III, we altered the ring size by adding or removing methylene groups, as well as substituting the

benzylic position. In zone IV, we pursued functional group interconversions as well as

replacement of the amide with heterocyclic groups. Synthesized analogs were tested for PKD1

inhibition *in vitro* to determine whether the structural modifications affected inhibitory activity.

Most of the zone I derivatives were considerably less active than CID755673 in the PKD screen.

In particular, carbon substituents *ortho* to the phenol and *O*-benzylations were detrimental. In

contrast, *ortho*-halogenation and *O*-methylation were well tolerated. Nitrogen replacements in

zone II were associated with loss of activity, whereas sulfur substitution was not only tolerated

well but often led to a substantial increase in activity. Among the zone III substitutions, a

thioether insertion *exo* to the five-membered heterocycle and an additional methylene group

(leading to an eight-membered fused ring) were well tolerated. Finally, all zone IV substitutions

were unsatisfactory, and we decided to retain the amide function of CID755673 in this position.

All compounds synthesized and tested, as well as their *in vitro* inhibitory activity toward PKD1 and their chemical structures, are listed in Appendix A.
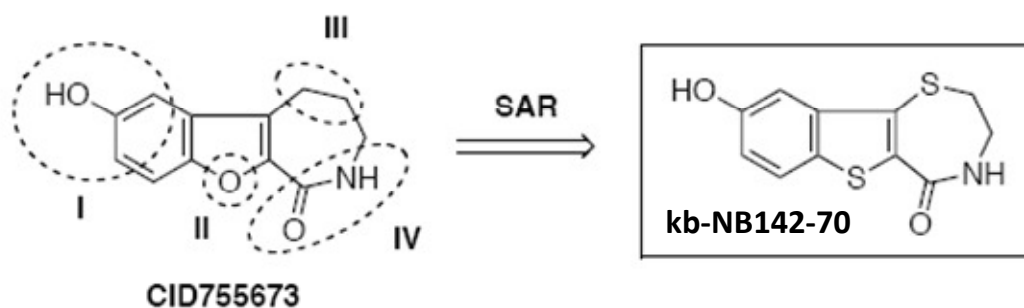
Figure 14. SAR of CID755673 and its analogs. Diagram describing the major structural zones dissected for SAR analysis.

After initial screening and SAR analysis on approximately 50 analogs summarized above, 5 novel compounds with equal or greater potency for PKD were selected for further testing (**Figure 15**).
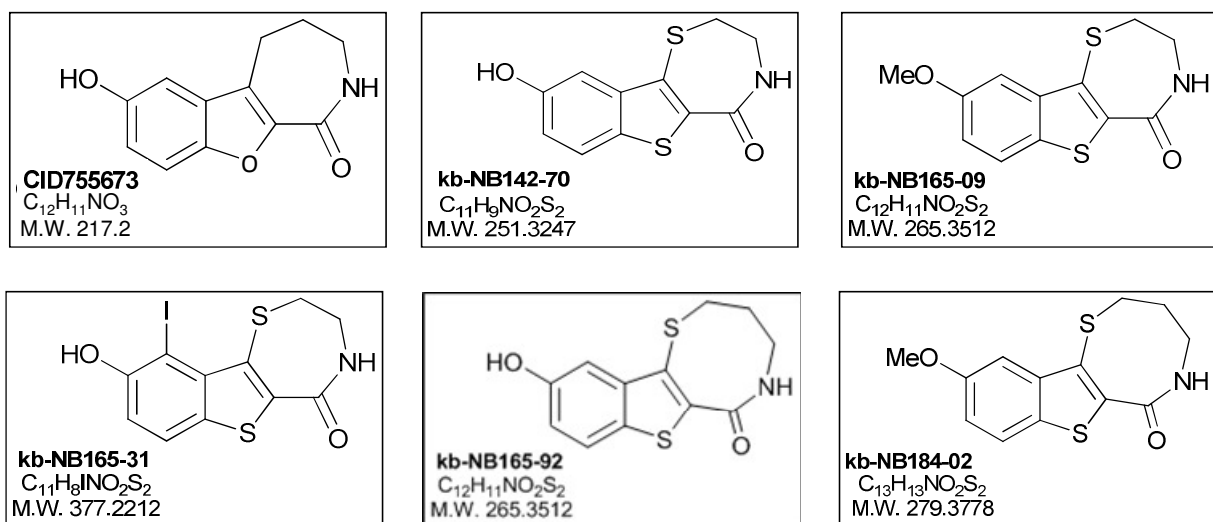
Figure 15. Chemical structures of CID755673 and its analogs. Chemical structures of the parental compound CID755673, previously identified and confirmed as a pan-PKD inhibitor, and of 5 analogs of CID755673.

3.2.2.2 *In vitro* activities of CID755673 analogs

The *in vitro* inhibitory activities of the novel compounds toward PKD were determined using radiometric PKD kinase activity assays. Recombinant human PKD1, -2, or -3 was incubated with the substrate, syntide-2, in the presence of 10 different concentrations of each compound. IC_{50} values were determined for each compound by plotting percent PKD activity versus compound concentration for each point. We found that while the compounds inhibited all 3 PKD isoforms, their potency and selectivity varied (**Figure 16** and **Table 3**). The most potent compound was found to be kb-NB142-70, which inhibited PKD1 with an IC_{50} of 28.3 ± 2.3 nM (n = 3), showing a 7-fold greater potency than the parental compound (**Table 3**). This compound was also a robust inhibitor of PKD2 and -3, demonstrating respective IC_{50}s of 58.7 ± 4.2 nM (n = 3) and 53.2 ± 3.5 nM (n = 3). Notably, kb-NB142-70 and kb-NB184-02 exhibited about 2-fold greater selectivity toward PKD1. In contrast, the compound kb-NB165-92 was more selective toward PKD3, showing approximately 2-fold greater potency toward PKD3 (IC_{50} = 58.8 ±7.3 nM, n = 3) than PKD1 or -2 (IC_{50} = 111.2 ± 6.0 and 100.7 ±10.9, n = 3, respectively), which is unique among the compounds tested. Other compounds, namely kb-NB165-09 and kb-NB165-31, showed similar inhibition of all 3 isoforms. Overall, our results demonstrated that core structural modification of CID755673 substantially enhanced its potency, but had less effect on isoform selectivity.
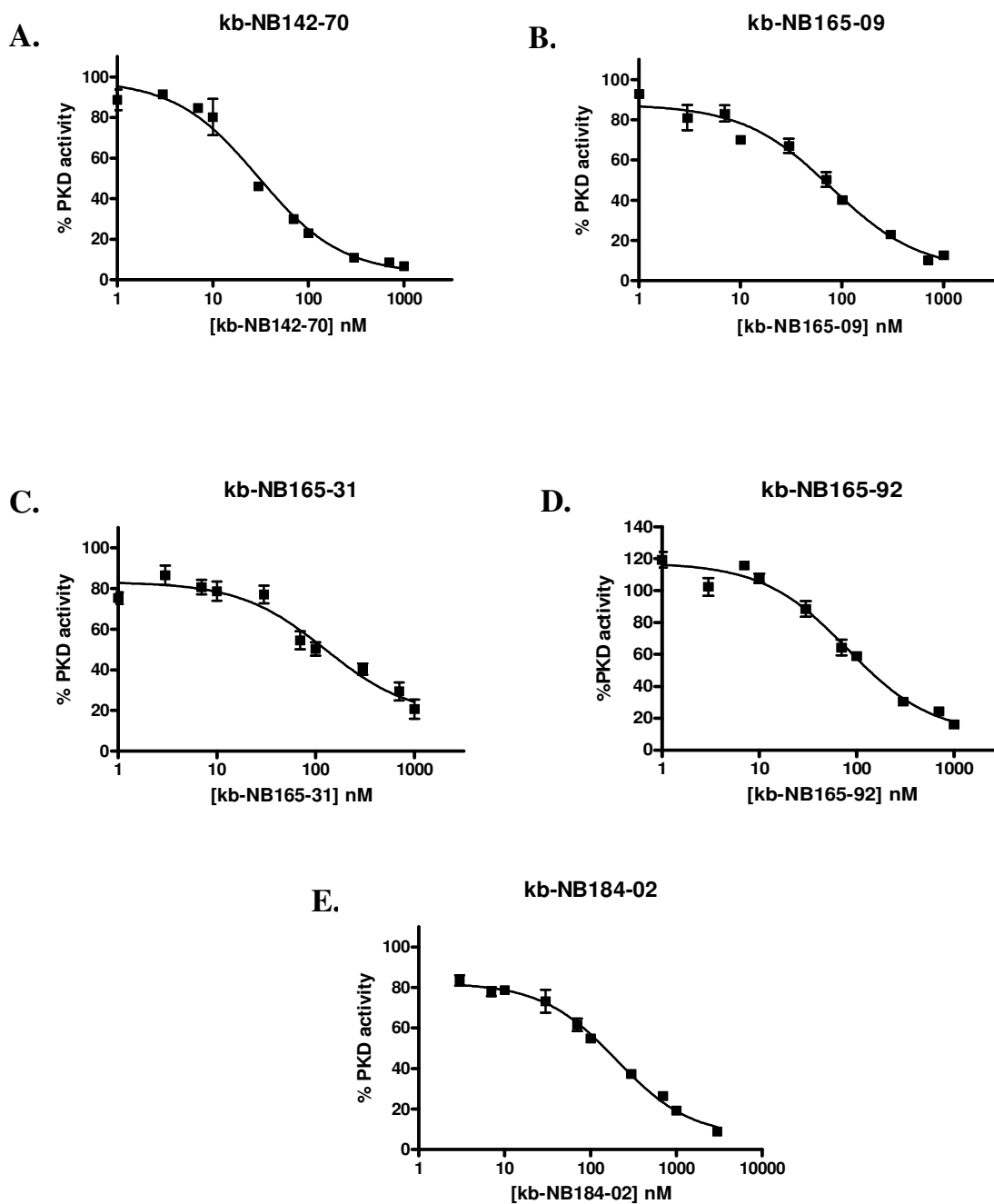
Figure 16. Inhibition of PKD activity by CID755673 analogs *in vitro*. A-E, inhibition of recombinant human PKD1 *in vitro*. PKD kinase activity was assayed by a radiometric kinase assay in the presence of increasing concentrations of the CID755673 analogs. A 10-point concentration curve was generated for each compound for IC_{50} determination. Each IC_{50} was determined as the mean ± S.E.M. of 3 independent experiments with triplicate determinations at each concentration in each experiment. Representative graphs are shown.

Table 3. *In vitro* **inhibitory activity of CID755673 and its analogs for PKD.** IC_{50} were determined for CID755673 and its analogs against PKD1, -2, and -3 using radiometric kinase activity assays. Each IC_{50} was calculated as the mean ± S.E.M. of at least 3 independent experiments with triplicate determinations at each concentration in each experiment as described in "Materials and Methods."

	IC_{50} (nM)		
Compound	PKD1	PKD2	PKD3
CID755673	182 ± 27 (n = 5)	280 ± 1.8 (n = 3)	227 ± 24 (n = 3)
kb-NB142-70	28.3 ± 2.3 (n = 3)	58.7 ± 4.2 (n = 3)	53.2 ± 3.5 (n = 3)
kb-NB165-09	82.5 ± 4.6 (n = 4)	141.6 ± 7.4 (n = 3)	98.5 ± 15.3 (n = 3)
kb-NB165-31	114.1 ± 23.9 (n = 3)	162.9 ± 20.5 (n = 3)	91.1 ± 17.2 (n = 3)
kb-NB165-92	111.2 ± 6 (n = 3)	100.7 ± 10.9 (n = 3)	58.8 ± 7.3 (n = 3)
kb-NB184-02	192.8 ± 27.4 (n = 3)	463.2 ± 38.2 (n = 4)	324.7 ± 39.0 (n = 3)

*n, number of independent experiments

3.2.2.3 CID755673 analogs inhibit PMA-induced endogenous PKD1 activation in prostate cancer cells

To determine whether the compounds were active in cells, we tested their ability to inhibit activation of PKD1 by PMA in LNCaP prostate cancer cells. We measured both p-Ser[916] and p-Ser[742] levels by Western blot analysis to track PKD1 activity. As is shown in **Figure 17** (*lane 2*), addition of PMA alone induced phosphorylation of both Ser[916] and Ser[742] of PKD1. When LNCaP cells were pretreated with the novel CID755673 analogs before PMA treatment, concentration-dependent inhibition of phosphorylation at both Ser[916] and Ser[742] of PKD1 was observed (**Figure 17**, *lanes 3-7*). This effect appeared to be most dramatic for the compound kb-NB142-70, with a calculated cellular IC_{50} for inhibition of Ser[916] phosphorylation of 2.2 ± 0.6 μM (n = 3) (**Table 4**). The compounds kb-NB165-09 and kb-NB165-92 showed similar cellular activity, with IC_{50}s of 3.1 ± 0.5 (n = 3) and 2.6 ± 0.7 μM (n = 3) respectively. Consistent with

our *in vitro* data, kb-NB184-02 was again the least potent compound, demonstrating a cellular

IC_{50} of 18.6 ± 2.0 µM (n = 3). GAPDH was used as a loading control instead of PKD1 because

the PKD1 antibody showed a slight inconsistency in detecting phosphorylated and non-

phosphorylated forms of PKD1 (**Figure 17** and *data not shown*). Taken together, these results

indicated that the analogs were capable of inhibiting PKD1 in intact cells.
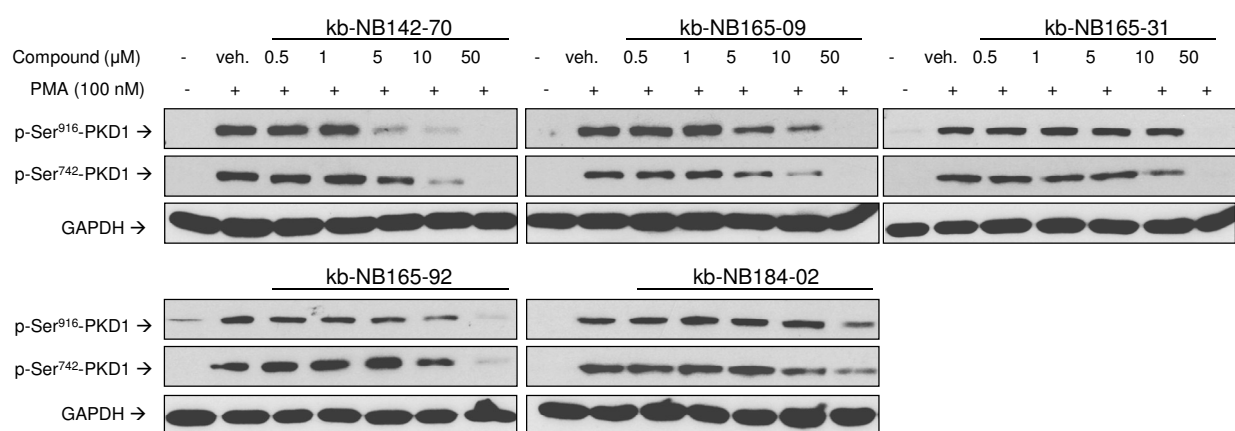
Figure 17. Inhibition of PMA-induced endogenous PKD1 activation in LNCaP cells. LNCaP cells were pretreated with indicated concentrations of the 5 analogs for 45 min, then stimulated with 100 nM PMA for 20 min. Cell lysates were immunoblotted for p-Ser^{916}-PKD1 and p-Ser^{742}-PKD1. GAPDH was blotted as a loading control. The experiment was repeated at least 3 times and representative blots are shown.

Table 4. Cellular inhibition of PKD1 autophosphorylation at Ser^{916} by CID755673 analogs. Cellular IC$_{50}$ was determined by densitometry analysis of Western blotting data for PKD1 autophosphorylation at Ser^{916} in LNCaP cells. Each IC$_{50}$ was calculated as the mean ± S.E.M. of at least 2 independent experiments.

Compound	Cellular IC$_{50}$ (μM)
kb-NB142-70	2.2 ± 0.6 (n = 3)
kb-NB165-09	3.1 ± 0.5 (n = 3)
kb-NB165-31	8.6 ± 2.0 (n = 3)
kb-NB165-92	2.6 ± 0.7 (n = 2)
kb-NB184-02	18.6 ± 2.0 (n = 3)

*n, number of independent experiments

3.2.2.4 Specificity of CID755673 and its analogs to PKD

We previously reported that CID755673 showed selectivity toward PKD and did not inhibit several other kinases tested, including PLK1, CAK, protein kinase B (AKT/PKB), PKCα, -βI, -δ, or CAMKIIα. To determine whether the novel analogs retained this specificity, we tested the compounds against their ability to inhibit PKCα, -βI, -δ, and CAMKIIα in *in vitro* radiometric kinase activity assays. All analogs were poor inhibitors of PKCα and PKCβI, with only slight (<50%) inhibitory activity at 10 μM concentration (**Figure 18A-B**). This was also true for PKCδ and CAMKIIα with the exception of kb-NB165-31, which did show nearly 50% inhibitory activity toward PKCδ and about 70% inhibition of CAMKIIα activity at 10 μM concentration (**Figure 18C-D**). As a positive control, the potent PKC inhibitor GF109203X showed strong inhibition of all 3 of these isoforms (**Figure 18A-C**).
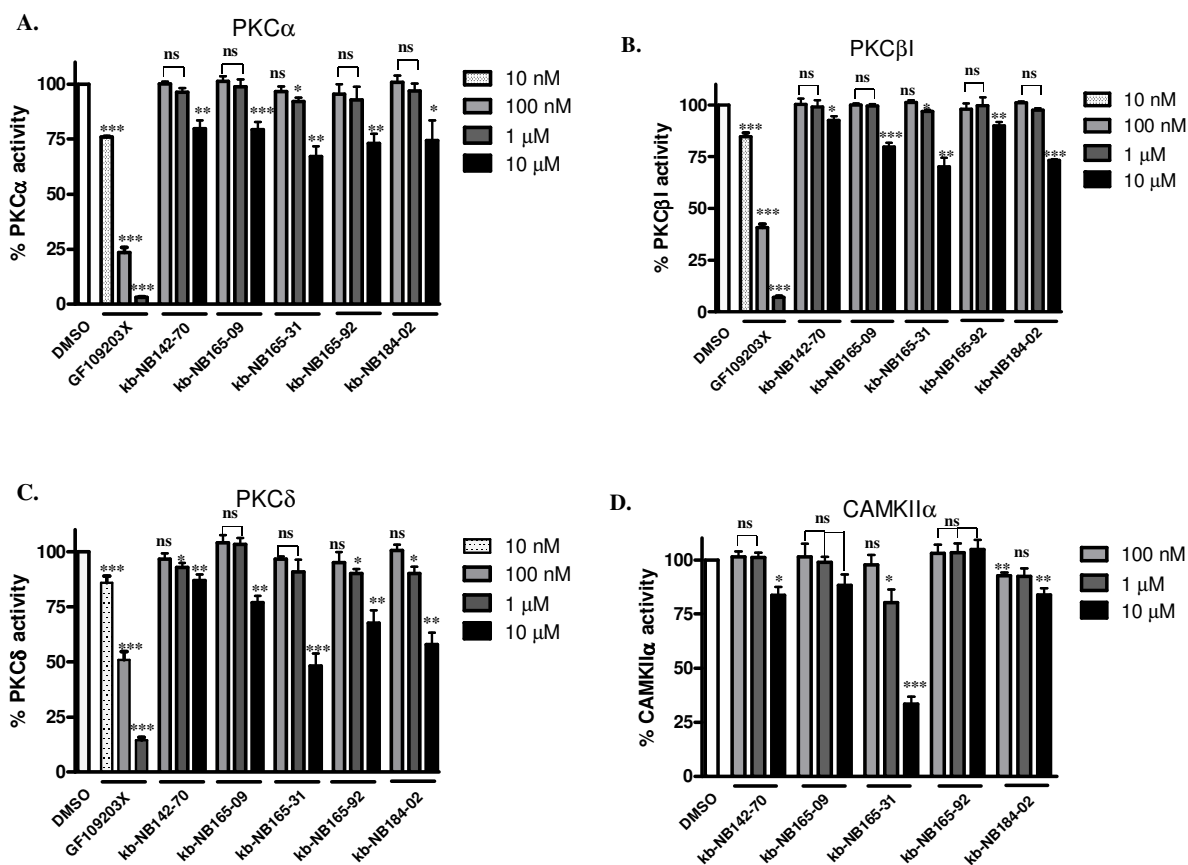
Figure 18. Selectivity of the CID755673 analogs. Inhibition of PKCα (**A**), PKCβI (**B**), PKCδ (**C**), or CAMKIIα (**D**) by each of the 5 analogs was determined at 100 nM, 1 μM, and 10 μM concentrations. In the PKC assays, the potent PKC inhibitor GF109203X was used as a control. Data are the mean ± S.E.M. of 3 independent experiments. ns, not statistically significant; *, $p < 0.05$; **, $p < 0.01$; ***, $p < 0.001$.

To further investigate the specificity of this series of compounds, a kinase profiling experiment was conducted on CID755673, testing 48 additional kinases (**Table 5**). CID755673 showed "significant" inhibition ($\geq 50\%$) of 6 out of a total 48 kinases – glycogen synthase kinase-3β (GSK3β), casein kinase 1δ (CK1δ), mitogen-activated protein kinase-activated protein kinase (MK) 5, MK2, ERK1, and cyclin-dependent kinase 2 (CDK2). As a control, PKD2 activity was reduced by 95% when treated with 10 μM CID755673. A separate, smaller scale

analysis of the kinase inhibition profile of all 5 of the CID755673 analogs was also conducted, and similar patterns of inhibition as the parental compound were observed, indicating that the analogs of CID75573 act on similar targets (data not shown).

Table 5. Kinase profiling report for CID755673. Forty-eight kinases were interrogated using a single-dose *in vitro* kinase assay at 10 µM CID755673. -20 to +20% inhibition, baseline levels; >20 to 49% inhibition, compound only marginally actively inhibits the kinase; >50% inhibition, compound is actively inhibiting the kinase. The assay was performed by Caliper Life Sciences (Hanover, MD).

	CID755673, 10 µM		CID755673, 10 µM
Kinase	**Average % Inhibition**	**Kinase**	**Average % Inhibition**
ABL	8	KDR	8
AKT1	3	**MAPKAPK2**	**95**
AKT2	4	MARK1	12
AMPK	35	MET	18
AurA	7	MSK1	7
BTK	-3	p38a	2
CAMK4	17	p70S6K	44
CDK2	**71**	PAK2	3
CHK1	7	PDGFRα	5
CHK2	4	PDK1	22
CK1δ	**82**	PIM2	6
c-Raf	2	PKA	6
EGFR	11	PKCη	40
ErbB4	1	PKCγ	30
Erk1	**50**	PKCθ	32
Erk2	31	PKCζ	-4
FGFR1	16	**PKD2**	**95**
FLT3	14	PKG1α	13
GSK3β	**86**	PKG1β	11
IGF1R	-2	**MK5/PRAK**	**75**
Ikkb	49	RSK1	29
IBSR	3	SGK1	9
IRAK4	0	SRC	7
JNK2	36	SYK	-8

3.2.2.5 Effects of the CID755673 analogs on tumor cell death, proliferation, and cell cycle distribution

Given the effects of PKD3 knockdown by siRNA or CID755673 in the inhibition of prostate cancer cell proliferation (Chen et al. 2008; Sharlow et al. 2008) and the implications that PKD regulates cell survival and proliferation (Guha et al. 2002; Wong and Jin 2005), we wanted to test whether the new compounds were cytotoxic and whether they also inhibited prostate cancer cell proliferation. Therefore, we determined the cytotoxic effects of the compounds on PC3 cells by MTT assay. As shown in **Figure 19**, the parental compound induced very little cell death, having an EC_{50} of 319.8 μM in this context. In contrast, the analogs showed considerable increases in cytotoxicity. The new lead compound kb-NB142-70 was again the most potent, causing considerable cell death and demonstrating an EC_{50} of 8.025 μM. The compounds kb-NB165-09, kb-NB165-31, and kb-NB184-02 showed similar effects on cell death, with EC_{50}s of 49.98 μM, 31.91 μM, and 33.84 μM, respectively.

In addition to the novel analogs demonstrating increased cytotoxicity when compared to the parental compound, they also caused dramatic arrest in prostate cancer cell proliferation when applied at 10 μM concentration to PC3, CFPAC, and PANC1 cells, as determined by cell counts over 6 consecutive days (**Figure 20A-C**). In contrast to the parental compound, which only slowed cell proliferation, the novel analogs markedly inhibited cancer cell proliferation, with kb-NB142-70 being most potent among these compounds.
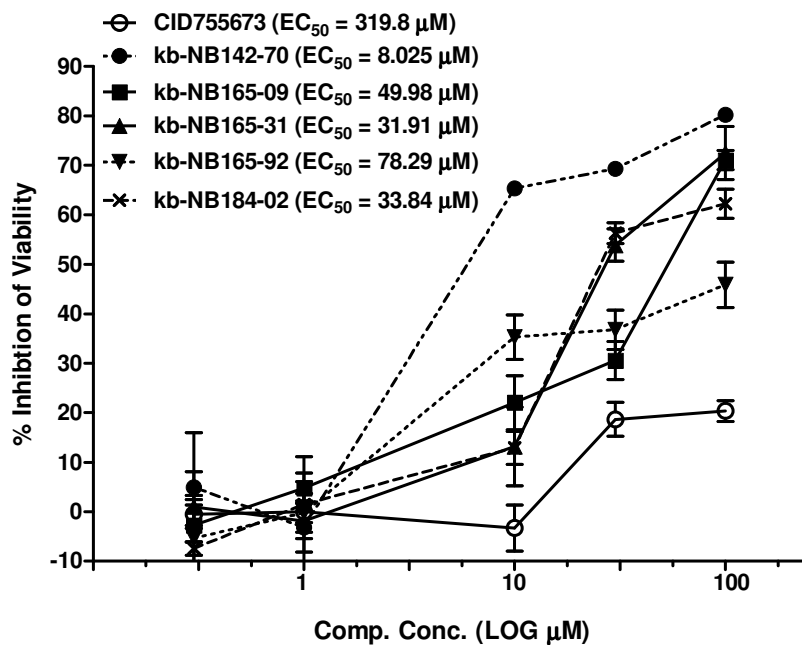
Figure 19. Cytotoxic effects of the CID755673 analogs in PC3 cells. PC3 cells were seeded into 96-well plates (3000 cells/well) and were then incubated in media containing 0.3-100 μM inhibitors for 72 h. MTT solution was added to each well and incubated for 4 h. Optical density was read at 570 nm to determine cell viability. The EC_{50} was determined as the mean ± S.E.M. of 3 independent experiments for each compound.
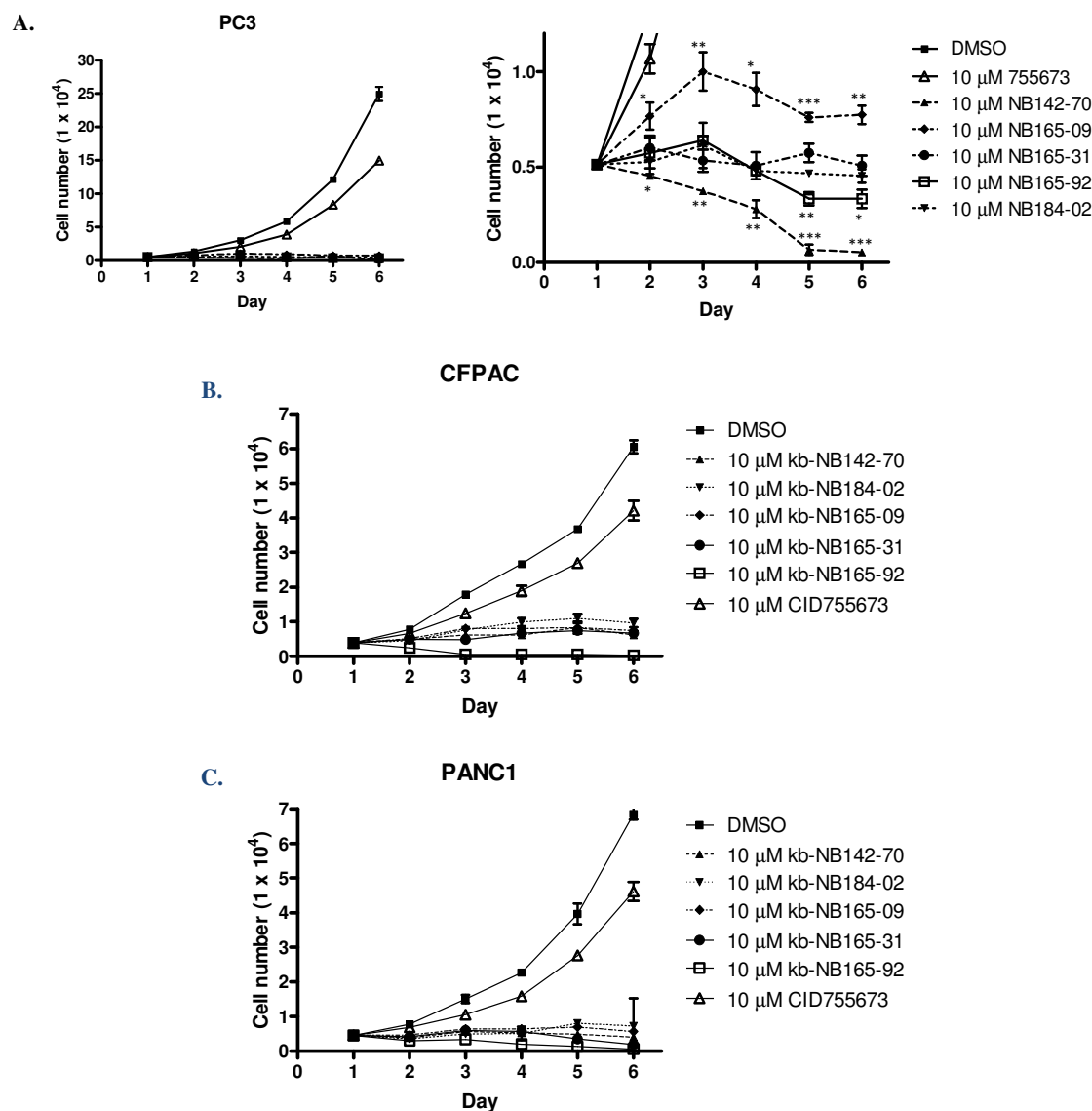
Figure 20. Effects of the CID755673 analogs on cancer cell proliferation. The analogs caused potent arrest in cancer cell proliferation. PC3 (A), CFPAC (B), or PANC1 (C) cells were plated in triplicate in 24-well plates. The next day, cells were counted and the indicated compound was added. Cells were counted daily for a total of 6 days. Media and inhibitor were refreshed every 2 days. The mean cell number ± S.E. was plotted over time. The experiment was repeated twice and a representative graph is shown. Statistical significance versus Day 1 cell count was determined by unpaired t-test for PC3 cells and is indicated. The right panel in (A) is an enlargement of the lower portion of the left panel in (A). *, $p < 0.05$; **, $p < 0.01$; ***, $p < 0.001$.

To gain insight into the mechanism of growth inhibition caused by the analogs, we conducted cell cycle analysis in PC3 cells. Our previous data indicated the parental compound CID755673 caused G_2/M phase cell cycle arrest when applied at 10 or 25 μM for 6 days (Sharlow et al. 2008). In the present study, PC3 cells were treated with 10 μM compound for 48 h and cell cycle distribution was analyzed by flow cytometry after propidium iodide labeling of fixed cells. Indeed, the compounds showed increased accumulation in the G_2/M phase of the cell cycle when compared to the DMSO treated control or to CID755673 (note that in this experiment, 48 h incubation of CID755673 was too short to induce G_2/M arrest) (**Figure 21**). Taken together, our data indicate that the novel analogs of CID755673 are efficacious inhibitors of survival and proliferation in prostate cancer cells.
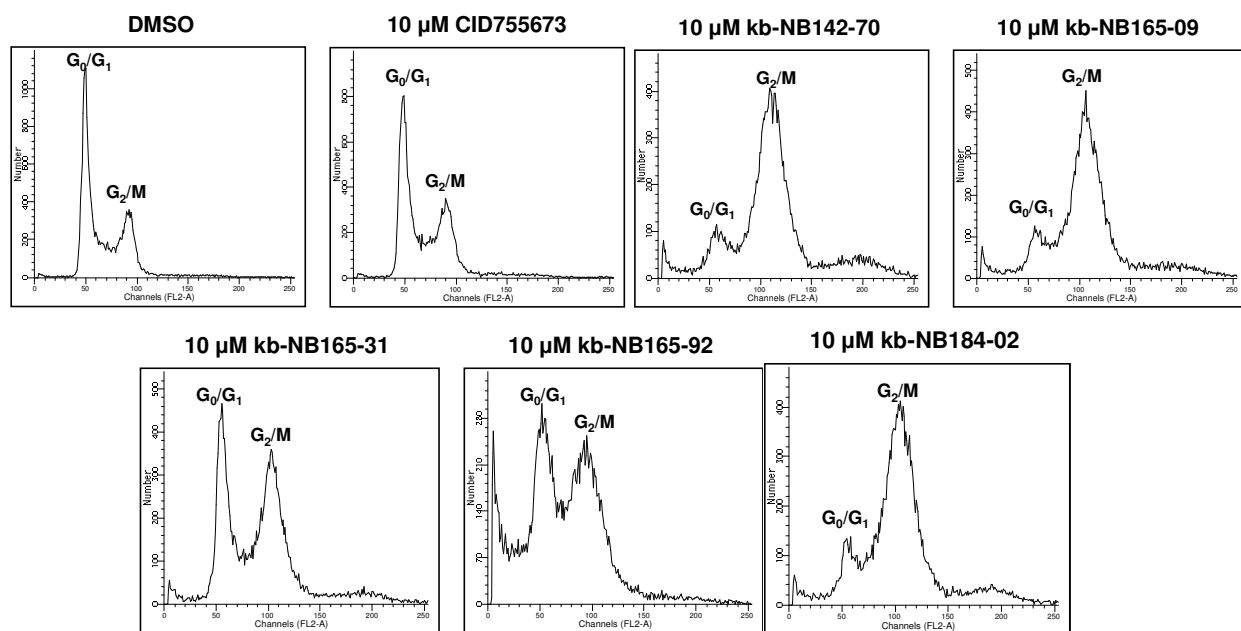
Figure 21. The analogs cause G_2/M phase cell cycle arrest in prostate cancer cells. PC3 cells were treated with either vehicle (DMSO) or 10 μM concentration of indicated compound for 48 h. Cell cycle distribution was determined by flow cytometry after propidium iodide labeling of fixed cells. G_0/G_1 and G_2/M phases are labeled. The experiment was repeated 3 times, and a representative is shown for each compound.

3.2.2.6 CID755673 and its analogs cause accumulation of cyclin D1 and cyclin D3

Though our evidence supports that CID755673 and its analogs induce cell cycle arrest at G_2/M phase, a recent study by Torres-Marquez *et al.* demonstrated that CID755673 treatment enhanced phorbol ester- and growth factor-induced DNA synthesis and G_1/S cell cycle progression in Swiss 3T3 cells independent of PKD1 (Torres-Marquez et al. 2010). In this study, it is important to note that both DNA synthesis and cell cycle distribution were determined after 40 h CID755673 treatment, while in our previous study cell proliferation was measured by counting cell numbers for 6 consecutive days of CID755673 treatment (Sharlow et al. 2008). Although it was clear based on counting cell numbers that CID755673 inhibited cell proliferation and ultimately caused G_2/M arrest, our study did not rule out the possibility that this compound could affect other stages of cell cycle progression. To investigate this possibility and to determine if CID755673 indeed affects the G_1/S transition, we measured the levels of cell cycle markers in response to treatment with CID755673 and its analogs. As shown in **Figure 22A**, CID755673 induced cyclin D1 and D3 expression in a concentration-dependent manner in PC3 cells, suggesting a role for CID755673 in promoting the G_1/S transition. Importantly however, the analogs of CID755673, with the exception of kb-NB165-09, showed much reduced effects on levels of cyclin D1 or D3, implying the specificity of these compounds was improved (**Figure 22B**). These data support the idea that CID755673 and its analogs have a complex effect on cell cycle progression: in addition to the induction of G_2/M arrest and subsequent inhibition of cell proliferation, these compounds may also promote the G_1/S transition.

A.

CID755673

Conc. (µM):   0   1   5   10   50

cyclin D1

cyclin D3

GAPDH

PC3

B.

DMSO · CID755673 · kb-NB142-70 · kb-NB165-09 · kb-NB165-92 · kb-NB184-02

cyclin D1

cyclin D3

GAPDH

PC3
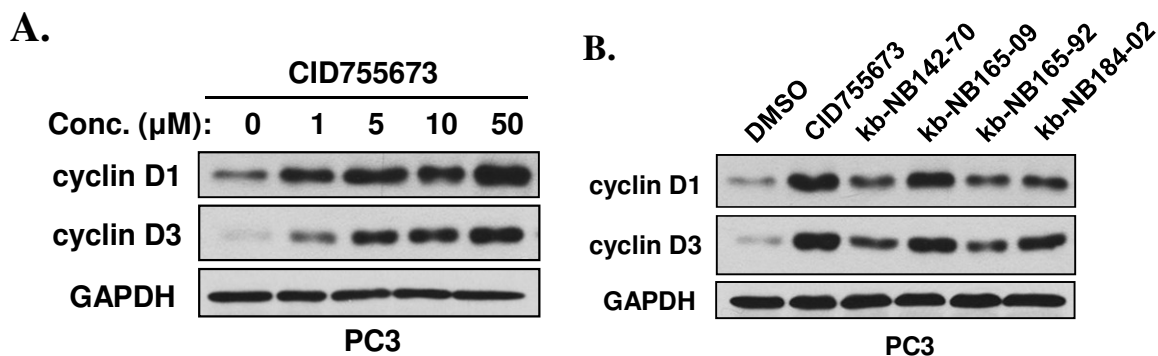
Figure 22. CID755673 and its analogs cause accumulation of cyclin D1 and cyclin D3. A, PC3 cells were treated with increasing concentrations of CID755673 for 48 h. Inhibitor and growth media were refreshed after 24 h. Western blots for cyclin D1 and cyclin D3 are shown. **B**, PC3 cells were treated with 25 µM CID755673, 10 µM kb-NB142-70, 10 µM kb-NB165-09, 1 µM kb-NB165-92, or 10 µM kb-NB184-02 for 48 h. Note that 1 µM kb-NB165-92 was used in this assay since this compound at 10 µM caused significant cell death. Inhibitors and growth media were refreshed after 24 h. Western blots for cyclin D1 and D3 are shown. GAPDH was used as a loading control.

3.2.2.7 Effects of the CID755673 analogs on tumor cell migration and invasion

Previous reports have indicated that PKD may have important roles in the regulation of cell motility, adhesion, and invasion (Bowden et al. 1999; Jaggi et al. 2005; Prigozhina and Waterman-Storer 2004). Additionally, we previously demonstrated that the PKD inhibitor CID755673 slowed cell migration and invasion in prostate and pancreatic cancer cells (Sharlow et al. 2008). In order to assess whether the novel analogs of CID755673 retained the ability to slow cancer cell migration and invasion, we performed 2 assays. First, we evaluated the effects of the compounds on migration in DU145, PC3, and PANC1 cells by wound healing assay. Confluent cells were wounded and then treated with either 5 µM or 25 µM inhibitor. Wound closure was inhibited in a concentration-dependent manner in all cell lines (**Figure 23A-D**). In this assay, treatment with kb-NB142-70 and kb-NB165-09 resulted in the most dramatic reduction in wound healing, with wounds showing only 25-35% closure when treated with 25

µM concentration of these two compounds in prostate cancer cells. The effect was a little less striking in pancreatic cancer cells, with wounds healing up to 50% when treated with kb-NB142-70 or kb-NB165-09. The compound kb-NB165-31 appeared to strongly resemble the efficacy of the parental compound, demonstrating 55-60% wound closure at 25 µM concentration in both PC3 and DU145 cells (**Figure 23A-B**).
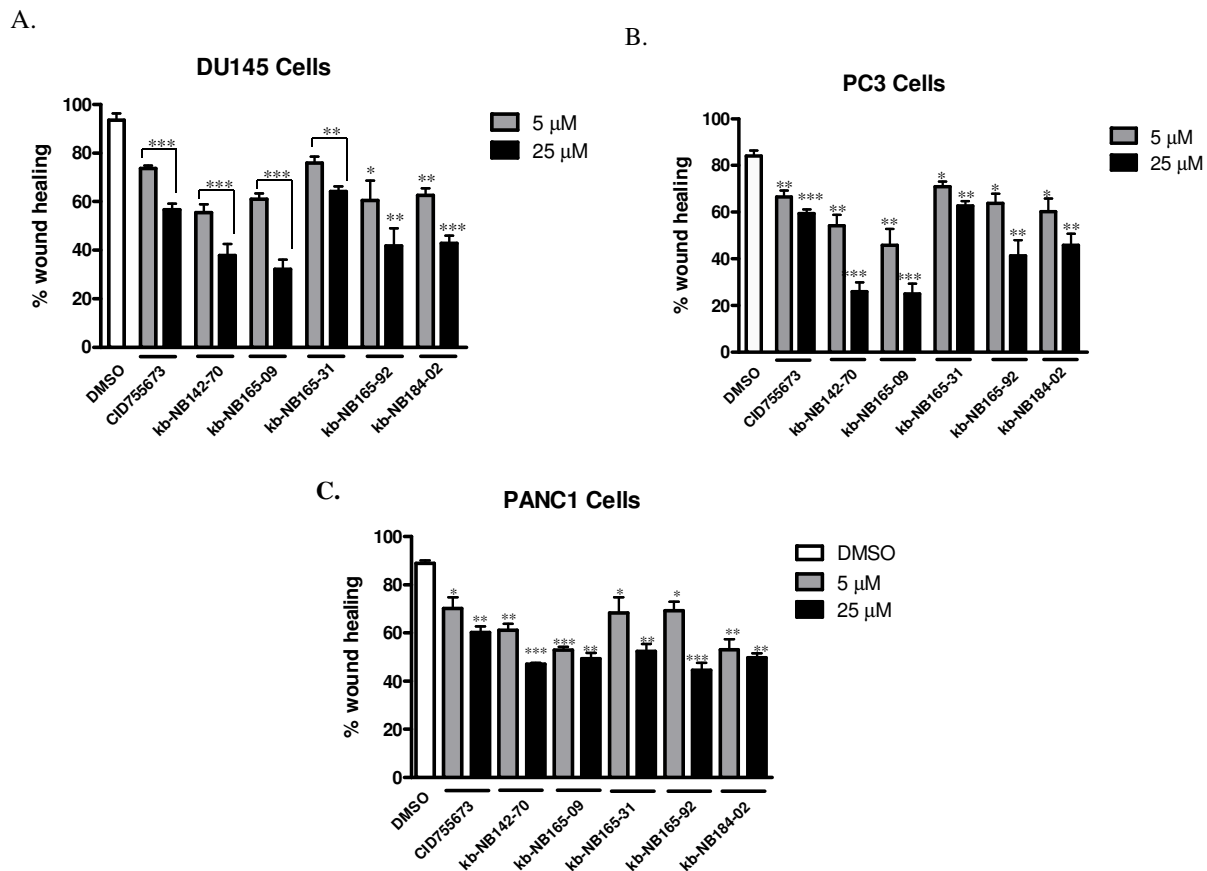
Figure 23. Effects of the CID755673 analogs on cancer cell migration. The analogs inhibited wound healing in prostate and pancreatic cancer cells. DU145 (A), PC3 (B), or PANC1 (C) cells were grown to confluence in 6-well plates. The monolayer was wounded and imaged immediately. Cells were then treated with either vehicle (DMSO) or analogs at indicated concentration for 24 h. Cells were then fixed and stained with 0.5% crystal violet. Percentage wound closure was calculated as described in "Materials and Methods." Data shown are the mean ± S.E.M. for 3 independent experiments. Statistical significance versus the DMSO control was determined by unpaired t-test in GraphPad Prism V. ns, not statistically significant; *, $p < 0.05$; **, $p < 0.01$; ***, $p < 0.001$.

The analogs also significantly inhibited tumor cell invasion measured by Matrigel invasion assay (**Figure 24A-B**). Consistent with our previously reported results, 10 μM CID755673 significantly inhibited invasion of DU145 cells. Invasion was also inhibited by kb-NB165-31, kb-NB165-92, and kb-NB184-02 at levels similar to the parental compound in DU145 cells. However, kb-NB142-70 and kb-NB165-09 showed increased activity in this assay, reducing percent invasion to only 10% in DU145 cells. The lead compound kb-NB142-70 reduced invasion to 20% in CFPAC cells. Taken together, these results support the conclusion that the novel analogs of CID755673 significantly inhibit prostate and pancreatic cancer cell migration and invasion.
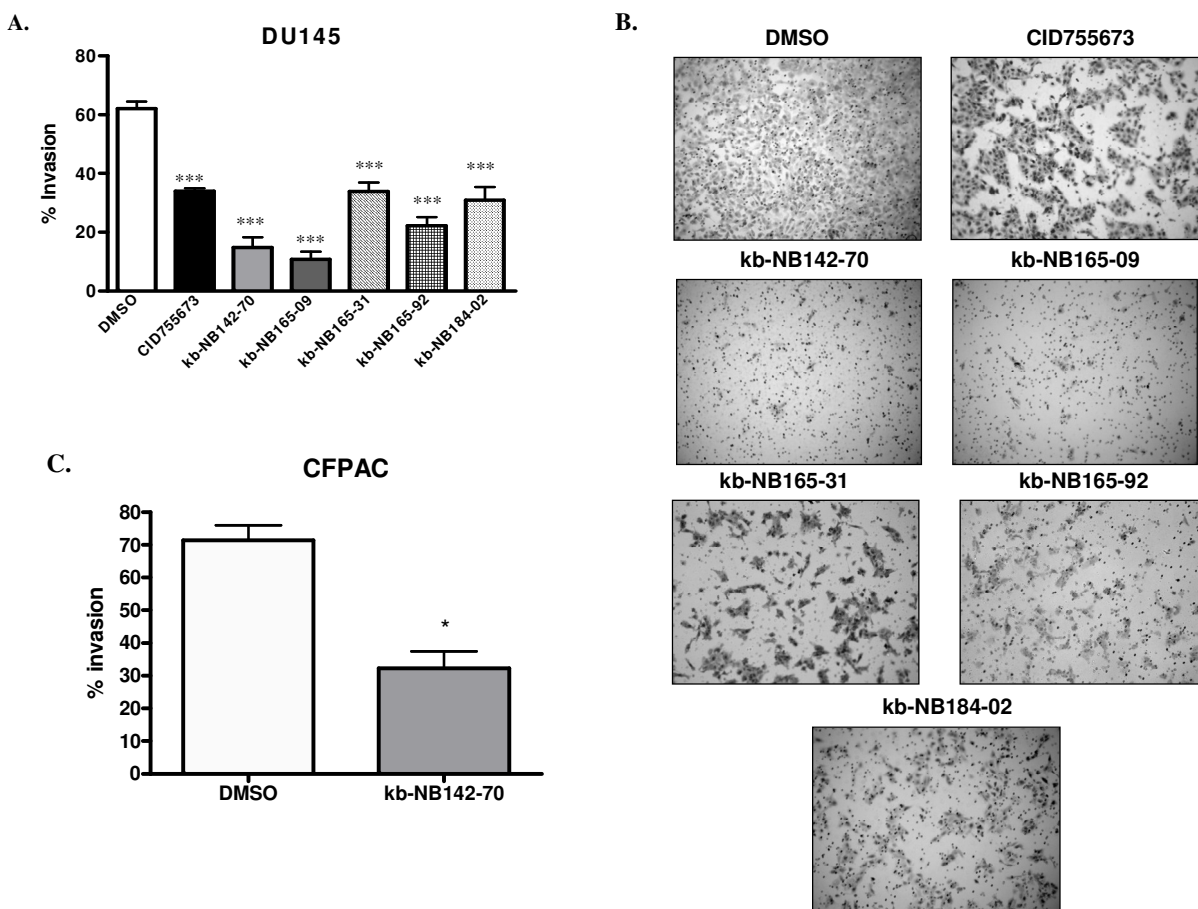
Figure 24. Analogs of CID755673 inhibit cancer cell invasion. A, The analogs inhibited invasion in DU145 cells. 0.08×10^6 DU145 cells in RPMI 1640 media containing 0.1% FBS and 10 μM of indicated compound were seeded into Matrigel inserts. After 22 h, noninvasive cells were removed and invasive cells were fixed in 100% methanol, stained in 0.5% crystal violet solution, and photographed. The number of cells that invaded the Matrigel matrix was determined by cell counts in at least 5 fields relative to the number of cells that migrated through the control insert. The data shown is the mean ± S.E.M. of 3 insert samples from 2 independent experiments (n = 6 per sample). Statistical significance versus the control DMSO was determined by unpaired t-test. ***, $p < 0.001$. B, Representative images comparing invasion of the vehicle (DMSO) and the compounds. C, The lead compound kb-NB142-70 inhibited invasion in CFPAC pancreatic cancer cells. The invasion assay was performed as above using 10 μM kb-NB142-70. The data shown is the mean ± S.E.M. of 3 insert samples from 2 independent experiments (n = 6 per sample).

3.2.2.8 A CID755673-derived photoaffinity-labeling compound inhibits PKD *in vitro* and in cells

To assist in elucidating the mechanism of action of CID755673 and its analogs, a series of photoaffinity-labeling compounds derived from a CID755673-based scaffold were synthesized in the laboratory of Dr. Peter Wipf (see Appendix A, Table 6, Entries 1–4). This series of analogs included modifications that would, in theory, allow for irreversible binding of the compound to PKD, facilitating subsequent determination of the binding site and providing insight into the mechanism through which these compounds inhibit PKD. We analyzed the *in vitro* activity of these compounds by radiometric kinase assay. Notably, the azide analog MCF292-08 retained high inhibitory activity toward PKD1 (IC_{50} = 74.9 nM, **Figure 25A-B**). Cellular activity was also comparable to the novel analogs, with a cellular IC_{50} of 2.2 µM toward inhibition of PMA-induced Ser[916]-PKD1 autophosphorylation in LNCaP cells (data not shown). Furthermore, initial investigations suggested that exposure to UV light resulted in irreversible binding of MCF292-08 to PKD1 *in vitro*, and enhanced inhibitory activity in cells (data not shown). Based on these encouraging results, ongoing studies that utilize this novel compound to elucidate the mechanism of PKD inhibition by this class of compounds are currently being conducted.

A.

MCF292-08

B.

MCF 292-08

$IC_{50}= 0.08 \pm 0.01 \ \mu M$
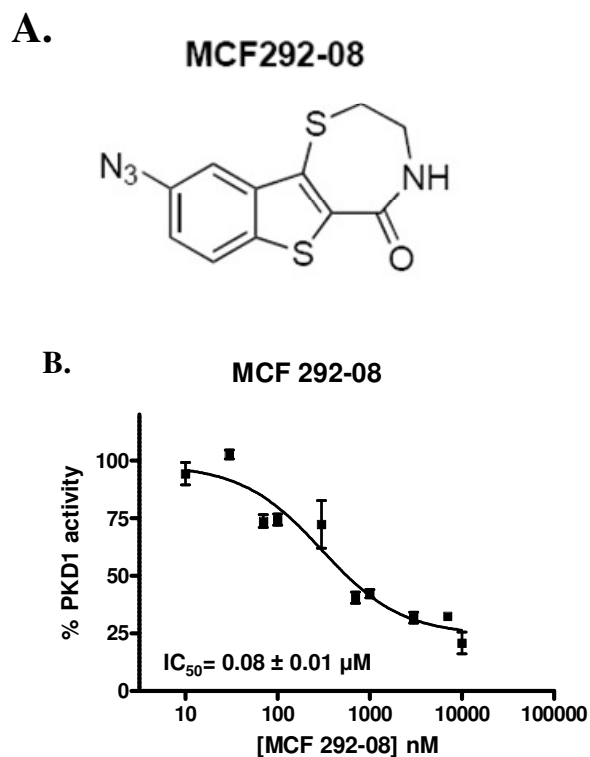
Figure 25. The photoaffinity-labeling compound MCF292-08 inhibits PKD1 *in vitro*. A, chemical structure of MCF292-08. B, PKD kinase activity was assayed by a radiometric kinase assay in the presence of increasing concentrations of MCF292-08. A 10-point concentration curve was generated for IC_{50} determination. The IC_{50} was determined by taking the mean ± S.E.M. of 5 independent experiments with triplicate determinations at each concentration in each experiment. A representative graph is shown.

3.3   DISCUSSION

In 2008, we reported the identification and characterization of CID755673, a benzoxoloazepinolone that inhibited all 3 isoforms of PKD with an IC_{50} of around 200 nM (**Figure 4**) (Sharlow et al. 2008). This significant discovery of the first potent, specific PKD inhibitor paved the way for the surge of additional novel PKD inhibitors which hit the literature

in the 2-3 years following our publication of CID755673 (Harikumar et al. 2010; LaValle et al. 2010a; Monovich et al. 2009; Raynham et al. 2008; Singh et al. 2009).

Our subsequent studies detailed the characteristics of PKD inhibition that CID755673 and its analogs demonstrated. CID755673 indeed showed some specificity toward PKD over several related kinases, and it did not inhibit the *in vitro* activity of PKCα, PKCβ, PKCδ, or CaMKIIα. Unlike the majority of commonly-used kinase inhibitors, CID755673 appeared to have a unique mechanism of action, inhibiting PKD1 in a non-ATP- and non-substrate-competitive fashion. Importantly, CID755673 retained cellular activity, albeit with a lower potency, inhibiting PKD1 autophosphorylation with an apparent IC_{50} of around 10 µM. Cellular studies also revealed that CID755673 reduced cell proliferation, migration, and invasion in prostate ans pancreatic cancer cells, highlighting the potential significance of the novel chemical structure in future drug development.

As mentioned, the evolving literature has revealed the discovery of several additional novel PKD inhibitors in recent years (Harikumar et al. 2010; LaValle et al. 2010a; Monovich et al. 2009; Raynham et al. 2008; Singh et al. 2009). In addition to CID755673 and its analogs, an interesting bipyridyl, BPKDi (2'-(cyclohexylamino)-6-(piperazin-1-yl)-[2,4'-bipyridine]-4-carboxamide), was recently identified as a very potent inhibitor of PKD1, -2, and -3 (IC_{50} of 1-9 nM) in a >650,000 compound high-throughput screen (**Figure 26**) (Monovich et al. 2009). BPKDi had very little or no activity toward CaMKIδ, CaMKIIα, CaMKIIβ, CaMKIIδ, CaMKIV, MARK1, MARK2, SIK1, GRK5, PKCδ, or PKCε. The compound caused substantial inhibition of PKD1 autophosphorylation at 1 µM concentration. Furthermore, treatment of cardiac myocytes with BPKDi resulted in reduced phosphorylation and increased nuclear retention of HDAC4 and HDAC5, validating these proteins as PKD substrates.
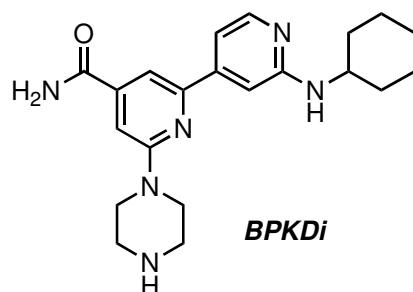
Figure 26. Chemical structure of BPKDi. This compound was discovered to be a potent and selective active site inhibitor of PKD.

Additional inhibitors emerging in the literature include a class of amino-ethyl-amino-aryl compounds **1**, **2**, and **3** (**Figure 27**) (Raynham et al. 2007). Compound **1** was shown to inhibit PDBu-stimulated PKD1 Ser^{916} phosphorylation in PANC-1 cells with an IC_{50} of 4 μM, while compounds **2** and **3** showed inhibition of PKD1 in the low and sub-nanomolar range, respectively. Additionally, compound **3** was reported to inhibit PKD2 with an IC_{50} of 4.1 nM. Furthermore, the pyrazine and pyridine benzamides **5** and **6** were reported to be inhibitors of PKD1 with low nanomolar IC_{50} values. Benzamides **4** and **6** were similarly potent, exhibiting IC_{50} values of 420 nM and 32 nM, respectively, against PKD1 (Raynham et al. 2008). Compounds containing the pyrimidinediamine scaffold, such as compound **7**, also demonstrated potent inhibition of PKD in the low nanomolar range (Singh et al. 2009). Another pan-PKD inhibitor, CRT0066101 (**Figure 27**, compound **8**), was reported very recently (Harikumar et al. 2010). CRT0066101 inhibits PKD1, PKD2, and PKD3 with *in vitro* IC_{50}s of 1, 2.5, and 2 nM, respectively, and has a cellular IC_{50} of 0.5 μM for PKD1 in intact PANC-1 cells. The structure of CRT0066101 appears to be derived from the core structure of compounds **1**, **2**, and **3** (**Figure 27**). The interesting scaffold **8** was reported to inhibit cell proliferation, induce apoptosis, and reduce viability of pancreatic cancer cells. Furthermore, treatment with CRT0066101 was shown

to affect levels of PKD biomarkers including phosphorylated Hsp27, activated NFκB, and expression of NFκB-regulated genes. The most attractive features of this inhibitor are that it is orally available and efficacious *in vivo*. CRT0066101 given orally at 80 mg/kg/d significantly suppressed the growth of subcutaneous (qd for 24 days) and orthotopic (qd for 21 days) pancreatic tumor xenografts in mice. This study provides strong support for targeting PKD in pancreatic cancer therapy (Harikumar et al. 2010), and the efficacy of this compound in other tumor types awaits further evaluation. Taken together, efforts at developing PKD-selective inhibitors have so far consistently demonstrated PKD as an effective target for cancer therapy.
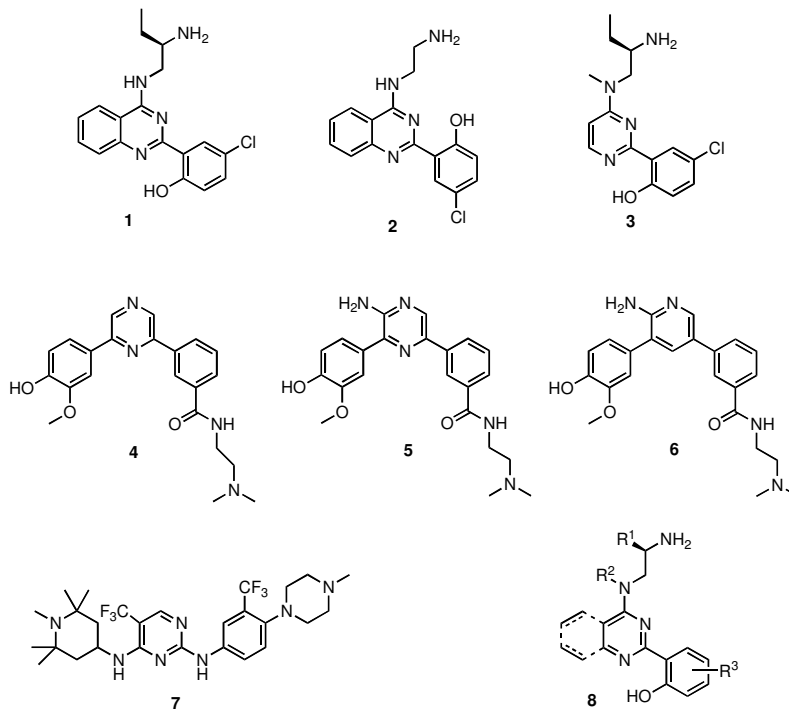
Figure 27. Recent active site PKD inhibitors reported in the literature.

It is important to note that both CID755673 and BPKDi were identified using PKD1 biochemical high throughput screens (Monovich et al. 2009; Sharlow et al. 2008) and display inhibitory activity against all 3 PKD isoforms. The individual screening strategies (*i.e.*, PKD

isoform and substrate pairing) used to identify these small molecule inhibitors may have directly impacted the specificity (or lack thereof) of the identified chemotypes. A more advantageous strategy may focus on a particular PKD-isoform paired with its isoform-specific substrate. As our understanding of the roles of each PKD isoform expands, and with the emergence of isoform-specific substrates, this strategy may prove to be more advantageous.

The novel analogs of CID755673, synthesized to have modifications in both the core structure and side chains, showed equal or increased potency to PKD1 inhibition *in vitro* and in cells when compared with CID755673. Additionally, we confirmed they also inhibited PKD2 and PKD3 *in vitro*, acting as pan-PKD inhibitors like the parental compound. Of the compounds reported here, the most potent was kb-NB142-70, which inhibited PKD1 with nearly a 7-fold greater potency compared to the parental compound. Furthermore, kb-NB142-70 inhibited PKD2 and PKD3 with about 4-fold increased potency than CID755673. The analogs also demonstrated increased inhibition of PMA-induced autophosphorylation of endogenous PKD1 in LNCaP prostate cancer cells when compared to the parental compound. In fact, the new lead compound, kb-NB142-70, was found to inhibit PKD1 with an IC_{50} of 28 nM *in vitro* and shows significantly increased cellular activity, inhibiting PKD1 autophosphorylation at Ser^{916} with an IC_{50} of around 2 µM in LNCaP cells. Thus, we have established that these small molecule analogs of CID755673 are also potent inhibitors of PKD both *in vitro* and in cells.

CID755673 is superior in specificity when compared with other compounds known to inhibit PKD, such as staurosporine and staurosporine-related the compounds K252a and Gö6976, even though these compounds have been reported to inhibit PKD in the low double- and single-digit nanomolar range (IC_{50}s of 40 nM, 7 nM, and 20 nM, respectively). This specificity may stem from the unique mechanism of action of CID755673 (**Table 2**). Though the exact

mechanism through which CID755673 and its analogs inhibit PKD has not yet been elucidated, we have shown that CID755673 is both non-ATP- and non-substrate-competitive. Ongoing studies utilitzing the novel photoaffinity-labeling compound MCF292-08 may provide significant insight into the mechanism of action of this class of compounds, including elucidation of the inhibitor binding site.

A kinase profiling report demonstrated that CID755673 may also target a few additional kinases, including GSK3β, CK1δ, MK5, MK2, ERK1, and CDK2. Importantly however, CID755673 lacks or shows only marginal activity towards almost all PKC isoforms that have been tested thus far (including PKC-α, -β, -γ, -δ, -η, -θ and -ζ), which distinguishes it from commonly used PKC/PKD inhibitors such as Gö6976. This feature may allow selective targeting of PKD-mediated signaling pathways and cellular processes, though discretion must be used since additional targets of CID755673 do indeed exist. Furthermore, when making conclusions as to the functional role of PKD in such cellular processes as proliferation, growth, and motility as presented here, it is important to confirm the results of inhibitor studies using specific PKD-targeting siRNA or shRNA. In previous studies published in our laboratory and in Chapter 4 of this dissertation, we demonstrated that transient PKD3 knockdown using specific PKD3-targeting siRNA and stable, inducible knockdown using specific shRNA vectors caused arrest in PC3 cell proliferation (Chen et al. 2008). Additionally, in Chapter 4 of this dissertation, we provide evidence that knockdown of PKD2 and PKD3 using siRNA or shRNA reduces migration and invasion, similar to the observed effects of our novel PKD inhibitors. Thus, we can conclude that the effects of our novel pan-PKD inhibitors on prostate cancer cell proliferation, migration, and invasion are at least in part due to inhibition of PKD.

Similar to the parental compound, the novel analogs for the most part retained specificity when tested against PKCα, -βI, -δ, and CAMKIIα. One compound, kb-NB165-31, did show significant inhibitory activity toward PKCδ and CAMKIIα when tested at 10 μM concentration. This compound has an iodine atom added as a side chain of the benzene ring in kb-NB142-70, which retained strong selectivity to PKD *in vitro*, suggesting that the increase in lipophilicity and the introduction of a polarizable group at the phenol *ortho*-position reduce compound specificity. Interestingly, in the case of kb-NB165-92, the expansion of the lactam by one carbon to a fused 8-membered ring reduced the potencies for PKD1 and PKD2 by 2-4 fold, while not altering potency for PKD3, implying that zone III of our pharmacophore may contain determinants for isoform-selectivity. However, this concept should be further exploited as methoxy analogs of kb-NB142-70 and kb-NB165-92, in contrast, did not exhibit an analogous shift in isoform-selectivity.

Cellular activity of the analogs was demonstrated through inhibition of PMA-induced activation of endogenous PKD1 by measuring the phosphorylation levels of Ser[916] and Ser[742]. Based on the canonical pathway of PKC-dependent PKD activation, phorbol ester-stimulated phosphorylation on Ser[738/742] by PKC followed by autophosphorylation of PKD1 on Ser[916] would result in full activation of PKD (Matthews et al. 1999; Waldron et al. 1999; Waldron et al. 2001; Zugaza et al. 1996). However, studies have also suggested that Ser[742] may be a site of both trans- and autophosphorylation. While initial, early catalytic activation of PKD requires rapid transphosphorylation on Ser[738/742] by PKC isoenzymes, and can be blocked by the PKC inhibitors Gö6983 and GF 109203X, the major mechanism required to maintain prolonged PKD activation is PKC-independent and relies on autophosphorylation at Ser[742] (Jacamo et al. 2008). Therefore, since *in vitro* studies failed to show inhibition of any PKC isoform tested, we can

conclude that the observed dose-dependent inhibition of Ser[742] phosphorylation on PKD1 after agonist stimulation (100 nM PMA for 20 min) by our novel PKD inhibitors likely reflects the inhibition of PKD1 autophosphorylation at this site, analogous to the inhibition of Ser[916] phosphorylation. Further analysis is required to determine the precise mechanism of inhibition of PKD by these novel compounds and to investigate the kinetics of PMA-induced Ser[916] and Ser[742] phosphorylation of PKD1 in the presence of these inhibitors, which may further establish Ser[742] as an additional autophosphorylation site and confirm the specificity of these inhibitors to PKD.

PKD has been implicated in the regulation of cell proliferation, survival, and apoptotic pathways in multiple cell types (Chen et al. 2008; Storz 2007; Trauzold et al. 2003). We have previously shown that PC3 cells predominantly express high levels of PKD3, potentially making them very sensitive to PKD3 inhibition, and that knockdown of PKD3 by siRNA causes strong arrest in cell proliferation in these cells (Chen et al. 2008). Here, we have shown that one of the more striking differences between the parental compound and its analogs is the increase in cytotoxicity and dramatic arrest in cell proliferation. While CID755673 is only minimally cytotoxic to prostate cancer cells, and can be tolerated at high concentrations for prolonged treatments (Sharlow et al. 2008), the novel analogs induced significant cytotoxicity in PC3 cells after much shorter treatments (48 h) and at much lower concentrations (5-10 μM). Based on our preliminary analysis, the effects of the compounds on viability in other prostate cancer cells (LNCaP and DU145) are comparable to those in PC3 cells (data not shown). The inhibitors appear to exhibit a general inhibitory effect on cell viability, with efficacy varying between different tumor cell types. Additionally, the analogs cause much more dramatic arrest in cell proliferation than the parental compound. This improvement in the antiproliferative effects of the analogs was accompanied by lowered IC_{50}s for PKD1 inhibition in LNCaP cells (2.2 μM for the

new lead compound, kb-NB-142-70, versus ~10-30 µM for the parental compound, CID755673).

Moreover, since the antiproliferative effects of the analogs phenocopied those caused by knockdown of PKD3 in PC3 cells (Chen et al. 2008), it is conceivable that these effects, at least to some extent, are mediated through inhibition of PKD. That said, we cannot exclude the possibility that CID755673 and its analogs have additional cellular targets whose inhibition may contribute to the elevated cytotoxicity and potent growth arrest observed in prostate cancer cells. Furthermore, since the analogs, mimicking the parental compound, all induced apparent G_2/M cell cycle arrest, it is likely that the mechanisms underlying the growth inhibition caused by the analogs are similar to those induced by the parental compound.

Although CID755673 and its analogs potently inhibited cell proliferation, their effects on cell cycle progression appeared to complex, involving two opposing effects on different stages of the cell cycle: 1) promotion of the G_1/S transition; 2) induction of G_2/M arrest. The G_2/M arrest ultimately leads to cessation of cell proliferation. However, the complexity of these effects is still not understood. In a recent study, CID755673 was found to enhance PDBu- and growth factor-stimulated DNA synthesis and G_1/S cell cycle transition independent of PKD1 in Swiss 3T3 cells (Torres-Marquez et al. 2010). Given that this report by Torres-Marquez *et al.* used DNA synthesis and cell cycle distribution as readouts, it remains to be determined if the potentiation effect reported indeed resulted in increased cell number (cell proliferation) in their assays since the G_2/M block may ultimately inhibit this effect. With regard to the potential targets that may account for this effect, we hypothesize, based on our kinase profiling data, that GSK-3β could play a role since active GSK-3β has a negative effect on cell cycle progression (Takahashi-Yanaga and Sasaguri 2008). Expression of the cell cycle proteins cyclin D1 and cyclin D3 is regulated by GSK-3β signaling at the transcriptional level and through protein degradation (De

Santa et al. 2007; Naderi et al. 2004; Takahashi-Yanaga and Sasaguri 2008). Thus, inhibition of GSK-3β may be in part responsible for the promotion of the G_1/S transition and the reported potentiation effect with other mitogens and may also explain our observed concentration-dependent increase in cyclin D1 and cyclin D3 levels with CID755673 treatment in prostate cancer cells (**Figure 22**) (LaValle et al. 2010a; Torres-Marquez et al. 2010). Additionally, since the analogs in general do not cause significant induction of cyclins D1 and D3 compared to the parental compound (**Figure 23**), they may not have mitogenic effects like CID755673 (Torres-Marquez et al. 2010), in part explaining the significantly increased effects of these novel analogs on arrest of cell proliferation. It is clear, however, that despite these unintended effects in our experimental system, the ultimate cell fate, i.e. cell growth arrest and subsequent cell death, was not altered.

Clearly, these new findings suggest that this class of compounds may target additional proteins, resulting in complex effects on cell cycle progression. Based on this kinase profiling data, we speculate that, in addition to PKD, the inhibitory effect of CID755673 and its analogs on cell proliferation may be contributed to the inhibition of CDK2, another potential target of CID755673. Although CDK2 is generally considered a regulator of S-phase entry (Bashir and Pagano 2005; Hu et al. 2001), some reports have also linked it to the G_2/M transition (Hu et al. 2001; Wang et al. 1997). According to the accepted model of cell cycle progression, CDK2 is activated by binding to cyclin E in late G_1 phase, resulting in phosphorylation of the retinoblastoma protein (Rb) and facilitating the G_1/S-phase transition (Satyanarayana and Kaldis 2009). It also promotes progression of S-phase by binding to cyclin A. However, it has been reported that inhibition of CDK2 by expression of a dominant negative CDK2 mutant or overexpression of p27[kip1] can cause accumulation in G_2/M (Hu et al. 2001; Wang et al. 1997).

Therefore, it is plausible that the G_2/M arrest and reduced cell proliferation caused by CID755673 and its analogs is in part due to inhibition of CDK2. It is also possible that CID755673 and its analogs may inhibit other members of the CDK family, for example CDK1, which plays a critical role in G_2/M cell cycle progression.

In addition to CDK2, casein kinase 1 delta (CK1δ) was also identified as a potential target of CID755673. This kinase belongs to a family of serine/threonine kinases that regulate a variety of cellular processes, including cell cycle progression, Wnt singaling, and the DNA damage response, and has been implicated in the progression of pancreatic cancer (Brockschmidt et al. 2008; Knippschild et al. 2005; Price 2006). Studies have shown that inhibition of CK1δ and CK1ε using the selective inhibitor IC261 resulted in dramatic arrest in pancreatic cancer cell growth and was accompanied by G_2/M cell cycle arrest (Brockschmidt et al. 2008). However, subsequent investigations have shown that IC261 can induce cell cycle arrest via regulation of the mitotic spindle at much lower concentrations than those required to inhibit CK1δ, therefore contesting whether CK1δ is indeed involved in regulating G_2/M arrest (Cheong et al. 2011), and studies demonstrating specific effects of CK1δ knockdown on cell cycle arrest are still lacking (Brockschmidt et al. 2008; Cheong et al. 2011; Cheong and Virshup 2011).

Finally, it must be stated that although CKD2, CK1δ, and a few other proteins were identified as potential hits in a single dose kinase profiling experiment (**Table 5**), the activities of CID755673 and its analogs toward these targets need to be further validated in 10-point dose-response kinase assays, and, more encouragingly, the activity profile of new analogs of CID755673 shows reduced off-target effects to accompany the markedly increased efficacy in tumor cells (**Figure 22**) (LaValle et al. 2010a).

In addition to the effects of these analogs on cell survival and proliferation, we also show that they are significant inhibitors of cancer cell migration and invasion. The compounds kb-NB142-70 and kb-NB165-09 in particular, strongly reduced wound healing in DU145, PC3, and PANC1 cells in a dose-dependent manner, and significantly inhibited invasion of DU145 and CFPAC cells through Matrigel invasion inserts when applied at 10 μM concentration. Furthermore, the pattern of inhibition exhibited by the analogs is fairly consistent with their inhibitory activities toward PKD. This suggests an important role for PKD in prostate and pancreatic cancer cell motility and supports the potential value of therapeutic targeting of PKD in the reduction or prevention of tumor metastases. Though the mechanism through which PKD may mediate migration and invasion is not yet known, several recent reports have begun to shed light onto the complexity of these signaling pathways, suggesting PKD involvement in both β-catenin and Akt signaling in prostate cancer cells (Chen et al. 2008; Jaggi et al. 2003; Jaggi et al. 2005).

In conclusion, we report the biochemical and functional analysis of CID755673 and several of its analogs. These analogs show equal and increased potency toward PKD inhibition both *in vitro* and in cells. The new lead compounds display prominent cytotoxic and anti-proliferative effects, and potently inhibit migration and invasion in prostate and pancreatic cancer cells. Although the molecular mechanisms underlying some of the biological effects of these compounds appear to be complex and may involve additional targets, their potent effects on multiple cancer-associated biologies warrant further development of this series of compounds toward possible clinical application in cancer therapy.

4.0   ANALYSIS OF THE FUNCTIONAL ROLE OF PROTEIN KINASE D IN PROSTATE CANCER

4.1   INTRODUCTION

Prostate cancer is the second leading cause of cancer-related death in men in the United States and the number one cause of death in men over age 75 (Jemal et al. 2009). Tumors arise in the prostate gland, a walnut-sized structure that wraps around the urethra, and may grow slowly, remaining benign for many years, or may grow rapidly and metastasize, leading to serious complications and even death (Jadvar 2011). Advances in screening procedures have resulted in earlier diagnosis; however, the benefits of catching this disease in its early stages remains a controversial topic (Cook and Nelson 2010; Shirai 2008). In particular, the discovery of prostate-specific antigen (PSA) as a serum marker for the detection of prostate carcinoma, and the development of screening procedures to measure PSA levels, have significantly increased early diagnosis (Cook and Nelson 2010; Zaviacic 1997). Still, despite early interventions and chemopreventive measures, therapeutic options are limited once the prostate tumor has metastasized (Shirai 2008). A more complete understanding of the molecular mechanisms underlying prostate cancer progression is necessary to facilitate the development of novel therapies.

In relatively recent years, the PKD family of serine/threonine kinases has been the subject of a variety of studies focusing on prostate cancer progression (LaValle et al. 2010b). These studies date back as early as 2003, when Balaji and colleagues reported that PKD1 appeared to be down-regulated in androgen-independent prostate cancer (Jaggi et al. 2003). Additional evidence from this same research group began to emerge showing that PKD1 was involved in regulating prostate cancer cell growth and motility, acting primarily as a tumor-suppressor (Biswas et al. 2010; Du et al. 2009; Jaggi et al. 2005; Mak et al. 2008; Syed et al. 2008). In 2008, our laboratory began to investigate PKD function in the context of prostate cancer. We showed that levels of PKD3, the least-studied of the PKD isoforms, were elevated in human prostate tumor tissues (Chen et al. 2008). Increased nuclear localization of PKD3 was found to be correlated with tumor grade, suggesting hyperactivity of this isoform in advanced prostate cancer (Chen et al. 2008). Furthermore, in cellular studies, our lab reported that transient knockdown of PKD3 reduced prostate cancer cell growth, likely through an Akt-mediated signaling pathway (Chen et al. 2008). The differential expression and distinct functions of the PKD isoforms apparent from these studies emphasizes the complexity of cancer pathology and progression, and underlies the need to elucidate the specific signaling events and molecular mechanisms involved in these processes.

As a Golgi resident protein, PKD has been shown to be essential for membrane fission and vesicle formation in the transport of cargo from the *trans*-Golgi network (TGN) to the plasma membrane (Bossard et al. 2007; Liljedahl et al. 2001; Malhotra and Campelo 2011). Although the mechanisms through which PKD regulates protein trafficking have been well studied, little is known of the identity of transported cargo, and the relevance of this regulation to tumor development remains to be determined. PKD1, the subject of the majority of studies on

PKD function, has been implicated in the secretion of several tumor-promoting cytokines such as IL-6, IL-8, and GROα/CXCL-1 (Hao et al. 2009; Ochi et al. 2011; Steiner et al. 2010), and matrix metalloproteinases (MMPs), secreted endopeptidases that play a major role in the degradation of the extracellular matrix (Biswas et al. 2010; Eiseler et al. 2009a; Lokeshwar 1999). However, it remains to be determined 1) how PKD regulates these processes, 2) whether these regulatory mechanisms affect tumor growth, and 3) what the functions of the other PKD isoforms are in modulating these events.

In this report, we provide substantial evidence for a tumor-promoting role for PKD3 in prostate cancer progression. Our results demonstrate that PKD3 modulates proliferation and motility of prostate cancer cells. Furthermore, we demonstrate that PKD3 mediates the secretion of multiple factors that stimulate cancer progression in multiple prostate cancer cell lines. These data validate PKD3 as a novel therapeutic target in the treatment of prostate cancer, and broaden our current understanding of the molecular mechanisms of PKD function in cancer progression.

4.2   RESULTS

4.2.1   Development of a stable, tetracycline-inducible PKD3 knockdown prostate cancer cell line

We have previously demonstrated that PC3 cells express high levels of PKD3, moderate PKD2, and no detectable PKD1 (Chen et al. 2008). Additionally, PKD3 was found to be overexpressed in human prostate tumors, highlighting the potential contribution of this isoform to prostate

cancer progression (Chen et al. 2008). Therefore, to facilitate the further study of PKD3 function in prostate cancer, we developed a PC3 cell line stably expressing a tet-inducible shRNA targeting PKD3 (**Figure 28**). In this model, PC3 cells express the tet-repressor (TR). In its unstimulated state, the TR binds to the promoter region, called the tet-operon (TO), of the integrated plasmid DNA, repressing transcription of the shRNA. When tetracycline (tet) is applied to the cells, the tet binds to the TR, causing dissociation of the TR from the TO, and allowing expression of the shRNA. Four stable clones were isolated that showed downregulation of PKD3 upon 5-day treatment with 1 µg/mL tet: shPKD3-1 C7, shPKD3-1 C26, shPKD3-1 C2-1, and shPKD3-1 C2-3. A clone expressing non-targeting, scrambled shRNA (shScr) was also isolated. Western blotting analysis revealed 50-75% knockdown of PKD3 protein levels from the isolated shPKD3-1 clones after 5-day tet treatment (**Figure 29A**). PKD3 levels of the shScr clone were unaffected. PKD2 levels were also unchanged in the tet-treated cells for all clones, evidence that our shRNA targeted specifically the PKD3 isoform. For further confirmation of the knockdown, we performed RT-qPCR analysis. With this method, we observed 50% and 65% reduction in PKD3 transcript levels for clones shPKD3-1 C2-1 and shPKD3-1 C2-3, respectively (**Figure 29B**).
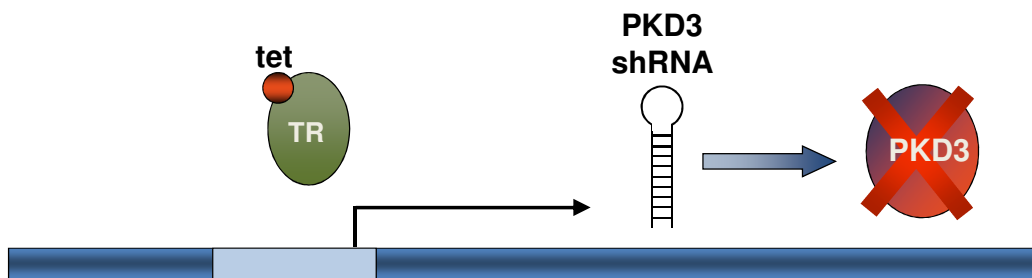
Figure 28. Model of tetracycline-inducible PKD3 knockdown. PC3 cells expressing the tet-repressor (TR) were transfected with the vector containing shRNA targeting PKD3 and stable cell lines were generated. Upon treatment with 1 µg/mL tetracycline, the PKD3 shRNA is expressed and PKD3 expression is reduced.

A.

B.
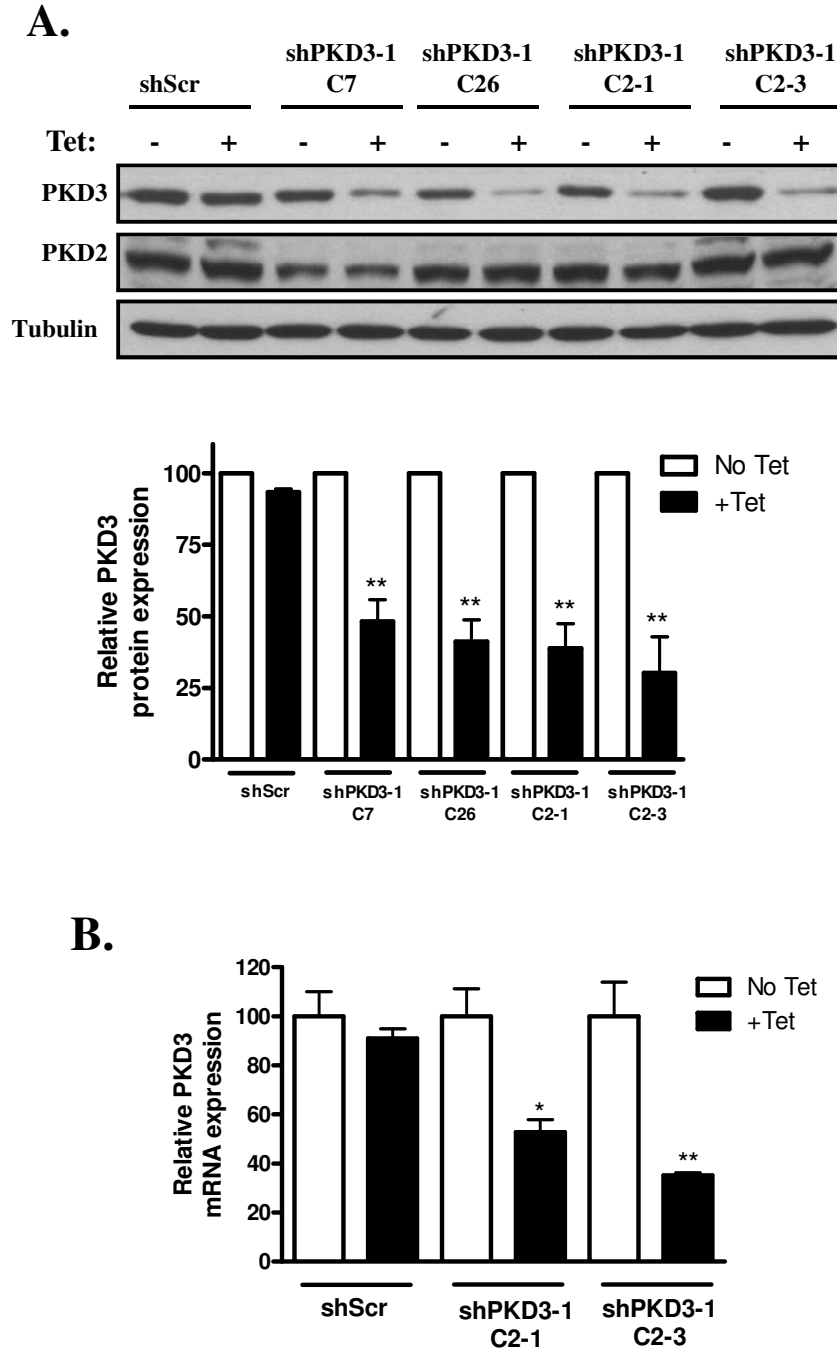
Figure 29. Tetracycline-induced knockdown of PKD3. PC3-TR cells were transfected with the pENTR/TO/H1 vector containing shRNA targeting PKD3, as described in "Materials and Methods." After stable selection, clones were treated with 1 µg/mL tet for up to 5 days. Cells were collected and PKD3 expression was analyzed by Western blotting (A) and RT-qPCR (B). Densitometry analysis of the Western blotting results is shown as the mean ± S.E.M. of 3 independent experiments. Statistical significance is indicated (*, $p < 0.05$; **, $p < 0.01$; ***, $p < 0.001$).

4.2.2. Tetracycline-induced knockdown of PKD3 reduces prostate cancer cell proliferation, migration, and invasion

Next, we wanted to determine the effects of PKD3 knockdown on several significant cancer-related phenotypes. We first investigated whether tet-induced knockdown of PKD3 caused a reduction in cell proliferation in this model system. After a 5-day pretreatment with 1 µg/mL tet, the number of viable cells was determined each day for 6 days.

As shown in **Figures 30A-F**, each of the 4 stable PKD3 knockdown clones showed a significant reduction in cell proliferation, whereas growth of both the parental PC3-TR cell line and the shScr clone were unaffected by tet treatment. This is consistent with our previous report that transient knockdown of PKD3 by siRNA causes a significant decrease in proliferation in PC3 cells (Chen et al. 2008).
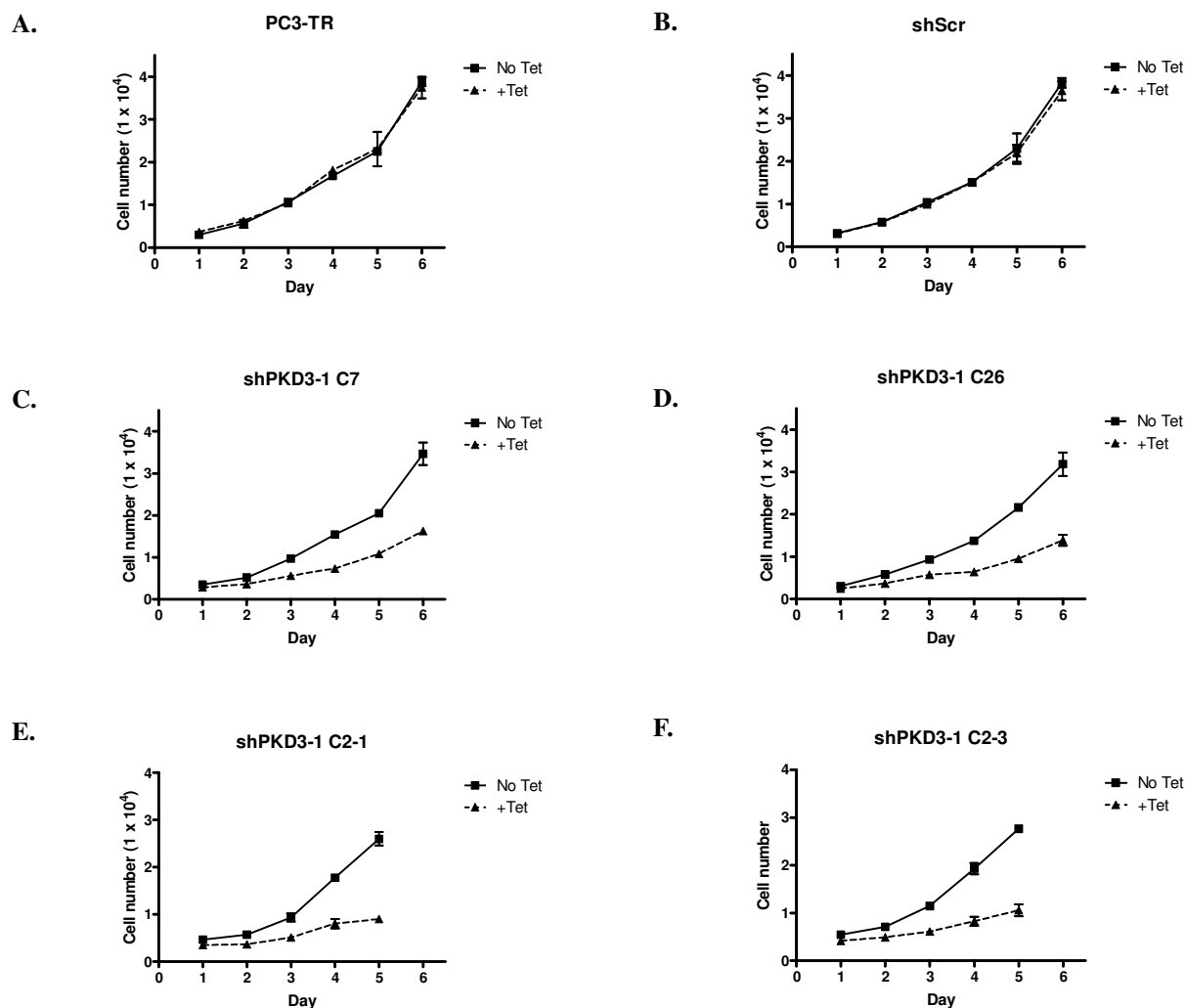
Figure 30. Tetracycline causes reduced proliferation in stable shPKD3-1 clones. PC3-TR (A), shScr (B), shPKD3-1 C7 (C), shPKD3-1 C26 (D), shPKD3-1 C2-1 (E), or shPKD3-1 C2-3 (F) cells were pre-treated with 1 µg/mL tet for 5 days then replated at 5000 cell/well in 24-well plates. Cell number was determined every day for up to 6 consecutive days. Media and tet were refreshed every 2 days. Experiments were repeated 3 times, and a representative graph is shown.

Cell motility is essential for the acquired ability of cancer cells to invade into surrounding tissue and form distant metastases, a key step in the progression of aggressive prostate cancer (Lee and Tenniswood 2004). To date, the role of PKD3 in prostate cancer cell motility has not been described. Therefore, we investigated whether tet-induced knockdown of PKD3 could alter cell migration and invasion. After a 5-day induction with 1 µg/mL tet, we performed a wound healing assay to measure cell migration using our stable clones and the shScr control. While the "wound" completely closed in both the parental PC3-TR cell line and the shScr cells, wound closure was reduced to only 45% and 35% in the PKD3 knockdown clones shPKD3-1 C7 and shPKD3-1 C26, respectively (**Figure 31A-B**). This result was further confirmed using transient knockdown of PKD2 and/or PKD3 by siRNA in PC3 cells, which resulted in nearly a 60% reduction in wound healing compared to the non-targeted siRNA control (**Figure 32A-B**). Interestingly, there did not appear to be an additive effect of the dual PKD2/PKD3 knockdown in this experiment, suggesting that these 2 isoforms may have non-redundant functions and may act on distinct pathways. However, it is also possible that a 60% decrease in wound healing is the maximum that can be achieved in this cell line under these conditions and any additive effects may not be able to be demonstrated.

A.

B.
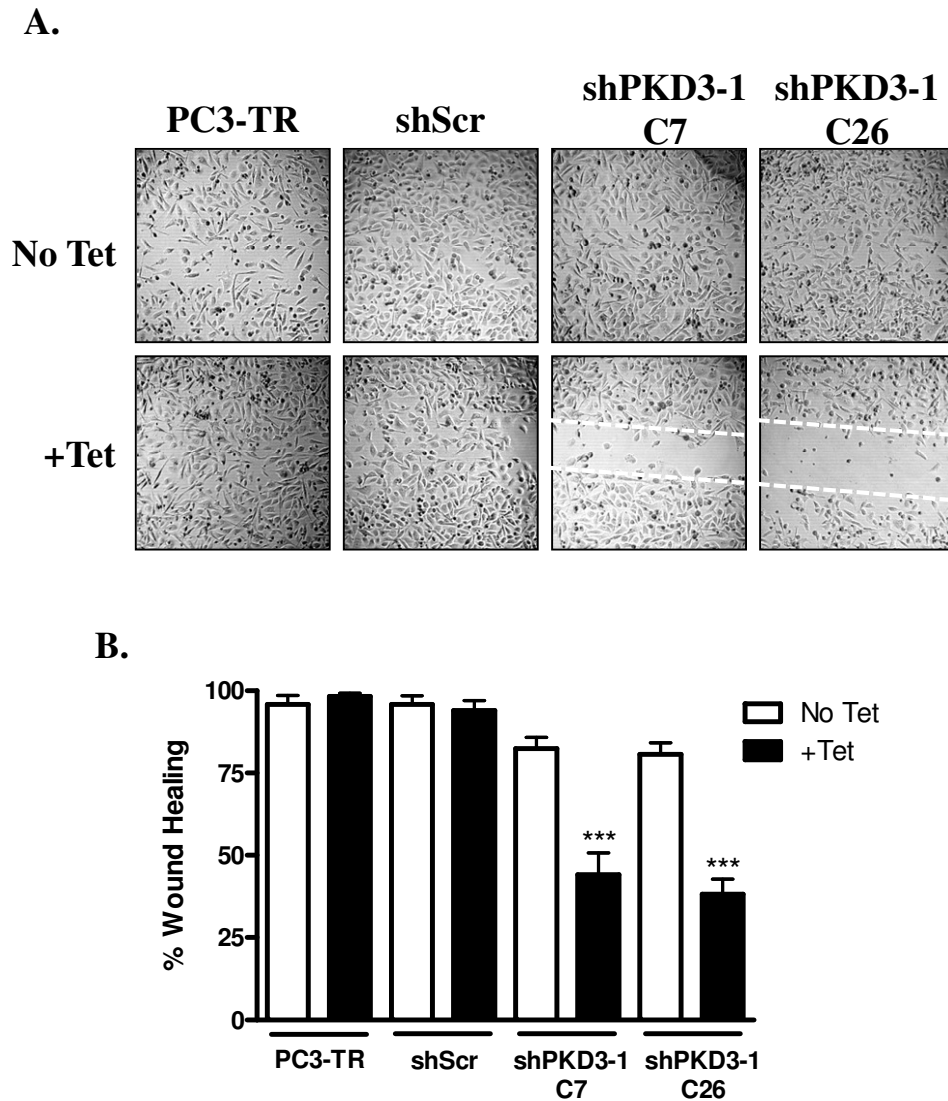
Figure 31. Inducible knockdown of PKD3 leads to reduced cell migration. PC3-TR, shScr, shPKD3-1 C7, or shPKD3-1 C26 cells were pre-treated with 1 µg/mL tet for 5 days, and then replated in 6-well plates. After growing to confluence, the monolayer was wounded using a 10 µL pipette tip, and an image was taken immediately. Twenty-four hours later, cells were fixed in methanol and stained with 0.5% crystal violet. A final image was taken (A), and the percent wound healing was calculated as described in the "Materials and Methods." The experiment was repeated 3 times. Data are the mean percent wound healing ± S.E.M. as determined from 3 separate measurements of the wound area from 3 independent experiments (B). Statistical significance is indicated (***, $p < 0.001$). Representative images are shown (A).

A.

B.

Figure 32. Transient knockdown of PKD2 and/or PKD3 reduces migration in PC3 cells. PC3 cells were transiently transfected with non-targeting siRNA (siNT) or siRNA targeting PKD2 (siPKD2), PKD3 (siPKD3), or both PKD2 and PKD3 (siPKD2+3). Two days later, cells were replated in 6-well plates and grown to confluence. Wound-induced migration was measured as described in the "Materials and Methods." Representative images at 0 h (top panels) or 18 h (bottom panels) are shown (A). The graph depicts the mean ± S.E.M. of 3 separate measurements of the wound area from 3 independent experiments (B).

In order to measure the effects of PKD3 knockdown on the ability of cells to invade, we performed a Matrigel invasion assay using our stable clone shPKD3-1 C7 and the shScr control cells. After a 5-day induction with tet, we replated the cells into the top chambers of Matrigel invasion inserts, in the presence or absence of tet. Twenty percent FBS was used in the bottom chamber as a chemoattractant. Our data showed that invasion of the tet-treated shPKD3-1 C7 cells was reduced to only 20%, compared to 65% invasion for the non-treated shPKD3-1 C7 cells (**Figure 33**). Invasive capacity of the shScr cells was not affected by the addition of tet. This result was again further confirmed using a transient knockdown of PKD2 and/or PKD3 (**Figure 34**). Taken together, these data demonstrate a novel role for PKD3 and PKD2 in the modulation of prostate cancer cell motility, a key capacity required for the progression and metastasis of aggressive prostate cancer.

A.

B.
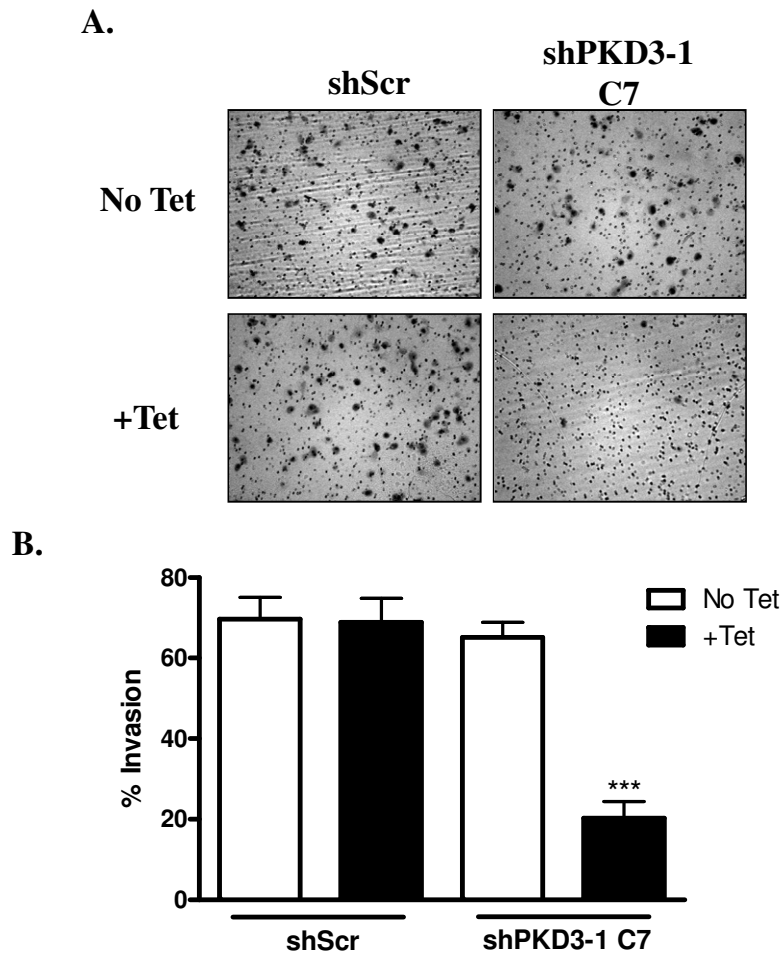
Figure 33. Tetracycline-induced PKD3 knockdown reduces invasion in PC3 cells. After pretreatment for 5 days with 1 µg/mL tet, 0.08M shScr or shPKD3-1 C7 cells in Ham's F12 media containing 0.1% FBS were seeded into Matrigel invasion or control inserts. Twenty percent FBS was added to the bottom chamber to stimulate invasion. In tet-treated cells, 1 µg/mL tet was added to both the top and bottom chambers. After 22 h, noninvasive cells were removed and invasive cells were fixed in 100% methanol, stained in 0.1% crystal violet solution, and photographed. The number of cells that invaded the Matrigel matrix was determined by cell counts in at least 5 fields relative to the number of cells that migrated through the control insert. A, Representative images comparing the invasiveness of shScr and shPKD3-1 C7 cells with and without tet are shown. B, The graphs show the mean ± S.E.M. of 3 independent experiments, each run in triplicate. Statistical significance versus the untreated control was determined. ***, $p < 0.001$.
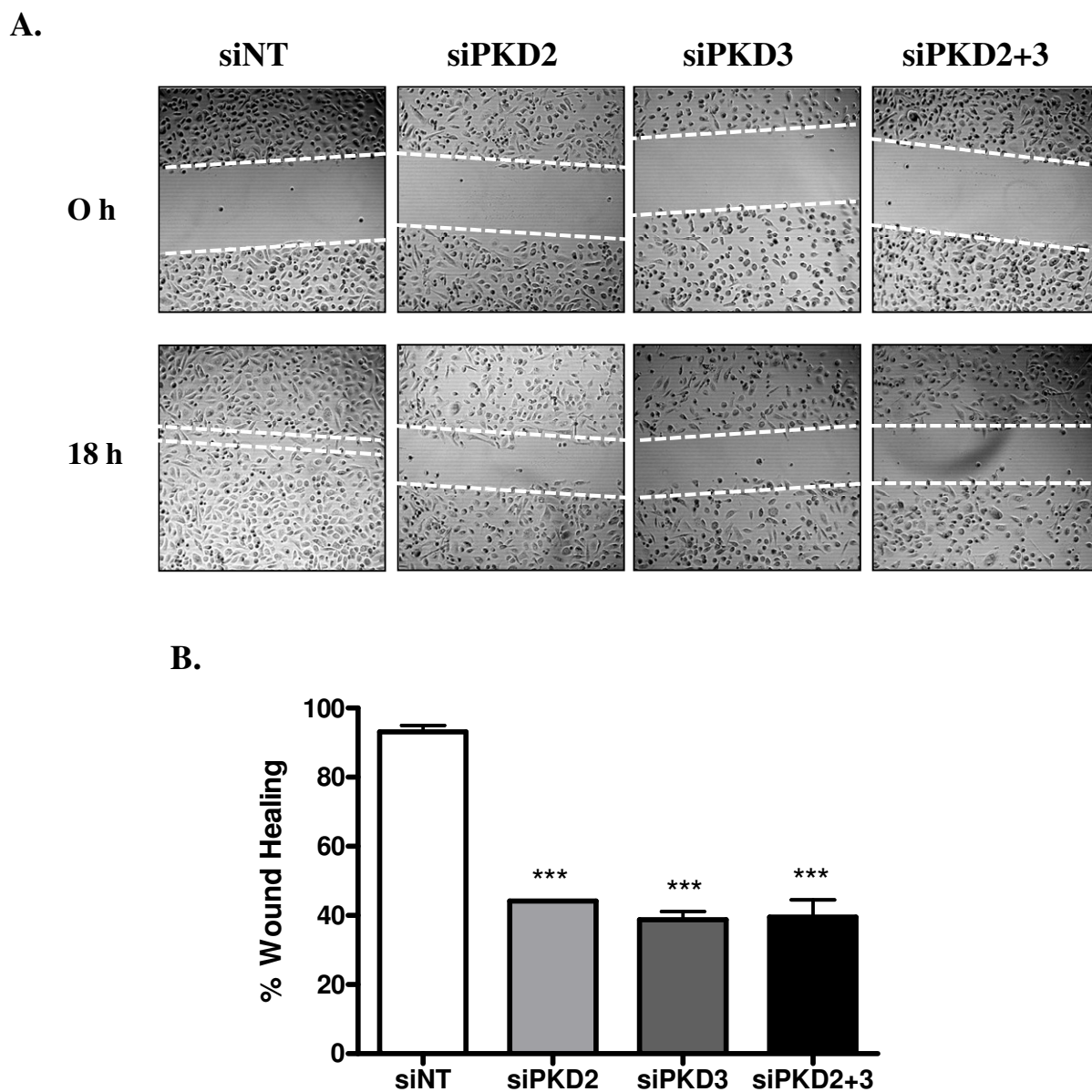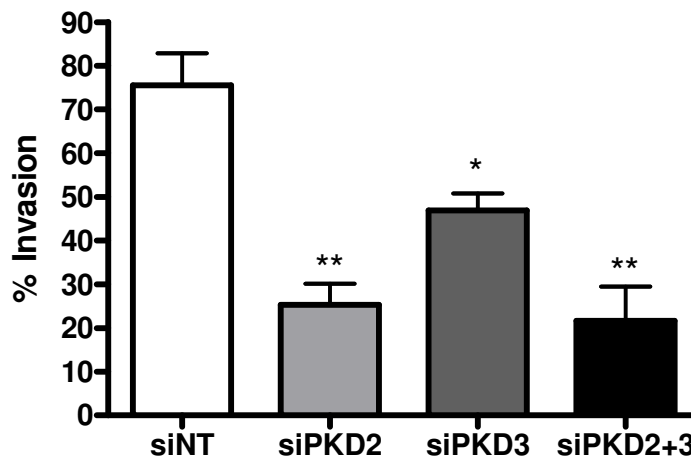
Figure 34. Transient knockdown of PKD2 and/or PKD3 reduces PC3 cell invasion. PC3 cells were transiently transfected with siRNAs targeting PKD2 (siPKD2), PKD3 (siPKD3), or both PKD2 and PKD3 (siPKD2+3). As a control, cells were transfected with non-targeting siRNA (siNT). Forty-eight hours following transfection, cells were replated into Matrigel invasion or control inserts at 0.08M cells/well in Ham's F12 media containing 0.1% FBS. Twenty percent FBS was added to the bottom chamber to act as a chemoattractant. After 22 h, noninvasive cells were removed and invasive cells were fixed in 100% methanol, stained in 0.1% crystal violet solution, and photographed. The number of cells that invaded the Matrigel matrix was determined by cell counts in at least 5 fields relative to the number of cells that migrated through the control insert. The data shown is the mean ± S.E.M. of 3 independent experiments, each run in triplicate. Statistical significance versus the untreated control was determined by unpaired t-test. *, $p < 0.05$; **, $p < 0.01$.

4.2.3 PKD3 knockdown leads to reduced secretion of MMPs

As a major traffic regulator, PKD has been shown to regulate cell motility through modulation of anterograde membrane traffic from the TGN to the plasma membrane (Prigozhina and Waterman-Storer 2004), which we hypothesized may impact the secretory pathways in tumor cells. Here, we investigated whether secreted factors may be involved in the PKD-mediated

regulation of PC3 cell migration. Indeed, we found that the conditioned medium collected from tet-treated shPKD3-1 C7 cells exhibited a significantly reduced capacity to promote PC3 cell migration compared to conditioned medium collected from untreated shPKD3-1 C7 cells and control shScr cells (**Figure 35**).
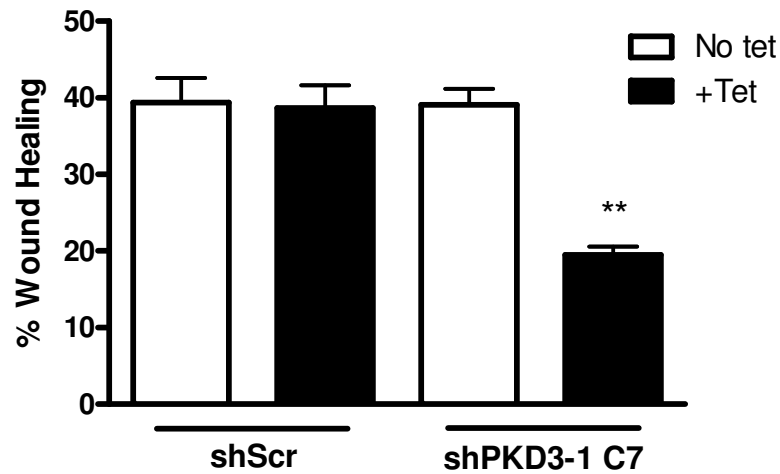
Figure 35. Conditioned media collected from tetracycline-treated shPKD3-1 C7 cells displays a reduced capacity to promote PC3 cell migration. PC3 cells stably expressing scrambled or PKD3-targeting shRNA (clones shScr and shPKD3-1 C7) were pretreated with or without 1 µg/mL tet for 5 days, then replated at equal densities in serum-free media. Conditioned media was collected after 48 h and applied to confluent, normal PC3 cells which had just been "wounded" using a 10 µL pipette tip, and the wound was imaged. Twenty-four hours later, images of the wound were captured again, and the percent wound healing was calculated by measuring the wound area at 3 locations along the wound for the initial wound and again at the 24-h time point. The graph shows the mean ± S.E.M. of the 3 independent experiments. **, $p < 0.01$.

MMPs are secreted endopeptidases that play critical roles in cell motility, angiogenesis, and invasion, and MMP-2 and MMP-9 in particular have been shown to be significant modulators of cancer progression (Lokeshwar 1999). While PKD1 has recently been implicated in the regulation of MMP-2 and MMP-9 in PC3 and DU145 prostate cancer cells (Biswas et al. 2010), the role of PKD3 in modulating MMPs has not been investigated. Therefore, we performed gelatin zymography to determine whether knockdown of PKD3 reduced the gelatinase activities of MMP-2 and MMP-9 detected in conditioned medium. Transient transfection typically resulted in 50-80% knockdown for all siRNAs excluding siPKD3-2, which was not effective at inhibiting PKD3 expression (**Figure 36**). Conditioned medium from PC3 cells transfected with siRNA targeting PKD3 was collected and then run on a polyacrylamide gel co-polymerized with 0.1% gelatin. Zymography revealed a reduction in MMP-9 levels in the conditioned medium from the PKD3 knockdown cells when using 4 different siRNAs (**Figure 37**). MMP-2 was expressed at low levels in these cells and its expression was not altered. This effect was also observed when PC3 cells were treated with 50 µM CID755673 or 25 µM kb-NB142-70, supporting the use of these compounds to study PKD function in prostate cancer cells (data not shown).
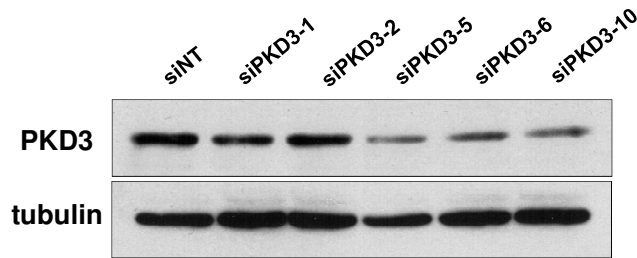
Figure 36. Knockdown of PKD3 using multiple siRNAs targeting PKD3. PC3 cells were transiently transfected with non-targeting siRNA (siNT) or one of 5 different siRNAs targeting PKD3. Cells were collected 48 h after transfection, and PKD3 levels were assessed by Western blot. With the exception of siPKD3-2, which did not inhibit PKD3 expression, all siRNAs (siPKD3-1, siPKD3-5, siPKD3-6, and siPKD3-10) typically resulted in 50-80% knockdown of endogenous PKD3. Tubulin was blotted as a loading control.
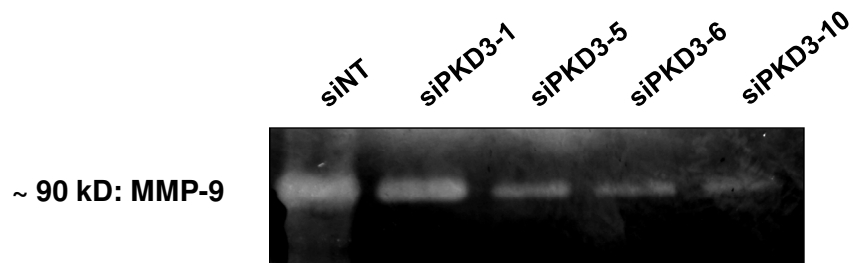
Figure 37. Zymography reveals reduced MMP-9 secreted from PKD3 knockdown cells. PC3 cells were transfected with siRNAs targeting different regions of PKD3 or a non-targeting siRNA. Forty-eight hours later, cells were replated at equal densities in 6-well plates into serum-free media. Conditioned media was collected after 48 h, and zymography analysis was conducted as described in the "Materials and Methods." The band represents MMP-9, as determined by molecular weight comparison with a purified, recombinant MMP-9 control.

To determine whether this reduction of MMP-9 activity was due to alteration in MMP-9 gene transcription rather than impairment of MMP-9 secretion, we performed RT-qPCR analysis and determined relative amounts of MMP-9 transcripts in multiple tet-induced PKD3 knockdown clones. Interestingly, we found that PKD3 knockdown caused no change in MMP-9

transcript levels for either clone shPKD3-1 C2-1 or clone shPKD3-1 C2-3 (**Figure 38A**).

Similarly, tet-treatment did not affect transcript levels of MMP-9 in control shScr cells. Since

PKD has also been implicated in the regulation of MMP-14 through modulation of class IIa

HDAC nuclear localization (Ha et al. 2008a; Wang et al. 2008), we investigated whether MMP-

14 levels were also altered in our PKD3 knockdown cells. We again found no changes in levels

of MMP-14 transcripts when shPKD3-1 C2-1 or shPKD3 C2-3 cells were treated with tet for 5

days (**Figure 38B**). These results suggest that PKD3 is not involved in the regulation of

transcription of these factors, but rather is altering their secretion.
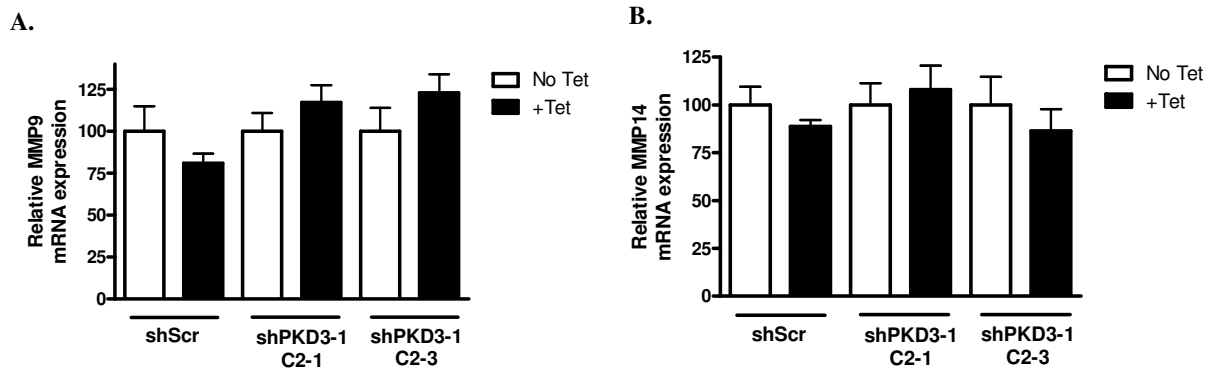
Figure 38. Inducible knockdown of PKD3 does not alter MMP-9 or MMP-14 mRNA. The stable clones shScr, shPKD3-1 C2-1, or shPKD3-1 C2-3 were pretreated with or without 1 µg/mL tet for 5 days. Cells were collected and total RNA was isolated. RT-qPCR analysis was performed as described in the "Materials and Methods" to determine MMP-9 (A) or MMP-14 (B) transcript levels relative to GAPDH.

4.2.4 PKD3 knockdown reduces secretion of several key cytokines

To examine if there might be a global effect on other secretory pathways, such as inflammatory pathways that have been implicated in prostate cancer progression (MacManus et al. 2007; Reiland et al. 1999; Seaton et al. 2008), we performed a cytokine antibody array using conditioned medium collected from our tet-induced shPKD3-1 C7 cells. The array revealed that tet-induced knockdown of PKD3 caused a significant reduction in the majority of the cytokines on the array (**Figure 39A-B, Appendix B for antibody array map**). For example, IL-3 and IL-6 were reduced to ~70% of the untreated control, TGFβ and TNFα were decreased to almost undetectable levels, and the chemoattractant proteins monocyte chemotactic protein (MCP) 1, -2, and -3 were reduced to only 20-40% of the untreated control. Tet-treatment itself had no effect on the secretion of cytokines in the shScr cells.
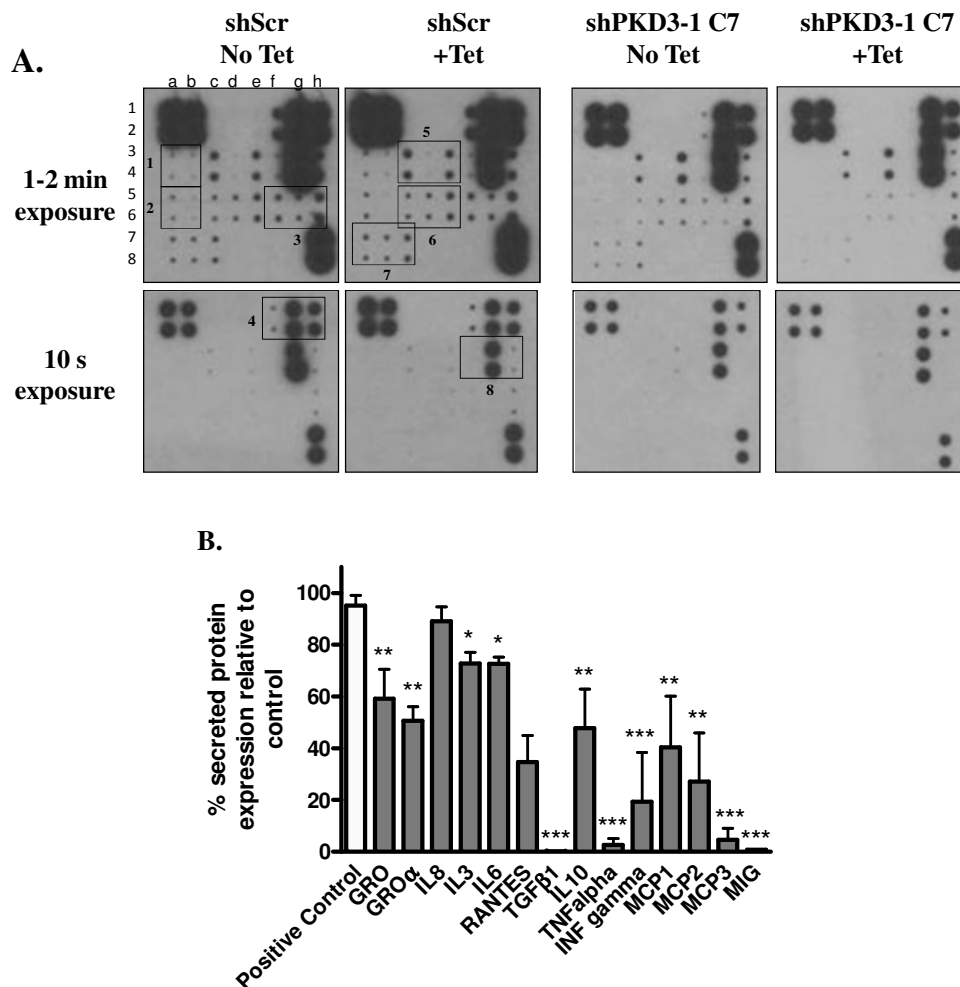
Figure 39. Knockdown of PKD3 modulates secretion of various cytokines in a membrane-based array. The stable clones shScr and shPKD3-1 C7 were pretreated with or without 1 µg/mL tet for 5 days and then replated at equal densities into serum-free media. Conditioned media was collected after 2 days and subjected to the cytokine antibody array following the manufacturer's directions. Chemiluminescent detection of protein spots for each of the 4 samples is shown (A). Boxes indicate spots corresponding to the following cytokines: Box 1, IL-1α, IL-2; Box 2, IL-13, IL-15; Box 3, MCP-3, MIG, RANTES; Box 4, GM-CSF, GRO, GROα; Box 5, IL-3, IL-5, Il-6; Box 6, INF-γ, MCP-1, MCP-2; Box 7, TGF-β1, TNF-α, TNF-β; Box 8, IL-7, Il-8, IL-10. B, Densitometry analysis arising from several exposures of the chemiluminescent blots. Statistical analysis was performed using the student's t-test. *, $p <$ 0.05; **, $p < 0.01$; ***, $p < 0.001$.

To confirm these array results, we analyzed the levels of several key cytokines secreted into the media by ELISA. Our data showed that tet-induced PKD3 knockdown caused a significant reduction in the levels of IL-6, IL-8, and GROα/CXCL-1 secreted from shPKD3-1 C2-3 cells (**Figure 40A**). Specifically, we found that tet-induced PKD3 knockdown in shPKD3-1 C2-3 cells reduced IL-8 secretion to less than 40% of the levels detected in conditioned medium from the untreated shPKD3-1 C2-3 cells and IL-6 secretion was reduced to only 75% of the control. To further validate our results, we measured cytokine secretion in prostate cancer cells depleted of endogenous PKD3 by multiple siRNAs. **Figure 40B** shows that transient knockdown of PKD3 using several siRNAs targeting different regions of PKD3 also caused a potent reduction in IL-6, IL-8, and GROα/CXCL-1 secretion in both PC3 and DU145 cells. To examine whether PKD kinase activity is required for this process, we investigated the effects of our previously-described novel PKD inhibitors CID755673 and kb-NB142-70 on cytokine secretion in PC3 cells (LaValle et al. 2010a; Sharlow et al. 2008). We found that treatment with either inhibitor caused a marked reduction in the secretion of IL-6, IL-8, and GROα/CXCL-1 (**Figure 41**). In fact, 25 µM kb-NB142-70 reduced secretion of each of these cytokines to only approximately 10% of the DMSO-treated control.
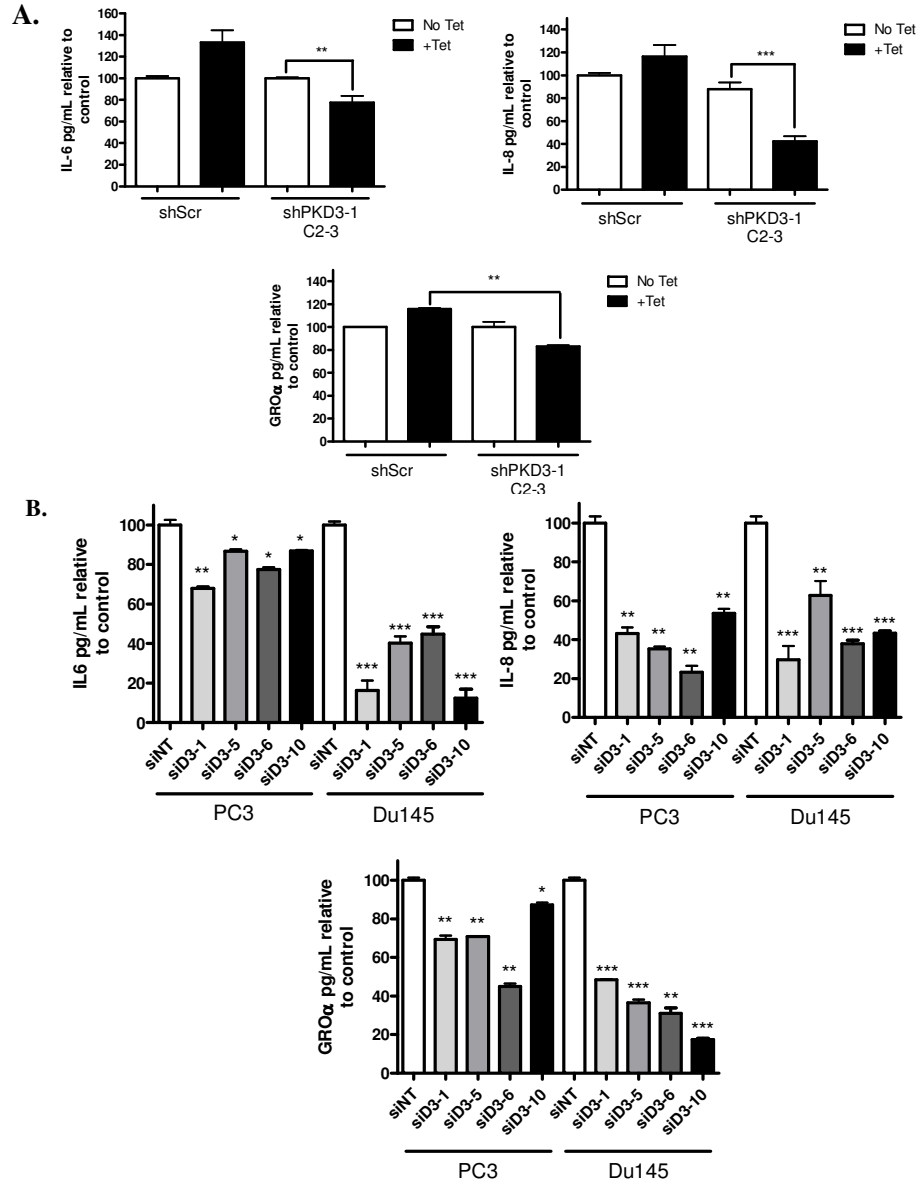
Figure 40. Knockdown of PKD3 reduces secretion of IL-6, IL-8, and GROα/CXCL-1. A, The stable clones shScr or shPKD3-1 C2-3 were pretreated with or without 1 µg/mL tet for 5 days and then replated at equal densities into serum-free media. Conditioned media was collected after 2 days and subjected to ELISA analysis to determine levels of IL-6, IL-8, or GROα/CXCL-1 secreted into the media. B, PC3 and DU145 cells were transfected with siRNAs targeting different regions of PKD3 or non-targeting siRNA. Two days after transfection, cells were replated at equal densities into serum-free media. Conditioned media was collected after 2 days and subjected to ELISA. For IL-8 ELISAs, conditioned media was diluted up to 20-fold in Assay Diluent B, provided in the ELISA kit. The data represent the mean ± S.E.M. from duplicate samples of 2-3 independent experiments (n = 4-6 for each sample). *, $p < 0.05$; **, $p < 0.01$; ***, $p < 0.001$.
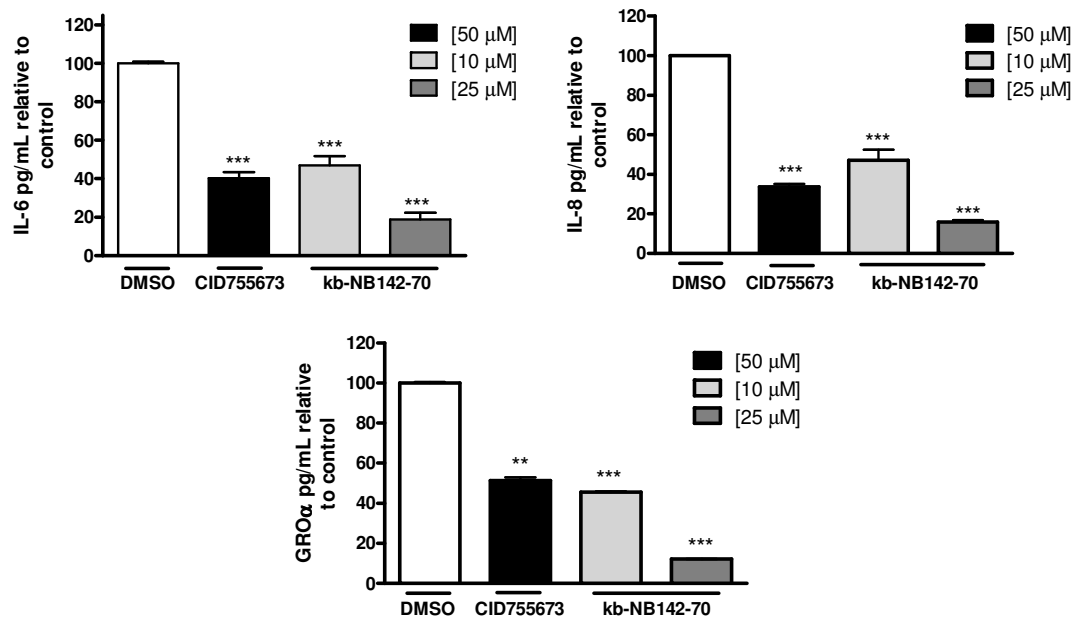
Figure 41. Antagonizing PKD activity reduces secretion of IL-6, IL-8, and GROα/CXCL-1. PC3 cells were treated with the indicated inhibitors for 48 h in serum-free media. The conditioned media was then collected, and ELISA was performed as before. For IL-8 ELISAs, conditioned media was diluted up to 20-fold in Assay Diluent B, provided in the ELISA kit. The data represent the mean ± S.E.M. from duplicate samples of 2-3 independent experiments (n = 4-6 for each sample). *, $p < 0.05$; **, $p < 0.01$; ***, $p < 0.001$.

To determine whether the effects of PKD3 knockdown on levels of secreted IL-6, IL-8, and GROα/CXCL-1 were due to transcriptional regulation rather than regulation of secretion, RT-qPCR was performed on total RNA extracted from shPKD3-1 C2-1 and shPKD3-1 C2-3 cells treated with or without tet. As shown in **Figure 42**, after 5-day tet treatment to induce PKD3 knockdown, no changes were detected in IL-6, IL-8, or GROα/CXCL-1 transcript levels compared to untreated control cells. Similarly, no changes in transcript levels were observed in the control shScr cells with or without tet treatment. These data suggest that knockdown of endogenous PKD3 or inhibition of PKD by chemical inhibitors blocks secretion, but not transcription, of key cancer-promoting factors in prostate cancer cells, likely due to global impairment of the secretory pathway.
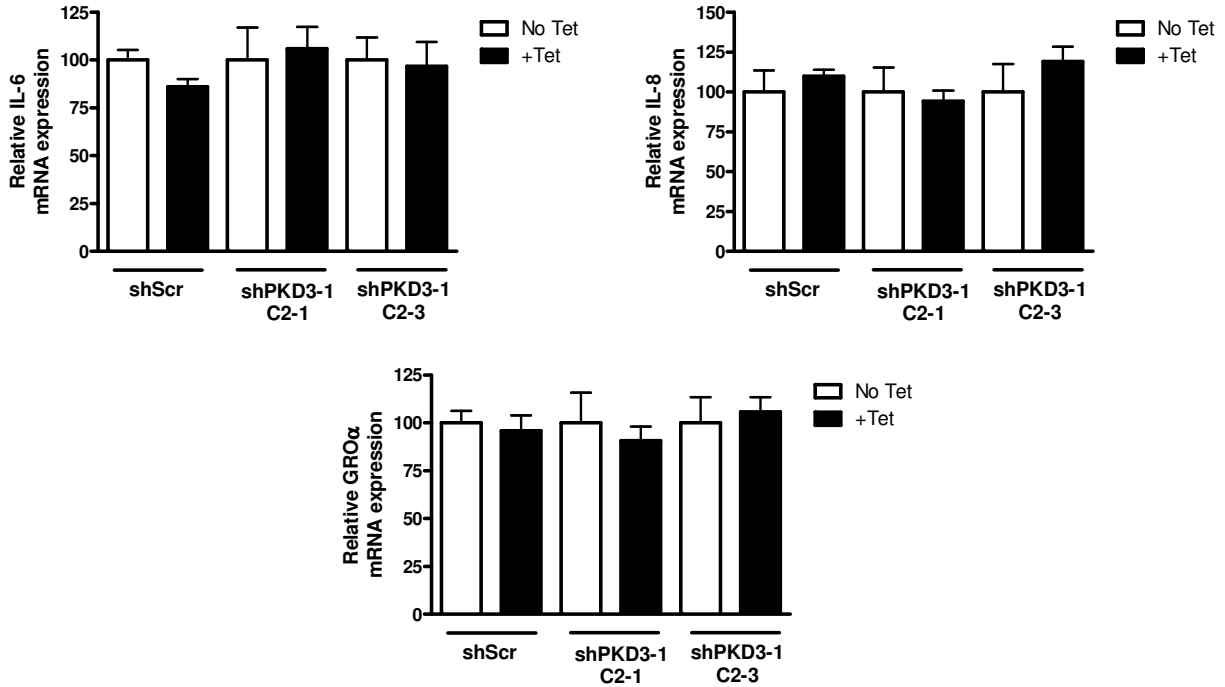
Figure 42. Tetracycline-induced knockdown of PKD3 does not modulate IL-6, IL-8, or GROα/CXCL-1 transcript levels. The stable clones shScr, shPDK3-1 C2-1, and shPKD3-1 C2-3 were pretreated with or without 1 µg/mL tet for 5 days. Cells were collected, and total RNA was isolated. RT-qPCR analysis was performed, and IL-6, IL-8, and GROα/CXCL-1 transcript levels relative to GAPDH control were determined.

4.3   DISCUSSION

Increasing evidence supports a major role for PKD in cancer progression. Here, we have established an essential role for PKD3, the least-studied member of the PKD family, in the progression of prostate cancer. We have demonstrated, in multiple prostate cancer cell lines, that specific knockdown of PKD3 expression using RNAi technology reduces proliferation, motility, and secretion of key cancer-promoting factors, including IL-6, IL-8, and GROα/CXCL-1. Furthermore, effects of our novel PKD inhibitors CID755673 and kb-NB142-70 have mimicked

those of targeted PKD knockdown. These data indicate that PKD3 is a viable target for the development of novel chemotherapeutics in prostate cancer treatment, and that our new class of PKD inhibitors can be used, albeit with caution, to study PKD function in cells.

In a previous report, we showed that PKD3 is upregulated in human prostate tumors and demonstrated increased nuclear accumulation in advanced-stage prostate cancer (Chen et al. 2008). Furthermore, transient knockdown of PKD3 by 2 different siRNAs caused a significant reduction in PC3 cell proliferation, an effect that was likely mediated by signaling through Akt and ERK (Chen et al. 2008). This is in contrast to reports by Balaji and colleagues, who have demonstrated an almost tumor-suppressor-like function for PKD1 in prostate cancer (Mak et al. 2008), highlighting potential isoform-specific functions of PKD and necessitating further study into the specific role of the PKD3 isoform in prostate carcinogenesis. Here, we have reported the development of a PC3 cell line stably expressing a tetracycline-inducible shRNA targeting PKD3. Addition of tet caused downregulation of endogenous PKD3 in 4 clones generated using this model (**Figure 29**). We found that this tet-induced PKD3 knockdown led to reduced cell proliferation, in accordance with our previous report using a transient knockdown approach. We also demonstrated that knockdown of PKD3 significantly inhibits prostate cancer cell migration and invasion, which implies that PKD3 may contribute to tumor metastasis and play a role in the progression of a primary prostate tumor into a more aggressive metastatic phenotype.

It is noteworthy that even with incomplete knockdown (50% - 65%) of PKD3, dramatic effects on prostate cancer cell proliferation and motility were observed, implying that PKD3 may affect multiple tumor-promoting pathways. In this study, when the conditioned medium from PKD3 knockdown cells was applied to normal PC3 cells, it resulted in significant inhibition of cell migration. Upon further investigation, we found that knockdown of PKD3 by shRNA caused

124

a global reduction in cytokine secretion in PC3 prostate cancer cells. These results were confirmed by ELISA for several significant targets, including IL-6, IL-8, and GROα/CXCL-1. Importantly, RT-qPCR analysis revealed no changes in the transcript levels of these proteins, suggesting that the reduced detection of cytokines was due to inhibition of secretion rather than gene expression. Thus, our data indicate that the robust effects of this partial PKD3 knockdown may be due to inhibition of the secretion of key cancer-promoting factors, thereby mediating several signaling pathways through reduction of autocrine and paracrine signaling.

Pro-inflammatory cytokines such as IL-6, IL-8, and GROα/CXCL-1 have well-documented, significant roles in prostate cancer progression (Mishra et al. 2011; Sciume et al. 2010). IL-8 in particular has been demonstrated to have various functions in cancer cells that promote angiogenesis, migration, metastasis, and proliferation, and is significantly upregulated in human prostate tumors (Murphy et al. 2005; Waugh and Wilson 2008). Functionally, IL-8 has been shown to regulate Akt expression and activity in androgen-independent prostate cancer cells (MacManus et al. 2007), promote the activity of the cell motility regulators RhoGTPase, RacGTPase, and Cdc42GTPase in prostate cancer cells (Waugh and Wilson 2008), and modulate expression of the androgen receptor and the androgen-independent state (Araki et al. 2007; Seaton et al. 2008), emphasizing the significance of this important cytokine in prostate cancer progression. Besides signaling in an autocrine fashion to stimulate cell growth and motility, these factors are also regulators of the tumor microenvironment (Coussens and Werb 2002). They have been shown to facilitate recruitment of immune system cells to the site of the tumor, which help tumors to "escape" immunosurveillance (Rescigno et al. 2007; Wilczynski and Duechler 2010), and also are potent stimulators of angiogenesis through communication with endothelial cells (Vindrieux et al. 2009). We have demonstrated that there is indeed reduced secretion of multiple

of these critical angiogenic cytokines with PKD3 knockdown, and this may account for the very potent effects on prostate cancer cell proliferation and motility seen in our cellular studies.

PKD has been long known to regulate protein trafficking; however, more recent studies have also begun to reveal a link between PKD function and the expression/secretion of cytokines. For example, a recent report showed that VEGF treatment of endothelial cells stimulated PKD1-dependent secretion of multiple cytokines, possibly mediating angiogenesis and the inflammatory response (Hao et al. 2009). In this study, researchers found that silencing of PKD1 or PKD2 through use of siRNA or treatment with the non-specific inhibitor Gö6976 caused reduced VEGF-stimulated expression and secretion of IL-6, IL-8, and GROα. However, they found no effects of PKD3 knockdown on cytokine secretion. In the present study, we demonstrate a very potent effect of PKD3 knockdown (using shRNA or siRNA) or pan-PKD inhibition (using PKD inhibitors) on secretion of these cytokines. This discrepancy can be explained by the relatively low expression of PKD3 in endothelial cells, which is in contrast to the high expression and likely aberrant hyperactivity of PKD3 in our PC3 and DU145 cells. It is plausible that the high expression of PKD3 in our multiple prostate cancer cell lines contributes to a constitutive hyperactivity of the secretory pathway, leading to increased secretion of key tumor-promoting factors and enhancing autocrine growth/motility signals. Furthermore, while specific PKD3 knockdown by shRNA and siRNA had robust effects on the secretion of multiple cytokines, pan-PKD inhibition by the PKD inhibitors CID755673 and kb-NB142-70 caused an even more dramatic reduction in cytokine secretion (**Figure 41**). This synergism suggests that PKD3 and PKD2, the other PKD isoform expressed in PC3 cells, likely have redundant effects in mediating cytokine secretion in prostate cancer cells, and this should be confirmed using specific PKD2 siRNAs in future studies. Thus, though it is clear that PKD has a role in the modulation of

126

cytokines, it is also clear that these events could be context- and isoform-dependent. Further investigations into the mechanisms through which PKD3 mediates secretion of these cytokines and potential isoform-specific effects are clearly warranted.

In conclusion, we present convincing evidence of the tumor-promoting functions of PKD3 in prostate cancer progression. We have shown that the cumulative effects of reduced cytokine secretion can cause significant changes in cancer cell proliferation and motility, and we have demonstrated that a reduction in PKD3 expression can have profound effects on cancer-related phenotype.

5.0 VALIDATION OF PROTEIN KINASE D3 AS A NOVEL THERAPEUTIC TARGET IN PROSTATE CANCER TREATMENT THROUGH USE OF TUMOR XENOGRAFT MODELS

5.1 INTRODUCTION

While the use of cell lines and *in vitro* studies are certainly useful, tumor xenograft models are much more effective means for understanding the biology and pathology of prostate cancer progression in a relavant tumor microenvironment (Chung et al. 2007). In the study of prostate cancer, a multitude of xenograft models, including subcutaneous xenografts, orthtopically implanted xenografts, cardiac injection models, and bone xenografts, have greatly increased our understanding of the mechanisms of progression to androgen dependence (Corey et al. 2003; Harper et al. 2004; Legrier et al. 2004; Zhou et al. 2004), functions of the tumor microenvironment (Kumano et al. 2008; Shaw et al. 2010; Yang et al. 2005), primary sites of metastasis and the ability of prostate cancer cells to form metastases (Angelucci et al. 2004; Chung et al. 2007; Margheri et al. 2005; Thudi et al. 2011), and the preclinical efficacy of potential novel chemotherapeutics (Dahmani et al. 2010; Hasegawa et al. 2011; Hwang et al. 2010; Kim et al. 2011). Furthermore, the use of xenograft models allows researchers to investigate the involvement of specific proteins in the progression of prostate cancer *in vivo*.

In Chapter 4, we discussed reports demonstrating aberrant and differential expression of PKD1 and PKD3 in human prostate cancer tissues and cell lines (Chen et al. 2008; Jaggi et al. 2003). The additional studies presented in this dissertation in Chapters 3 and 4 suggest that the PKD isoenzymes, or, more specifically, PKD2 and PKD3, promote tumor cell growth and motility in the context of prostate cancer, and that targeting them via specific RNAi or inhibitors causes substantial reductions in prostate cancer cell growth and motility. Thus, although the PKD isoforms are differentially implicated in prostate cancer, it is undeniable that they play critical roles in the regulation of prostate cancer cell proliferation and invasion.

Despite the variety of studies in prostate cancer cell lines and evidence of aberrant expression in human tumor tissues, *in vivo* animal studies providing evidence of the role of PKD in prostate cancer progression have previously not been reported. Here, we describe the use of a tetracycline-inducible PKD3 knockdown prostate cancer cell line in both subcutaneous and orthotopic xenograft models, providing significant evidence that PKD3 plays a tumor-promoting role in prostate cancer progression *in vivo*. Our results demonstrate that inducible knockdown of PKD3 causes substantial reduction in the growth of subcutaneous xenograft tumors in nude mice. Furthermore, we show that inhibition of PKD3 expression results in decreased levels of intratumoral GROα/CXCL-1, a cytokine involved in multiple cancer-promoting pathways. These data validate PKD3 as a promising therapeutic target in prostate cancer treatment, expand our understanding of the molecular mechanisms of PKD function in prostate cancer progression, and support the further development of potential chemotherapeutic agents targeting this crucial family of serine/threonine kinases.

5.2   RESULTS

5.2.1   Knockdown of PKD3 halts growth of subcutaneous xenograft tumors in mice

In order to validate that PKD3 is indeed a significant regulator of prostate tumor growth *in vivo*, we studied the ability of PKD3 knockdown to inhibit growth of PC3 tumors inoculated subcutaneously in nude mice. We first established tumors in nude male mice using shScr or shPKD3-1 C7 cells from our tet-inducible PKD3 knockdown model system. Five days after inoculation of the tumor cells, we administered 1 mg/mL doxycycline (dox), a tetracycline analog, via drinking water to half the mice bearing shScr tumors and half the mice bearing shPKD3-1 C7 tumors (4 groups: shScr No Dox, shScr +Dox, shPKD3-1 C7 No Dox, shPKD3-1 C7 +Dox; n = 10-11 mice per group). We measured tumor volume 3 times a week for 25 days at which time the shScr tumors were nearing 20 mm in diameter, necessitating euthanasia. While dox itself had no effect on tumor growth in the shScr mice, we saw a very potent reduction in tumor volume in dox-treated mice bearing shPKD3-1 C7 tumors (**Figure 43A, C**). After the 25-day experiment, tumor volume for the shPKD3-1 C7 +dox group measured only 100 mm^3 on average, compared to an average of 325 mm^3 for the no dox shPKD3-1 C7 group, a reduction of nearly 70%. Mice experienced no changes in weight due to tumor growth or dox treatment during the course of the study (**Figure 43B**).

A.

B.

C.

10 mm

| shScr No Dox | shScr +Dox | shPKD3-1 C7 No Dox | shPKD3-1 C7 +Dox | shPKD3-1 C7 +Dox |
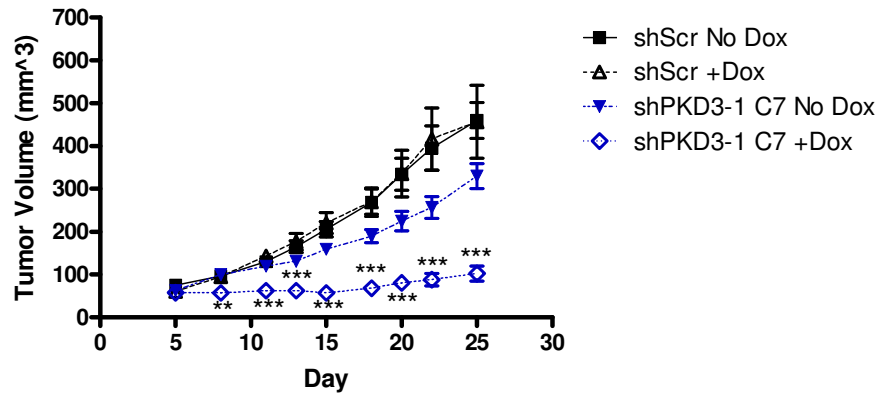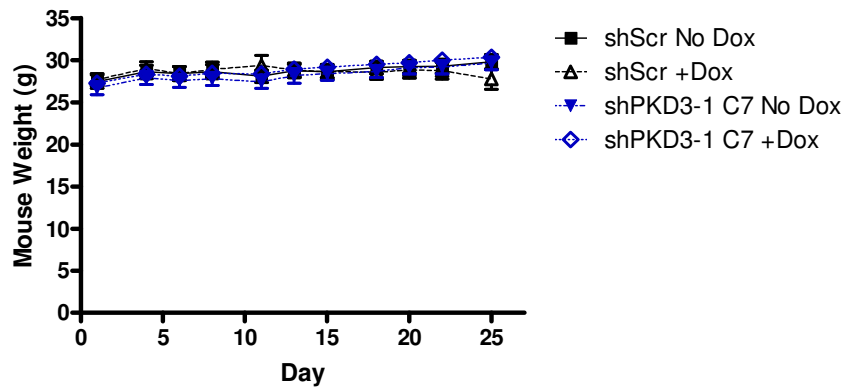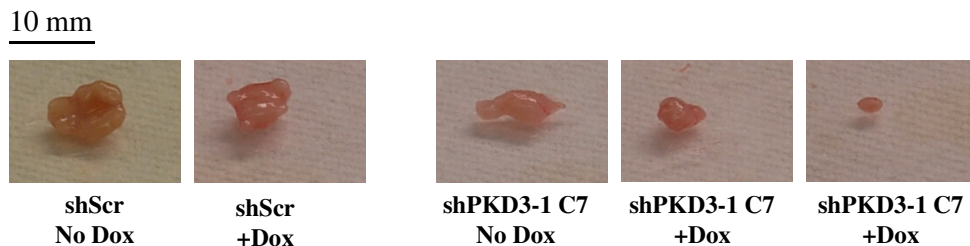
Figure 43. Doxycycline-induced knockdown of PKD3 in PC3 cells slows growth of subcutaneous tumor xenografts in mice. Male nude mice were injected subcutaneously in the right flank with either shScr or shPKD3-1 C7 cells (4.0×10^6 cells resuspended 1:1 in BD Matrigel). Five days following injection, mice were randomized and half the mice from each group were given dox at 1 mg/mL via drinking water. Tumor volume (A) and mouse weight (B) were measured every 2-3 days. The experiment was performed using 5-6 mice per group and was independently repeated twice for a total of 10-11 mice per group. Statistical significance was determined using the Mann-Whitney-Wilcoxon test. C, Representative images of the excised tumors. **, $p < 0.01$; ***, $p < 0.001$.

131

5.2.2 Inducible knockdown of PKD3 results in reduced levels of intratumoral GROα/CXCL-1

To investigate the potential mechanisms leading to reduced tumor growth in our model, we performed ELISA analysis of lysates prepared from the excised tumors. The ELISAs revealed a significant reduction in intratumoral GROα/CXCL-1, but not IL-8 (**Figure 44**). In fact, in shPKD3-1 C7 +Dox tumors, levels of GROα/CXCL-1 were reduced to approximately 55% of the no dox control. This significant difference indicates that PKD3 modulates levels of this cytokine *in vivo*, and this may contribute to the reduced tumor growth we saw in shPKD3-1 C7-derived tumors.
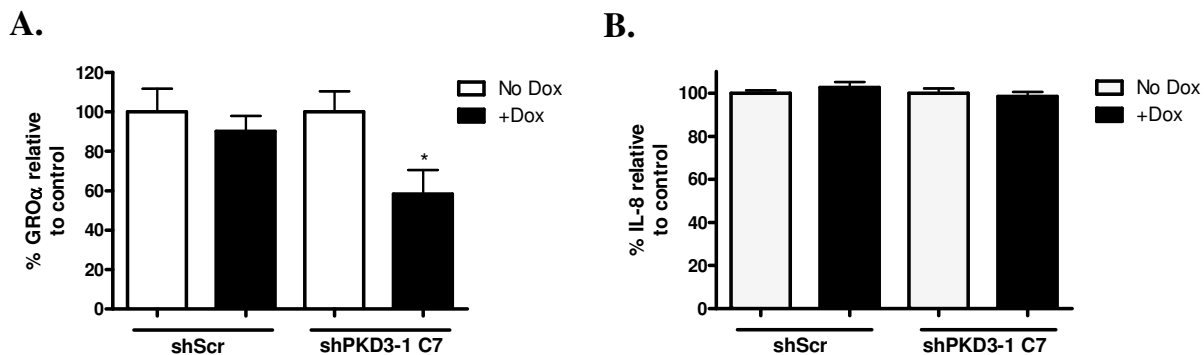
Figure 44. PKD3 knockdown causes reduction in intratumoral GROα/CXCL-1, but not IL-8. Excised tumors were cut into small pieces and lysed as described in the "Materials and Methods." Protein concentration was determined by BCA Protein Concentration Assay Kit, and equal amounts of protein were subjected to ELISA for detection of GROα/CXCL-1 (A) or IL-8 (B) following the manufacturer's instructions. For each tumor sample, duplicate measurements were determined, and tumors from 4-5 mice in each group were analyzed. *, $p < 0.05$.

5.2.3 Inducible knockdown of PKD3 reduces growth of orthotopic prostate xenograft tumors

While the above subcutaneous xenograft mouse model gives us vital information about the ability of prostate cancer cells to form tumors and vascularize, it is well recognized that there are many limitations to using this model (Chung et al. 2007; Kerbel 2003). For example, tumor bits or cells implanted subcutaneously rarely metastasize, are not exposed to the site-specific microenvironment, and are not always accurate predictors of subsequent clinical investigations (Sano and Myers 2009). Therefore, many researchers have begun using orthotopic implantation models to study the pathogenesis of specific cancers in mouse models, including prostate cancer (Chung et al. 2007; Park et al. 2010).

Here, we have developed an orthotopic xenograft model using our inducible PKD3-knockdown cell lines. In this small-scale study using 3-4 mice for each group, we investigated whether dox-induced PKD3 knockdown could reduce growth of orthotopic prostate tumors. For each cell line, we injected 0.5×10^6 cells into the dorsolateral lobe of the prostate in 8-week old male nude mice. Fourteen days following injection, we began treatment using 1 mg/mL dox in the animals' drinking water. We continuously monitored mice for signs of pain, discomfort, difficulties urinating, and weight loss. In general, we noticed that mice inoculated with shScr cells began to lose weight around day 20 and more rapid weight loss was observed after day 25 (**Figure 45C**). Mice were euthanized at day 31, and full necropsies were performed. Also, primary tumors were excised and weighed. We found that the average weight of the tumors arising from shPKD3-1 C7 cells was less, though statistical significance was not indicated due to the small sample size (**Figure 45A-B**). Necropsies revealed that the shScr +Dox mice, in

addition to having larger primary tumors, generally had small tumors growing all over the abdomen, with some found on the liver and in the mesentery. At the time, we were unable to quantify the number of these tumors. Notably, none of the shPKD3-1 C7 +Dox mice had these peritoneal tumors, but only had generally small tumors localized in the prostate. All mice in the study developed at least primary prostate tumors, giving us a 100% tumor take rate. This high take rate was unexpected since this was an early pilot study; however, very high tumor take rates have been reported for several orthotopic prostate xenograft models in the literature, particularly if the tumor cells are injected with Matrigel (Ruggeri et al. 2003; Saar et al. 2010). These promising data indicate that a more in-depth, full-scale study using this inducible PKD3 knockdown model is warranted.

A.

B.

shScr +Dox	shPKD3-1 C7 +Dox

C.
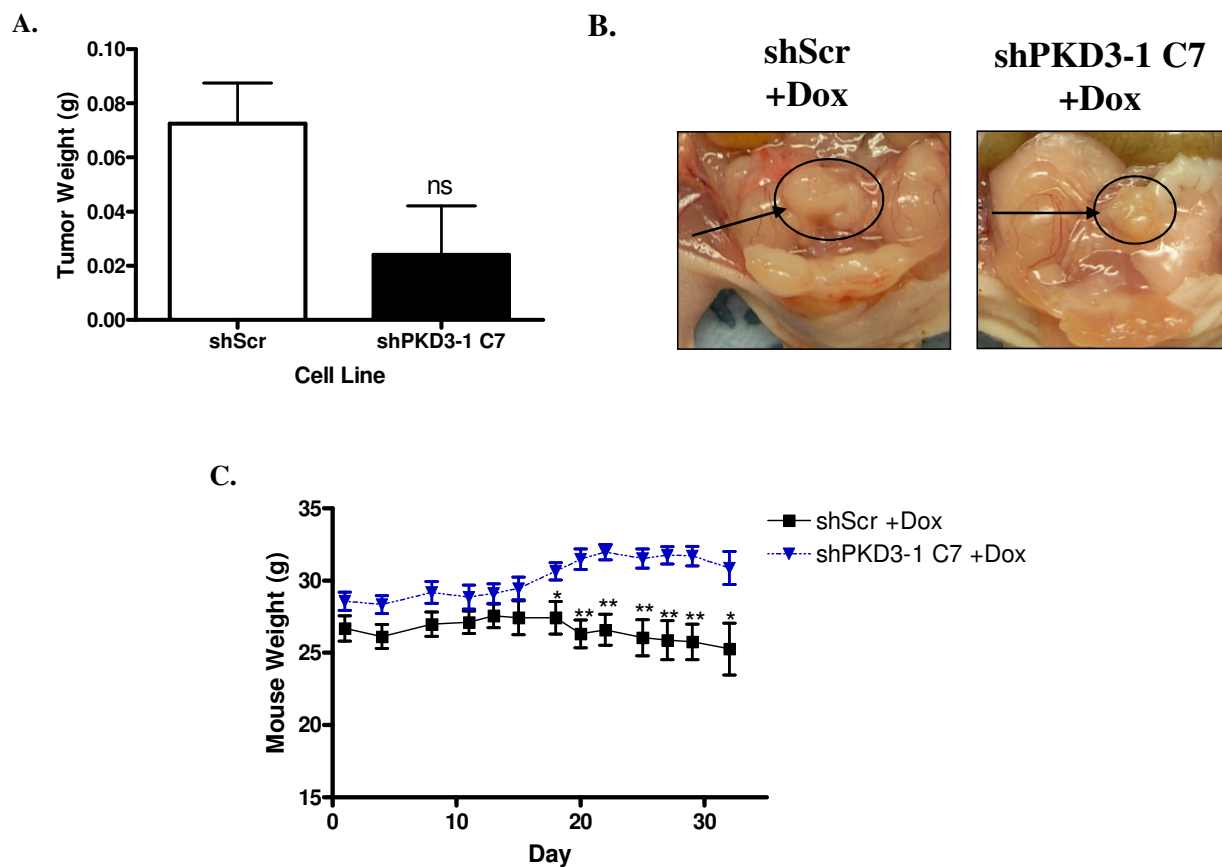
Figure 45. PKD3 knockdown causes reduced growth of orthotopic prostate tumors in mice. For orthotopic prostate xenograft, 0.5 x 10^6 shScr (n = 4) or shPKD3-1 C7 (n = 3) cells were resuspended 1:1 in BD Matrigel (total volume 10 µL) and injected directly into the dorsolateral lobe of the prostates of 8-week old male nude mice. Fourteen days following the injection, mice were given drinking water containing 1 mg/mL dox. Dox-containing water was refreshed every 2 days, and mice were monitored as described in the "Materials and Methods" for weight loss, pain, and discomfort. Thirty-one days following orthotopic injection, mice were sacrificed, and tumors were excised and weighed. Total necropsies were performed to determine the presence of metastases. Weight of the excised tumor was plotted (A), and representative images of shScr and shPKD3-1 C7 primary prostate tumors are shown (B). Mouse weight was monitored over the course of the experiment (C). ns, not significant; *, $p < 0.05$; **, $p < 0.01$.

5.3   DISCUSSION

Recent studies of PKD function in prostate cancer cells have revealed multiple roles in cell proliferation and motility pathways, often with conflicting evidence for PKD1 and PKD3 reported in the literature (Biswas et al. 2010; Chen et al. 2008; Jaggi et al. 2005) Furthermore, the studies presented in Chapters 3 and 4 of this dissertation clearly support a tumor-promoting role for PKD2 and PKD3 in prostate cancer. However, though we can gain much mechanistic insight from cellular models, it is *in vivo* models of cancer progression that bestow us with the most useful and clinically-relevant information. Therefore, we sought to establish whether PKD3 could modulate the growth of prostate tumors *in vivo,* as an extension to the cellular work we completed in Chapter 4. In this study, we provide evidence that inhibition of PKD3 expression using a tetracycline-inducible PKD3 knockdown model reduces the growth of both subcutaneous and orthotopic prostate xenografts. We found significant changes in the level of GROα/CXCL-1 in excised tumors, suggesting that PKD3 may regulate tumor growth through modulation of cytokine levels. The results presented here validate PKD3 as a promising therapeutic target in the treatment of prostate cancer and support the further development of PKD-targeted therapies.

The chemokine GROα/CXCL-1 has been studied in a variety of cancers, and has been found to promote proliferation, invasion, and angiogenesis in many different contexts (Haghnegahdar et al. 2000; Ogata et al. 2010; Reiland et al. 1999; Wen et al. 2006). In prostate cancer, GROα/CXCL-1 was shown to promote invasion and chemotaxis in PC3 cells (Reiland et al. 1999). Thus, the significant PKD3-dependent reduction in intratumoral GROα/CXCL-1 is an important observation that may explain in part the reduced tumor growth we observed in the shPKD3-1 C7-derived tumors. Though we do not yet know the mechanisms through which

PKD3 is mediating GROα/CXCL-1 expression *in vivo,* our cellular studies suggest that downregulation of PKD3 impairs the secretory pathway rather than transcription of this important tumor-promoting factor.

The subcutaneous xenograft model is the most commonly used tumor xenograft model, largely because of the relative ease of implementation when compared to orthotopic models (Chung et al. 2007). However, it is becoming increasingly clear that subcutaneous xenograft models are inferior to orthotopic models in predicting the success of future clinical trials (Kerbel 2003; Park et al. 2010; Sano and Myers 2009). Since implantation of tumor cells or xenografts orthotopically creates a much more physiologically-relevant tumor microenvironment, the orthotopic model is thought to more closely mimic actual tumor development (Chung et al. 2007). Furthermore, orthotopic tumors often give rise to metastases, whereas the occurrence of secondary tumors is very rare in subcutaneous models (Chung et al. 2007). Therefore, with the intention of studying PKD3 function in the progression of metastatic prostate cancer, we initiated a pilot study using an orthotopic prostate xenograft model. We found slightly reduced growth of the primary tumor in the shPKD3-1 C7 +Dox group, compared to the shScr +Dox group. Additionally, we observed dramatic weight loss and growth of a substantial number of secondary tumors in the abdomen and mesentery in mice inoculated with shScr cells, but not in mice from the shPKD3-1 C7 group. The weight loss observed in the shScr group was not due to the dox treatment itself, since the mice in the shPKD3-1 C7 group as well as the mice in our subcutaneous studies also received this same treatment and did not experience weight loss (**Figure 43B** and **Figure 45C**). From the necropsies performed on these mice bearing shScr tumors, we observed a number of secondary tumors in the abdomen and mesentery, with 1 mouse showing lesions on the liver, and much larger primary tumors localized at the prostate.

These differences, though not statistically significant due to the small sample size, suggest that PKD3 may indeed promote the aggressiveness of prostate cancer *in vivo*, and it is clear that a larger study is warranted.

The results of the xenograft models described in this chapter also demonstrate the potential usefulness of this inducible knockdown model system in studying the role of PKD function *in vivo*. A larger scale orthotopic study is underway to investigate whether PKD3 knockdown inhibits the metastasis of prostate tumors. Future studies using this model can also be used to investigate PKD3-mediated mechanisms of *in vivo* tumor growth and metastasis including regulation of angiogenesis by Matrigel plug assay (Akhtar et al. 2002). Additionally, this model can be used to determine whether PKD knockdown sensitizes tumors to established chemotherapeutic agents such as docetaxel.

In conclusion, we have presented evidence that PKD3 is a valid and promising therapeutic target in prostate cancer, and that targeting PKD3 *in vivo* results in substantially reduced prostate tumor growth. Future *in vivo* studies using the orthotopic model are required to determine the role of PKD3 in prostate cancer metastasis.

6.0   CONCLUSIONS

In 1955, the National Cancer Institute made an observation that agents tested and validated in tumor xenograft models prior to being introduced in the clinic vastly out-performed those that were prescreened only in cellular models (Gellhorn and Hirschberg 1955). From this correlation, a paradigm shift occurred, and the NCI commenced a large-scale study to screen anticancer drugs against a panel of xenograft tumors in mice (Goldin et al. 1961a; Goldin et al. 1961b; Goldin et al. 1961c; Oettel and Wilhelm 1955; Stock et al. 1960). The past few decades have seen another shift in thought, moving toward anticancer drug development platforms that attempt to develop cytotoxic agents through targeting a specific protein or class of proteins (Suggitt and Bibby 2005). The protein kinase D family has become one of these promising targets in many cancer types, and our understanding of cancer-related PKD functions is rapidly evolving (LaValle et al. 2010b).

In collaboration with our colleagues, Drs. John S. Lazo, Elizabeth R. Sharlow, and Peter Wipf, at the University of Pittsburgh, we have developed and characterized a novel class of PKD inhibitors. This class of compounds shows high selectivity toward the PKD isoforms and has anticancer activities in cellular models of both prostate and pancreatic cancer. Through SAR analysis, the parental compound CID755673 evolved into the new lead compound kb-NB142-70, which showed greatly increased potency *in vitro* and in cells. This class of compounds has been

used to study PKD function in cells by multiple groups now, and is proving to be a useful pharmacological tool (Pilankatta et al. 2011).

Further studies of PKD function in prostate cancer cells revealed that PKD2 and PKD3 modulate cell growth and motility. We made a significant observation that conditioned media collected from PKD3 knockdown cells slowed cell migration when applied to normal PC3 cells, implicating changes in the profile of secreted proteins. Analysis showed substantial reduction in MMP-9 secretion and the secretion of multiple cytokines, including IL-8, IL-6, and GROα/CXCL-1. Experimental evidence suggests that this effect is not a transcriptionally-mediated process, but rather may be accounted for by the known role of PKD in modulating protein trafficking and fission of plasma membrane-bound vesicles from the Golgi. Finally, subcutaneous and orthotopic xenograft models using a tetracycline-inducible PKD3 knockdown PC3 cell line have validated PKD as a promising therapeutic target in prostate cancer treatment.

In this thesis, we have come full circle, describing a novel class of PKD inhibitors with anticancer activity in prostate and cancer cells, discovering novel functions for PKD in the regulation of tumor-promoting factors and cytokines, and finally using *in vivo* analysis to validate PKD3 as a strong candidate for anticancer therapy in prostate cancer. Though there is still much to be learned about the details of PKD function, our studies have provided substantial evidence that targeting PKD in cancer cells may lead to novel and potentially efficacious therapeutic alternatives to current treatment regimens in prostate cancer and other cancers.

APPENDIX A. COMPOUNDS TESTED DURING SAR ANALYSIS AND STRUCTURAL OPTIMIZATION

The following Tables detail the structures and activity of all the compounds synthesized and tested during SAR analysis and structural optimization of the PKD inhibitors described in this dissertation. All Tables were published in the following manuscript:

George KM, Frantz MC, Bravo-Altamirano K, LaValle CR, Tandon M, Leimgruber S, Sharlow ER, Lazo JS, Wang QJ, Wipf P. 2011. Design, synthesis, and biological evaluation of PKD inhibitors. Pharmaceutics 3(2):186-228.

Table 1. Chemical structures and PKD1 inhibitory activities of **CID797718** and its analogs.
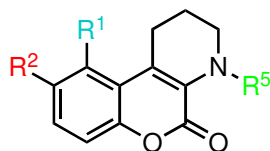
Entry	Compound	Structure			IC_{50}	
		R^1	R^2	R^5	IMAP-FP PKD1 (μM)	radiometric PKD1 (μM)
1	**CID797718**	H	OH	H	13.7 ± 0.42 ($n = 3$)	2.34 ± 0.16 ($n = 3$)
2	**kb-NB77-83**	H	OAllyl	H	not inhibitory	n.d.
3	**kb-NB77-78**	H	OTBS	H	not inhibitory	n.d.
4	**kb-NB77-91**	H	OH	Cbz	not inhibitory	n.d.
5	**kb-NB96-47-1**	Cl	OH	H	not inhibitory	n.d.
Entry	Compound	Structure			IC_{50}	
		R^1	R^2	R^5	IMAP-FP PKD1 (μM)	radiometric PKD1 (μM)
1	**CID797718**	H	OH	H	$13.7? \pm 0.42$ ($n = ?$)	2.34 ± 0.16 ($n = 3$)
2	**kb-NB77-83**	H	OAllyl	H	not inhibitory	n.d.
3	**kb-NB77-78**	H	OTBS	H	not inhibitory	n.d.
4	**kb-NB77-91**	H	OH	Cbz	not inhibitory	n.d.
5	**kb-NB96-47-1**	Cl	OH	H	not inhibitory	n.d.

Table 2. Chemical structure and PKD1 inhibitory activity of **CID755673** and its analogs.
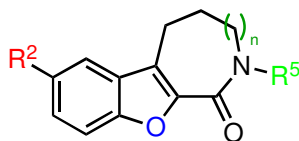
Entry	Compound	Structure R^2	Structure R^5	Structure N	IC$_{50}$ IMAP-FP PKD1 (μM)	IC$_{50}$ radiometric PKD1 (μM)	IC$_{50}$ cellular PKD1 (μM)
1	**CID755673**	OH	H	1	0.64 ± 0.03 (*n* = 3)	0.18 ± 0.02 (*n* = 5)	11.8 ± 4.0 (*n* = 3)
2	**kb-NB123-23A**	OH	H	0	12.6 ± 1.3 (*n* = 3)	1.41 (*n* = 1)	n.d.
3	**kb-NB123-32**	OMe	H	0	>100	n.d.	n.d.
4	**kb-NB96-53**	OH	H	2	8.3 ± 0.6 (*n* = 3)	1.03 (*n* = 1)	n.d.
5	**kb-NB96-59**	OMe	H	2	>100	n.d.	n.d.
6	**kb-NB77-56**	OMe	H	1	2.40 ± 0.14 (*n* = 3)	2.39 (*n* = 1)	n.d.
7	**kb-NB77-84**	OAllyl	H	1	2.6 ± 0.2 (*n* = 3)	1.23 (*n* = 1)	n.d.
8	**kb-NB123-36**	OAc	H	1	84.89 ± 3.21 (*n* = 3)	n.d.	n.d.
9	**kb-NB77-77**	OTBS	H	1	not inhibitory	n.d.	n.d.
10	**kb-NB123-37**	OMe	Me	0	not inhibitory	n.d.	n.d.
11	**kb-NB142-25**	OH	Me	1	n.d.	4.0 ± 1.1 (*n* = 2)	n.d.
12	**kb-NB96-04**	OMe	Me	1	>100	n.d.	n.d.
13	**kb-NB123-45-1**	OAc	Ac	1	not inhibitory	n.d.	n.d.
14	**kb-NB165-15**				n.d.	not inhibitory	n.d.

Entry	Compound	Structure R^2	Structure R^5	Structure N	IC$_{50}$ IMAP-FP PKD1 (μM)	IC$_{50}$ radiometric PKD1 (μM)	IC$_{50}$ cellular PKD1 (μM)
1	**CID755673**	OH	H	1	0.64 ± 0.03 (*n* = ?)	0.18 ± 0.02 (*n* = 5)	11.8 ± 4.0 (*n* = 3)
2	**kb-NB123-23A**	OH	H	0	12.6 ± 1.3 (*n* = ?)	1.41 (*n* = 1)	n.d.
3	**kb-NB123-32**	OMe	H	0	not inhibitory	n.d.	n.d.
4	**kb-NB96-53**	OH	H	2	8.3 ± 0.6 (*n* = ?)	1.03 (*n* = 1)	n.d.
5	**kb-NB96-59**	OMe	H	2	not inhibitory	n.d.	n.d.
6	**kb-NB77-56**	OMe	H	1	2.40 ± 0.14 (*n* = ?)	2.39 (*n* = 1)	n.d.
7	**kb-NB77-84**	OAllyl	H	1	2.6 ± 0.2 (*n* = ?)	1.23 (*n* = 1)	n.d.
8	**kb-NB123-36**	OAc	H	1	84.89 ± 3.21 (*n* = ?)	n.d.	n.d.
9	**kb-NB77-77**	OTBS	H	1	not inhibitory	n.d.	n.d.
10	**kb-NB123-37**	OMe	Me	0	not inhibitory	n.d.	n.d.
11	**kb-NB142-25**	OH	Me	1	n.d.	4.0 ± 1.1 (*n* = 2)	n.d.
12	**kb-NB96-04**	OMe	Me	1	not inhibitory	n.d.	n.d.
13	**kb-NB123-45-1**	OAc	Ac	1	not inhibitory	n.d.	n.d.
14	**kb-NB165-15**				n.d.	not inhibitory	n.d.

Table 3. Chemical structures and PKD1 inhibitory activities of **CID755673** analogs.
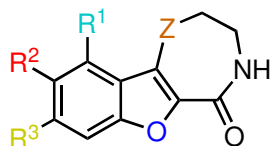
Entry	Compound	Structure				IC$_{50}$	
		Z	R^1	R^2	R^3	IMAP-FP PKD1 (μM)	radiometric PKD1 (μM)
1	**kb-NB77-88**	CH$_2$	Cl	OH	H	1.4 ± 0.1 (n = 3)	0.89 (n = 1)
2	**kb-NB96-21**	CH$_2$	F	OH	H	1.3? ± 0.05 (n = 3)	0.24 (n = 1)
3	**kb-NB96-50**	CH$_2$	Cl	OAllyl	H	not inhibitory	n.d.
4	**kb-NB96-47-5**	CH$_2$	H	OH	Cl	>100	n.d.
5	**kb-NB96-43**	CH$_2$	Cl	OH	Cl	not inhibitory	n.d.
6	**kb-NB96-02**	CH$_2$	Allyl	OH	H	2.4 ± 0.3 (n = 3)	1.58 (n = 1)
7	**kb-NB96-30**	CH$_2$	Propenyl	OH	H	1.0 ± 0.1 (n = 3)	0.24 (n = 1)
8	**kb-NB123-63**	C=O	H	OH	H	14.9 ± 1.2 (n = 3)	0.85 ± 0.11 (n = 2)
9	**kb-NB123-89**	CHOH	H	OH	H	24.09 ± 0.71 (n = 3)	1.23 ± 0.21 (n = 2)
10	**kb-NB142-05**	C=NNHPh	H	OH	H	21.70 ± 0.52 (n = 3)	1.13 (n = 1)
11	**kb-NB142-11**	C=NNHTs	H	OH	H	38.21 ± 1.17 (n = 3)	n.d.
12	**kb-NB142-10**	C=NOBn	H	OH	H	not inhibitory	n.d.

Table 4. Chemical structure and PKD1 inhibitory activity of the β-carboline analogs.
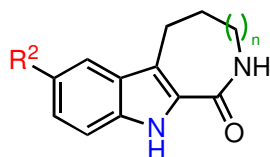
| Entry | Compound | Structure | | IC$_{50}$ | | |
		R^2	n	IMAP-FP PKD1 (μM)	radiometric PKD1 (μM)	cellular PKD1 (μM)
1	**kb-NB123-59**	OH	0	19.4 ± 1.4 (*n* = 3)	1.57 ± 0.20 (*n* = 2)	n.d.
2	**kb-NB123-57**	OH	1	2.14 ± 0.12 (*n* = 3)	0.13 ± 0.01 (*n* = 3)	>50 (*n* = 3)
3	**kb-NB123-52**	OBn	0	not inhibitory	n.d.	n.d.
4	**kb-NB123-53**	OBn	1	not inhibitory	n.d.	n.d.
5	**kb-NB142-08**	NH$_2$	0	74.4 ± 2.2 (*n* = 3)	15.74 ± 0.19 (n=2)	n.d.
6	**kb-NB142-01**	NH$_2$	1	47.1 ± 2.5 (*n* = 3)	9.68 ± 1.01 (n=2)	n.d.
7	**kb-NB123-93**	NHAc	0	not inhibitory	n.d.	n.d.
8	**kb-NB123-94**	NHAc	1	not inhibitory	n.d.	n.d.

Table 5. Chemical structures and PKD1 inhibitory activities of benzothienothiazepinone analogs.
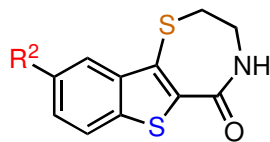
Entry	Compound	Structure R^2	IMAP-FP PKD1 (μM)	radiometric PKD1 (μM)	cellular PKD1 (μM)
				IC$_{50}$	
1	**kb-NB123-66**	OBn	not inhibitory	n.d.	n.d.
2	**kb-NB142-70**	OH	0.71 ± 0.02 (*n* = 3)	0.028 ± 0.002 (*n* = 3)	2.22 ± 0.59 (*n* = 3)
3	**kb-NB165-09**	OMe	n.d.	0.08 ± 0.01 (*n* = 4)	3.13 ± 0.54 (*n* = 3)

Table 6. Chemical structures and PKD1 inhibitory activities of analogs with zone I modifications.
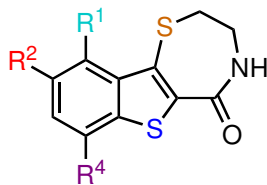
Entry	Compound	Structure			IC$_{50}$		
		R^1	R^2	R^4	% PKD1 activity at 1 μM	radiometric PKD1 (μM)	cellular PKD1 (μM)
1	**mcf292-03**	H	NH$_2$	H	74.4 ± 1.1 ($n = 2$)	3.17 ($n = 1$)	n.d.
2	**mcf292-08**	H	N$_3$	H	n.d.	0.08 ± 0.01 ($n = 5$)	2.17 ± 0.22 ($n = 3$)
3	**mcf292-05**	H	N=C=S	H	n.d.	2.77 ($n = 1$)	n.d.
4	**mcf292-09**	H	NHCOCH$_2$Cl	H	n.d.	1.50 ($n = 1$)	n.d.
5	**kb-NB165-31**	I	OH	H	13.6 ($n = 1$)	0.11 ± 0.02 ($n = 3$)	8.6 ± 2.0 ($n = 3$)
6	**kb-NB184-52**	Br	OH	H	12.7 ± 0.2 ($n = 2$)	0.048 ($n = 1$)	n.d.
7	**kb-NB184-38**	H	H	OBn	98.6 ± 4.1 ($n = 2$)	n.d.	n.d.
8	**kb-NB184-40**	H	H	OH	99 ± 11 ($n = 2$)	n.d.	n.d.
9	**kb-NB184-44**	H	H	OMe	77.5 ± 3.6 ($n = 2$)	n.d.	n.d.

Table 7. Chemical structures and PKD1 inhibitory activities of zone II and III modifications.
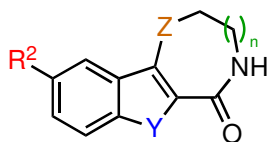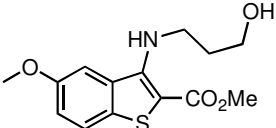
Entry	Compound	Structure				IC$_{50}$		
		Y	Z	R^2	n	% PKD1 activity at 1 μM	radiometric PKD1 (μM)	cellular PKD1 (μM)
1	**kb-NB184-22**	S=O	S	OH	1	66.5 ± 6.1 ($n = 2$)	n.d.	n.d.
2	**kb-NB184-25**	S=O	S	OMe	1	50.4 ± 2.3 ($n = 2$)	1.08 ($n = 1$)	n.d.
3	**kb-NB184-45**	S	S=O	OMe	1	97 ± 16 ($n = 2$)	n.d.	n.d.
4	**kb-NB165-89**	S	S	OBn	2	84.3 ($n = 1$)	21.7 ($n = 1$)	n.d.
5	**kb-NB165-92**	S	S	OH	2	16.7 ($n = 1$)	0.11 ± 0.01 ($n = 3$)	2.56 ± 0.66 ($n = 2$)
6	**kb-NB184-02**	S	S	OMe	2	29.5 ($n = 1$)	0.19 ± 0.03 ($n = 3$)	18.6 ± 2.0 ($n = 3$)
7	**kb-NB184-36**	S	O	OBn	2	83.3 ± 3.8 ($n = 2$)	n.d.	n.d.
8	**kb-NB184-57**	S	O	OMe	2	62.0 ± 3.5 ($n = 2$)	n.d.	n.d.
9	**kb-NB184-80**					91.3 ± 1.5 ($n = 2$)	not inhibitory	n.d.

Table 8. Chemical structures and PKD1 inhibitory activities of zone IV modifications.
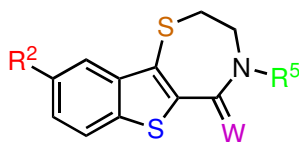
| Entry | Compound | Structure | | | IC$_{50}$ | |
		W	R^2	R^5	% PKD1 activity at 1 μM	radiometric PKD1 (μM)
1	**kb-NB165-16**	O	OMe	Me		4.57 ± 0.78 (*n* = 2)
2	**kb-NB165-17**	O	OH	Me		0.45 ± 0.05 (*n* = 2)
3	**kb-NB165-75**	O	OH	(CH$_2$)$_2$NH$_2$	55.6 (*n* = 1)	0.757 (*n* = 1)
4	**kb-NB165-81**	--	OBn	H	78.3 (*n* = 1)	39.6 (*n* = 1)
5	**kb-NB165-83**	--	OH	H	92.4 (*n* = 1)	16.4 (*n* = 1)

Table 9. Chemical structures and PKD1 inhibitory activities of analogs with zone I modifications to the pyrimidine scaffold.
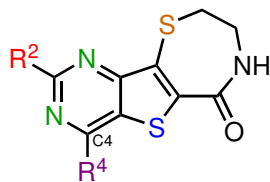
Entry	Compound	Structure		IC_{50}	
		R^2	R^4	radiometric PKD1 (μM)	cellular PKD1 (μM)
1	**kmg-NB4-23**	OMe	H	0.12 ± 0.03 ($n = 4$)	6.8 ± 1.3 ($n = 3$)
2	**kmg-NB4-69A**	OH	H	25.3 ($n = 1$)	n.d.
3	**kmg-NB5-13C**	OMe	OMe	>30.0 ($n = 2$)	n.d.
4	**kmg-NB5-15A**	OMe	OH	>30.0 ($n = 2$)	n.d.

APPENDIX B: CYTOKINE ANTIBODY ARRAY MAP

	a	b	c	d	e	f	g	h
1	Pos	Pos	Neg	Neg	GCSF	GM-CSF	GRO	GRO-alpha
2	Pos	Pos	Neg	Neg	GCSF	GM-CSF	GRO	GRO-alpha
3	IL-1 alpha	IL-2	IL-3	IL-5	IL-6	IL-7	IL-8	IL-10
4	IL-1 alpha	IL-2	IL-3	IL-5	IL-6	IL-7	IL-8	IL-10
5	IL-13	IL-15	IFN-gamma	MCP-1	MCP-2	MCP-3	MIG	RANTES
6	IL-13	IL-15	IFN-gamma	MCP-1	MCP-2	MCP-3	MIG	RANTES
7	TGF-beta1	TNF-alpha	TNF-beta	Blank	Blank	Blank	Blank	Pos
8	TGF-beta1	TNF-alpha	TNFbeta	Blank	Blank	Blank	Blank	Pos

APPENDIX C: LIST OF ABBREVIATIONS

Akt: also known as protein kinase B (PKB)
AR: androgen receptor
ATP: adenosine triphosphate
BCA: bicinchoninic acid
Bcl-2: B-cell lymphoma 2
BCR-ABL: a fusion protein of Bcr (breakpoint cluster region) and Abl
Bit1: Bcl-2 inhibitor of transcription 1
BPKDi: 2'-(cyclohexylamino)-6-(piperazin-1-yl)-[2,4'-bipyridine]-4-carboxamide
BSA: bovine serum albumin
C1 domain: phorbol ester/diacylglycerol binding domain
CaMK: calcium-calmodulin-dependent kinase
CDK: cyclin-dependent kinase
CXCL: chemokine (C-X-C motif) ligand
DAG: diacylglycerol
DMSO: dimethyl sulfoxide
dox: doxycycline
ECL: enhanced chemiluminescence
ECM: extracellular matrix
EDTA: ethylenediaminetetraacetic acid
EGFR: epithelial growth factor receptor
ELISA: enzyme-linked immunosorbent assay
EMT: epithelial-to-mesenchymal transition
ERK: extracellular signal-regulated kinase
FBS: fetal bovine serum
GM-CSF: granulocyte-macrophage colony stimulating factor
GPCR: G protein-coupled receptor
GRK: G protein-coupled receptor kinase
GRO: growth-regulated oncogene
GSK-3β: glycogen synthase kinase 3 beta
HDAC: histone deacetylase
HRP: horse radish peroxidase
Hsp: heat-shock protein
IC$_{50}$: half maximal inhibitory concentration
IL: interleukin
INF-γ: interferon gamma
JNK: c-Jun N-terminal kinase
MARK: microtubule-affinity-regulated kinase
MCP: monocyte chemotactic protein
MEF2: myocyte enhancer factor 2
MEK: mitogen-activated protein kinase kinase
MET: hepatocyte growth factor receptor
MIG: monokine induced by INF-γ
MLCK: myosin light-chain kinase
MMP: matrix metalloproteinase
MTT: 3-(4,5-Dimethylthiazol-2-yl)-2,5-diphenyltetrazolium bromide methyl thiazolyl tetrazolium
NCI: National Cancer Institute

NKκB: nuclear factor kappa-B
Par-1: protease-activated receptor-1
PC3-TR: PC3 prostate cancer cells stably expressing the tetracycline repressor
PCNA: proliferating cell nuclear antigen
PDBu: phorbol 12, 13-dibutyrate
PGF2α: Prostaglandin F2α
PH: pleckstrin homology domain
PI3K: phosphoinositide 3-kinase
PKC: protein kinase C
PKD: protein kinase D
PMA: phorbol 12-myristate 13-acetate
PMSF: phenylmethylsulfonyl fluoride
PTEN: phosphatase and tensin homolog
qd: once a day
Rac-1: Ras-related C3 botulinum toxin substrate 1
RANTES: regulated upon activation, normal T-cell expressed, and secreted
RIN1: Ras and Rab interactor 1
RTK: receptor tyrosine kinase
RT-qPCR: quantitative real-time reverse-transcription polymerase chain reaction
SAR: structure-activity relationship
SDS-PAGE: sodium dodecyl sulfate-polyacrylamide gel electrophoresis
shRNA: short hairpin RNA
SIK: salt-inducible kinase
siRNA: short interfering RNA
SphK2: sphingosine kinase 2
SSH1L: slingshot homolog 1-like
TBS-T: Tris-buffered saline with 0.01% Tween-20
tet: tetracycline
TGF: transforming growth factor
TGN: *trans* Golgi network
TNF: tumor necrosis factor
VEGF: vascular endothelial growth factor

BIBLIOGRAPHY

Aggarwal BB, Bhardwaj A, Aggarwal RS, Seeram NP, Shishodia S, Takada Y. 2004. Role of resveratrol in prevention and therapy of cancer: preclinical and clinical studies. Anticancer Res 24(5A):2783-840.

Akhtar N, Dickerson EB, Auerbach R. 2002. The sponge/Matrigel angiogenesis assay. Angiogenesis 5(1-2):75-80.

Altschmied J, Haendeler J. 2008. A new kid on the block: PKD1: a promising target for antiangiogenic therapy? Arterioscler Thromb Vasc Biol 28(10):1689-90.

Amir N, Motonishi, M., Fujita, M., Miyashita, Y., Fujisawa, K., Okamoto, K. . 2006. Synthesis of novel S-bridged heterotrinuclear complexes containing six-membered chelate rings: structural, spectroscopic, and electrochemical properties of [Co{Rh(apt)3}2]3+ (apt = 3-aminopropanethiolate). . Eur. J. Inorg. Chem. :1041-1049.

Angelucci A, Gravina GL, Rucci N, Festuccia C, Muzi P, Vicentini C, Teti A, Bologna M. 2004. Evaluation of metastatic potential in prostate carcinoma: an in vivo model. Int J Oncol 25(6):1713-20.

Araki S, Omori Y, Lyn D, Singh RK, Meinbach DM, Sandman Y, Lokeshwar VB, Lokeshwar BL. 2007. Interleukin-8 is a molecular determinant of androgen independence and progression in prostate cancer. Cancer Res 67(14):6854-62.

Bankaitis VA. 2002. Cell biology. Slick recruitment to the Golgi. Science 295(5553):290-1.

Bashir T, Pagano M. 2005. Cdk1: the dominant sibling of Cdk2. Nat Cell Biol 7(8):779-81.

Behrens MM, Strasser U, Choi DW. 1999. Go 6976 is a potent inhibitor of neurotrophin-receptor intrinsic tyrosine kinase. J Neurochem 72(3):919-24.

Bertos NR, Wang AH, Yang XJ. 2001. Class II histone deacetylases: structure, function, and regulation. Biochem Cell Biol 79(3):243-52.

Biliran H, Jan Y, Chen R, Pasquale EB, Ruoslahti E. 2008. Protein kinase D is a positive regulator of Bit1 apoptotic function. J Biol Chem 283(42):28029-37.

Biswas MH, Du C, Zhang C, Straubhaar J, Languino LR, Balaji KC. 2010. Protein kinase D1 inhibits cell proliferation through matrix metalloproteinase-2 and matrix metalloproteinase-9 secretion in prostate cancer. Cancer Res 70(5):2095-104.

Bossard C, Bresson D, Polishchuk RS, Malhotra V. 2007. Dimeric PKD regulates membrane fission to form transport carriers at the TGN. J Cell Biol 179(6):1123-31.

Bowden ET, Barth M, Thomas D, Glazer RI, Mueller SC. 1999. An invasion-related complex of cortactin, paxillin and PKCmu associates with invadopodia at sites of extracellular matrix degradation. Oncogene 18(31):4440-9.

Bravo-Altamirano K, George KM, Frantz MC, LaValle CR, Tandon M, Leimgruber S, Sharlow ER, Lazo JS, Wang QJ, Wipf P. 2011. Synthesis and structure−activity relationships of benzothienothiazepinone inhibitors of protein kinase D. ACS Med Chem Lett 2(2):154–159.

Brockschmidt C, Hirner H, Huber N, Eismann T, Hillenbrand A, Giamas G, Radunsky B, Ammerpohl O, Bohm B, Henne-Bruns D et al. 2008. Anti-apoptotic and growth-

stimulatory functions of CK1 delta and epsilon in ductal adenocarcinoma of the pancreas are inhibited by IC261 in vitro and in vivo. Gut 57(6):799-806.

Cawthorne C, Swindell R, Stratford IJ, Dive C, Welman A. 2007. Comparison of doxycycline delivery methods for Tet-inducible gene expression in a subcutaneous xenograft model. J Biomol Tech 18(2):120-3.

Chen J, Deng F, Singh SV, Wang QJ. 2008. Protein kinase D3 (PKD3) contributes to prostate cancer cell growth and survival through a PKCepsilon/PKD3 pathway downstream of Akt and ERK 1/2. Cancer Res 68(10):3844-53.

Cheong JK, Nguyen TH, Wang H, Tan P, Voorhoeve PM, Lee SH, Virshup DM. 2011. IC261 induces cell cycle arrest and apoptosis of human cancer cells via CK1delta/varepsilon and Wnt/beta-catenin independent inhibition of mitotic spindle formation. Oncogene 30(22):2558-69.

Cheong JK, Virshup DM. 2011. Casein kinase 1: Complexity in the family. Int J Biochem Cell Biol 43(4):465-9.

Chun YJ, Kim MY, Guengerich FP. 1999. Resveratrol is a selective human cytochrome P450 1A1 inhibitor. Biochem Biophys Res Commun 262(1):20-4.

Chung LWK, Isaacs WB, Simons JW, Corey E, Vessella RL. 2007. Xenograft Models of Human Prostate Cancer. In: Nickoloff JA, editor. Prostate Cancer: Humana Press. p 3-31.

Connor DT, Cetenko WA, Mullican MD, Sorenson RJ, Unangst PC, Weikert RJ, Adolphson RL, Kennedy JA, Thueson DO, Wright CD et al. 1992. Novel benzothiophene-, benzofuran-, and naphthalenecarboxamidotetrazoles as potential antiallergy agents. J Med Chem 35(5):958-65.

Connor DT, Sorenson, R. J., Mullican, M. D.; Thueson, D. O. . 1989. Preparation and testing of tetrazolyl-substituted benzothiophene-2-carboxamides and benzofurancarboxamides as antiallergic agents. (Warner-Lambert Co., USA). Eur. Pat. Appl. 20 pp. EP 299457 A2 19890118. Application: EP 88-111224 19880713.

Cook ED, Nelson AC. 2010. Prostate cancer screening. Curr Oncol Rep 13(1):57-62.

Cook PF, Cleland WW. 2007. Enzyme kinetics and mechanism. New York: Garland Science. 416 p.

Corey E, Quinn JE, Buhler KR, Nelson PS, Macoska JA, True LD, Vessella RL. 2003. LuCaP 35: a new model of prostate cancer progression to androgen independence. Prostate 55(4):239-46.

Coussens LM, Werb Z. 2002. Inflammation and cancer. Nature 420(6917):860-7.

Cuenda A, Nebreda AR. 2009. p38delta and PKD1: kinase switches for insulin secretion. Cell 136(2):209-10.

Dahmani A, de Plater L, Guyader C, Fontaine JJ, Berniard A, Assayag F, Beuzeboc P, Marangoni E, Nemati F, Poupon MF et al. 2010. A preclinical therapeutic schedule optimizing docetaxel plus estramustine administration in prostate cancer. Anticancer Drugs 21(10):927-31.

De Kimpe L, Janssens K, Derua R, Armacki M, Goicoechea S, Otey C, Waelkens E, Vandoninck S, Vandenheede JR, Seufferlein T et al. 2009. Characterization of cortactin as an in vivo protein kinase D substrate: interdependence of sites and potentiation by Src. Cell Signal 21(2):253-63.

De Santa F, Albini S, Mezzaroma E, Baron L, Felsani A, Caruso M. 2007. pRb-dependent cyclin D3 protein stabilization is required for myogenic differentiation. Mol Cell Biol 27(20):7248-65.

Ding G, Sonoda H, Yu H, Kajimoto T, Goparaju SK, Jahangeer S, Okada T, Nakamura S. 2007. Protein kinase D-mediated phosphorylation and nuclear export of sphingosine kinase 2. J Biol Chem 282(37):27493-502.

Doppler H, Storz P, Li J, Comb MJ, Toker A. 2005. A phosphorylation state-specific antibody recognizes Hsp27, a novel substrate of protein kinase D. J Biol Chem 280(15):15013-9.

Du C, Jaggi M, Zhang C, Balaji KC. 2009. Protein kinase D1-mediated phosphorylation and subcellular localization of beta-catenin. Cancer Res 69(3):1117-24.

Eiseler T, Doppler H, Yan IK, Goodison S, Storz P. 2009a. Protein kinase D1 regulates matrix metalloproteinase expression and inhibits breast cancer cell invasion. Breast Cancer Res 11(1):R13.

Eiseler T, Doppler H, Yan IK, Kitatani K, Mizuno K, Storz P. 2009b. Protein kinase D1 regulates cofilin-mediated F-actin reorganization and cell motility through slingshot. Nat Cell Biol 11(5):545-56.

Endo K, Oki E, Biedermann V, Kojima H, Yoshida K, Johannes FJ, Kufe D, Datta R. 2000. Proteolytic cleavage and activation of protein kinase C [micro] by caspase-3 in the apoptotic response of cells to 1-beta -D-arabinofuranosylcytosine and other genotoxic agents. J Biol Chem 275(24):18476-81.

Fielitz J, Kim MS, Shelton JM, Qi X, Hill JA, Richardson JA, Bassel-Duby R, Olson EN. 2008. Requirement of protein kinase D1 for pathological cardiac remodeling. Proc Natl Acad Sci U S A 105(8):3059-63.

Gellhorn A, Hirschberg E. 1955. Investigation of diverse systems for cancer chemotherapy screening. I. Summary of results and general correlations. Cancer Res Suppl. 3:1-13.

George KM, Frantz MC, Bravo-Altamirano K, LaValle CR, Tandon M, Leimgruber S, Sharlow ER, Lazo JS, Wang QJ, Wipf P. 2011. Design, synthesis, and biological evaluation of PKD inhibitors. Pharmaceutics 3(2):186-228.

Ghanekar Y, Lowe M. 2005. Protein kinase D: activation for Golgi carrier formation. Trends Cell Biol 15(10):511-4.

Goldin A, Venditti JM, Kline I, Mantel N. 1961a. Evaluation of antileukemic agents employing advanced leukemia L1210 in mice. IV. Cancer Res 21(3)Pt 2:27-92.

Goldin A, Venditti JM, Kline I, Mantel N. 1961b. Evaluation of chemical agents against carcinoma CA-755 in mice. Cancer Res 21:617-91.

Goldin A, Venditti JM, Mantel N. 1961c. Preclinical screening and evaluation of agents for the chemotherapy of cancer: a review. Cancer Res 21:1334-51.

Grandage VL, Everington T, Linch DC, Khwaja A. 2006. Go6976 is a potent inhibitor of the JAK 2 and FLT3 tyrosine kinases with significant activity in primary acute myeloid leukaemia cells. Br J Haematol 135(3):303-16.

Graziani Y, Erikson E, Erikson RL. 1983. The effect of quercetin on the phosphorylation activity of the Rous sarcoma virus transforming gene product in vitro and in vivo. Eur J Biochem 135(3):583-9.

Grimm JB, Stables JP, Brown ML. 2003. Design, synthesis, and development of novel caprolactam anticonvulsants. Bioorg Med Chem 11(18):4133-41.

Gschwendt M, Dieterich S, Rennecke J, Kittstein W, Mueller HJ, Johannes FJ. 1996. Inhibition of protein kinase C mu by various inhibitors. Differentiation from protein kinase C isoenzymes. FEBS Lett 392(2):77-80.

Gschwendt M, Kittstein W, Johannes FJ. 1998. Differential effects of suramin on protein kinase C isoenzymes. A novel tool for discriminating protein kinase C activities. FEBS Lett 421(2):165-8.

Guha S, Rey O, Rozengurt E. 2002. Neurotensin induces protein kinase C-dependent protein kinase D activation and DNA synthesis in human pancreatic carcinoma cell line PANC-1. Cancer Res 62(6):1632-40.

Ha CH, Jhun BS, Kao HY, Jin ZG. 2008a. VEGF stimulates HDAC7 phosphorylation and cytoplasmic accumulation modulating matrix metalloproteinase expression and angiogenesis. Arterioscler Thromb Vasc Biol 28(10):1782-8.

Ha CH, Jin ZG. 2009. Protein kinase D1, a new molecular player in VEGF signaling and angiogenesis. Mol Cells 28(1):1-5.

Ha CH, Wang W, Jhun BS, Wong C, Hausser A, Pfizenmaier K, McKinsey TA, Olson EN, Jin ZG. 2008b. Protein kinase D-dependent phosphorylation and nuclear export of histone deacetylase 5 mediates vascular endothelial growth factor-induced gene expression and angiogenesis. J Biol Chem 283(21):14590-9.

Haghnegahdar H, Du J, Wang D, Strieter RM, Burdick MD, Nanney LB, Cardwell N, Luan J, Shattuck-Brandt R, Richmond A. 2000. The tumorigenic and angiogenic effects of MGSA/GRO proteins in melanoma. J Leukoc Biol 67(1):53-62.

Hanahan D, Weinberg RA. 2000. The hallmarks of cancer. Cell 100(1):57-70.

Hao Q, Wang L, Tang H. 2009. Vascular endothelial growth factor induces protein kinase D-dependent production of proinflammatory cytokines in endothelial cells. Am J Physiol Cell Physiol 296(4):C821-7.

Harikumar KB, Kunnumakkara AB, Ochi N, Tong Z, Deorukhkar A, Sung B, Kelland L, Jamieson S, Sutherland R, Raynham T et al. 2010. A novel small-molecule inhibitor of protein kinase D blocks pancreatic cancer growth in vitro and in vivo. Mol Cancer Ther 9(5):1136-46.

Harper ME, Goddard L, Smith C, Nicholson RI. 2004. Characterization of a transplantable hormone-responsive human prostatic cancer xenograft TEN12 and its androgen-resistant sublines. Prostate 58(1):13-22.

Hasegawa M, Miyajima A, Kosaka T, Yasumizu Y, Tanaka N, Maeda T, Shirotake S, Ide H, Kikuchi E, Oya M. 2011. Low-dose docetaxel enhances the sensitivity of S-1 in a xenograft model of human castration resistant prostate cancer. Int J Cancer.

Hassan S, Biswas MH, Zhang C, Du C, Balaji KC. 2009. Heat shock protein 27 mediates repression of androgen receptor function by protein kinase D1 in prostate cancer cells. Oncogene 28(49):4386-96.

Hausser A, Storz P, Martens S, Link G, Toker A, Pfizenmaier K. 2005. Protein kinase D regulates vesicular transport by phosphorylating and activating phosphatidylinositol-4 kinase IIIbeta at the Golgi complex. Nat Cell Biol 7(9):880-6.

Haworth RS, Avkiran M. 2001. Inhibition of protein kinase D by resveratrol. Biochem Pharmacol 62(12):1647-51.

Hayashi A, Seki N, Hattori A, Kozuma S, Saito T. 1999. PKCnu, a new member of the protein kinase C family, composes a fourth subfamily with PKCmu. Biochim Biophys Acta 1450(1):99-106.

Hu B, Mitra J, van den Heuvel S, Enders GH. 2001. S and G2 phase roles for Cdk2 revealed by inducible expression of a dominant-negative mutant in human cells. Mol Cell Biol 21(8):2755-66.

Hwang JJ, Kim YS, Kim MJ, Kim DE, Jeong IG, Kim CS. 2010. Histone deacetylase inhibitor potentiates anticancer effect of docetaxel via modulation of Bcl-2 family proteins and tubulin in hormone refractory prostate cancer cells. J Urol 184(6):2557-64.

Iglesias T, Rozengurt E. 1998. Protein kinase D activation by mutations within its pleckstrin homology domain. J Biol Chem 273(1):410-6.

Jacamo R, Sinnett-Smith J, Rey O, Waldron RT, Rozengurt E. 2008. Sequential protein kinase C (PKC)-dependent and PKC-independent protein kinase D catalytic activation via Gq-coupled receptors: differential regulation of activation loop Ser(744) and Ser(748) phosphorylation. J Biol Chem 283(19):12877-87.

Jacobson PB, Kuchera SL, Metz A, Schachtele C, Imre K, Schrier DJ. 1995. Anti-inflammatory properties of Go 6850: a selective inhibitor of protein kinase C. J Pharmacol Exp Ther 275(2):995-1002.

Jadvar H. 2011. Prostate cancer. Methods Mol Biol 727:265-90.

Jaggi M, Chauhan SC, Du C, Balaji KC. 2008. Bryostatin 1 modulates beta-catenin subcellular localization and transcription activity through protein kinase D1 activation. Mol Cancer Ther 7(9):2703-12.

Jaggi M, Rao PS, Smith DJ, Hemstreet GP, Balaji KC. 2003. Protein kinase C mu is down-regulated in androgen-independent prostate cancer. Biochem Biophys Res Commun 307(2):254-60.

Jaggi M, Rao PS, Smith DJ, Wheelock MJ, Johnson KR, Hemstreet GP, Balaji KC. 2005. E-cadherin phosphorylation by protein kinase D1/protein kinase C{mu} is associated with altered cellular aggregation and motility in prostate cancer. Cancer Res 65(2):483-92.

Jamora C, Yamanouye N, Van Lint J, Laudenslager J, Vandenheede JR, Faulkner DJ, Malhotra V. 1999. Gbetagamma-mediated regulation of Golgi organization is through the direct activation of protein kinase D. Cell 98(1):59-68.

Jemal A, Siegel R, Ward E, Hao Y, Xu J, Thun MJ. 2009. Cancer statistics, 2009. CA Cancer J Clin 59(4):225-49.

Johannes FJ, Prestle J, Eis S, Oberhagemann P, Pfizenmaier K. 1994. PKCu is a novel, atypical member of the protein kinase C family. J Biol Chem 269(8):6140-8.

Kerbel RS. 2003. Human tumor xenografts as predictive preclinical models for anticancer drug activity in humans: better than commonly perceived-but they can be improved. Cancer Biol Ther 2(4 Suppl 1):S134-9.

Khatana SS, Boschelli, D. H., Kramer, J. B., Connor, D. T., Barth, H.; Stoss, P. . 1996. Preparation of benzothieno[2,3-f]-1,4-oxazepin- and -thiazepin-5(2H)-ones and of benzothieno[3,2-e]-1,4-diazepin-5-ones. . J. Org. Chem. 61:6060-6062.

Kim M, Jang HR, Kim JH, Noh SM, Song KS, Cho JS, Jeong HY, Norman JC, Caswell PT, Kang GH et al. 2008. Epigenetic inactivation of protein kinase D1 in gastric cancer and its role in gastric cancer cell migration and invasion. Carcinogenesis 29(3):629-37.

Kim SH, Bae HC, Park EJ, Lee CR, Kim BJ, Lee S, Park HH, Kim SJ, So I, Kim TW et al. 2011. Geraniol inhibits prostate cancer growth by targeting cell cycle and apoptosis pathways. Biochem Biophys Res Commun 407(1):129-34.

Kitanaka J, Ishibashi T, Baba A. 1993. Phloretin as an antagonist of prostaglandin F2 alpha receptor in cultured rat astrocytes. J Neurochem 60(2):704-8.

Kleiner DE, Stetler-Stevenson WG. 1994. Quantitative zymography: detection of picogram quantities of gelatinases. Anal Biochem 218(2):325-9.

Knippschild U, Gocht A, Wolff S, Huber N, Lohler J, Stoter M. 2005. The casein kinase 1 family: participation in multiple cellular processes in eukaryotes. Cell Signal 17(6):675-89.

Kovalevska LM, Yurchenko OV, Shlapatska LM, Berdova GG, Mikhalap SV, Van Lint J, Sidorenko SP. 2006. Immunohistochemical studies of protein kinase D (PKD) 2 expression in malignant human lymphomas. Exp Oncol 28(3):225-30.

Kumano M, Miyake H, Kurahashi T, Yamanaka K, Fujisawa M. 2008. Enhanced progression of human prostate cancer PC3 cells induced by the microenvironment of the seminal vesicle. Br J Cancer 98(2):356-62.

LaValle CR, Bravo-Altamirano K, Giridhar KV, Chen J, Sharlow E, Lazo JS, Wipf P, Wang QJ. 2010a. Novel protein kinase D inhibitors cause potent arrest in prostate cancer cell growth and motility. BMC Chem Biol 10:5.

LaValle CR, George KM, Sharlow ER, Lazo JS, Wipf P, Wang QJ. 2010b. Protein kinase D as a potential new target for cancer therapy. Biochim Biophys Acta 1806(2):183-92.

Lee EC, Tenniswood MP. 2004. Emergence of metastatic hormone-refractory disease in prostate cancer after anti-androgen therapy. J Cell Biochem 91(4):662-70.

Lee JW, Kwak HJ, Lee JJ, Kim YN, Lee JW, Park MJ, Jung SE, Hong SI, Lee JH, Lee JS. 2008. HSP27 regulates cell adhesion and invasion via modulation of focal adhesion kinase and MMP-2 expression. Eur J Cell Biol 87(6):377-87.

Legrier ME, de Pinieux G, Boye K, Arvelo F, Judde JG, Fontaine JJ, Bara J, Poupon MF. 2004. Mucinous differentiation features associated with hormonal escape in a human prostate cancer xenograft. Br J Cancer 90(3):720-7.

Mouse Genome Database (MGD) at the Mouse Genome Informatics website. Lexicon Phenotypic Analysis, project NIH-1194. http://www.informatics.jax.org/external/ko/lexicon/1574.html. July 8, 2011.

Liljedahl M, Maeda Y, Colanzi A, Ayala I, Van Lint J, Malhotra V. 2001. Protein kinase D regulates the fission of cell surface destined transport carriers from the trans-Golgi network. Cell 104(3):409-20.

Lokeshwar BL. 1999. MMP inhibition in prostate cancer. Ann N Y Acad Sci 878:271-89.

Lyubchanskaya VM, Alekseeva, L. M., Savina, S. A., Shashkov, A. S., and Granik, V. G. 2002. a -Oxolactam enamines as new synthons in the Nenitzescu reaction. Russ. Chem. Bull., Int. Ed. 51:1886-1893.

MacManus CF, Pettigrew J, Seaton A, Wilson C, Maxwell PJ, Berlingeri S, Purcell C, McGurk M, Johnston PG, Waugh DJ. 2007. Interleukin-8 signaling promotes translational regulation of cyclin D in androgen-independent prostate cancer cells. Mol Cancer Res 5(7):737-48.

Mak P, Jaggi M, Syed V, Chauhan SC, Hassan S, Biswas H, Balaji KC. 2008. Protein kinase D1 (PKD1) influences androgen receptor (AR) function in prostate cancer cells. Biochem Biophys Res Commun 373(4):618-23.

Malhotra V, Campelo F. 2011. PKD regulates membrane fission to generate TGN to cell surface transport carriers. Cold Spring Harb Perspect Biol 3(2).

Margheri F, D'Alessio S, Serrati S, Pucci M, Annunziato F, Cosmi L, Liotta F, Angeli R, Angelucci A, Gravina GL et al. 2005. Effects of blocking urokinase receptor signaling by antisense oligonucleotides in a mouse model of experimental prostate cancer bone metastases. Gene Ther 12(8):702-14.

Marklund U, Lightfoot K, Cantrell D. 2003. Intracellular location and cell context-dependent function of protein kinase D. Immunity 19(4):491-501.

Martin M, Kettmann R, Dequiedt F. 2007. Class IIa histone deacetylases: regulating the regulators. Oncogene 26(37):5450-67.

Martiny-Baron G, Kazanietz MG, Mischak H, Blumberg PM, Kochs G, Hug H, Marme D, Schachtele C. 1993. Selective inhibition of protein kinase C isozymes by the indolocarbazole Go 6976. J Biol Chem 268(13):9194-7.

Matthews SA, Liu P, Spitaler M, Olson EN, McKinsey TA, Cantrell DA, Scharenberg AM. 2006. Essential role for protein kinase D family kinases in the regulation of class II histone deacetylases in B lymphocytes. Mol Cell Biol 26(4):1569-77.

Matthews SA, Navarro MN, Sinclair LV, Emslie E, Feijoo-Carnero C, Cantrell DA. 2010. Unique functions for protein kinase D1 and protein kinase D2 in mammalian cells. Biochem J 432(1):153-63.

Matthews SA, Pettit GR, Rozengurt E. 1997. Bryostatin 1 induces biphasic activation of protein kinase D in intact cells. J Biol Chem 272(32):20245-50.

Matthews SA, Rozengurt E, Cantrell D. 1999. Characterization of serine 916 as an in vivo autophosphorylation site for protein kinase D/Protein kinase Cmu. J Biol Chem 274(37):26543-9.

McKinsey TA. 2007. Derepression of pathological cardiac genes by members of the CaM kinase superfamily. Cardiovasc Res 73(4):667-77.

Medeiros RB, Dickey DM, Chung H, Quale AC, Nagarajan LR, Billadeau DD, Shimizu Y. 2005. Protein kinase D1 and the beta 1 integrin cytoplasmic domain control beta 1 integrin function via regulation of Rap1 activation. Immunity 23(2):213-26.

Mishra P, Banerjee D, Ben-Baruch A. 2011. Chemokines at the crossroads of tumor-fibroblast interactions that promote malignancy. J Leukoc Biol 89(1):31-9.

Monovich L, Vega RB, Meredith E, Miranda K, Rao C, Capparelli M, Lemon DD, Phan D, Koch KA, Chapo JA et al. 2009. A novel kinase inhibitor establishes a predominant role for protein kinase D as a cardiac class IIa histone deacetylase kinase. FEBS Lett.

Morotti A, Mila S, Accornero P, Tagliabue E, Ponzetto C. 2002. K252a inhibits the oncogenic properties of Met, the HGF receptor. Oncogene 21(32):4885-93.

Murphy C, McGurk M, Pettigrew J, Santinelli A, Mazzucchelli R, Johnston PG, Montironi R, Waugh DJ. 2005. Nonapical and cytoplasmic expression of interleukin-8, CXCR1, and CXCR2 correlates with cell proliferation and microvessel density in prostate cancer. Clin Cancer Res 11(11):4117-27.

Naderi S, Gutzkow KB, Lahne HU, Lefdal S, Ryves WJ, Harwood AJ, Blomhoff HK. 2004. cAMP-induced degradation of cyclin D3 through association with GSK-3beta. J Cell Sci 117(Pt 17):3769-83.

Nelson EC, Evans CP, Mack PC, Devere-White RW, Lara PN, Jr. 2007. Inhibition of Akt pathways in the treatment of prostate cancer. Prostate Cancer Prostatic Dis 10(4):331-9.

Nishita M, Tomizawa C, Yamamoto M, Horita Y, Ohashi K, Mizuno K. 2005. Spatial and temporal regulation of cofilin activity by LIM kinase and Slingshot is critical for directional cell migration. J Cell Biol 171(2):349-59.

Ochi N, Tanasanvimon S, Matsuo Y, Tong Z, Sung B, Aggarwal BB, Sinnett-Smith J, Rozengurt E, Guha S. 2011. Protein kinase D1 promotes anchorage-independent growth, invasion, and angiogenesis by human pancreatic cancer cells. J Cell Physiol 226(4):1074-81.

Oettel H, Wilhelm G. 1955. Tests of compounds against Ehrlich ascites tumor, sarcoma 180 and Walker carcino-sarcoma 256. Cancer Res Suppl. 2:129-44.

Ogata H, Sekikawa A, Yamagishi H, Ichikawa K, Tomita S, Imura J, Ito Y, Fujita M, Tsubaki M, Kato H et al. 2010. GROalpha promotes invasion of colorectal cancer cells. Oncol Rep 24(6):1479-86.

Park SI, Kim SJ, McCauley LK, Gallick GE. 2010. Pre-clinical mouse models of human prostate cancer and their utility in drug discovery. Curr Protoc Pharmacol 51:14 15-14 15 27.

Peterman EE, Taormina P, 2nd, Harvey M, Young LH. 2004. Go 6983 exerts cardioprotective effects in myocardial ischemia/reperfusion. J Cardiovasc Pharmacol 43(5):645-56.

Picq M, Dubois M, Munari-Silem Y, Prigent AF, Pacheco H. 1989. Flavonoid modulation of protein kinase C activation. Life Sci 44(21):1563-71.

Pilankatta R, Lewis D, Inesi G. 2011. Involvement of protein kinase D in expression and trafficking of ATP7B (copper ATPase). J Biol Chem 286(9):7389-96.

Prevarskaya N, Skryma R, Vacher P, Bresson-Bepoldin L, Odessa MF, Rivel J, San Galli F, Guerin J, Dufy-Barbe L. 1994. Gonadotropin-releasing hormone induced Ca2+ influx in nonsecreting pituitary adenoma cells: role of voltage-dependent Ca2+ channels and protein kinase C. Mol Cell Neurosci 5(6):699-708.

Price MA. 2006. CKI, there's more than one: casein kinase I family members in Wnt and Hedgehog signaling. Genes Dev 20(4):399-410.

Prigozhina NL, Waterman-Storer CM. 2004. Protein kinase D-mediated anterograde membrane trafficking is required for fibroblast motility. Curr Biol 14(2):88-98.

Qin L, Zeng H, Zhao D. 2006. Requirement of protein kinase D tyrosine phosphorylation for VEGF-A165-induced angiogenesis through its interaction and regulation of phospholipase Cgamma phosphorylation. J Biol Chem 281(43):32550-8.

Raynham TM, Hammonds TR, Charles MD, Pave GA, Foxton CH, Blackaby WP, Stevens AP, Ekwuru CT; 2008. Pyridine Benzamides and Pyrazine Benzamides Used as PKD Inhibitors

Raynham TM, Hammonds TR, Gillatt JH, Charles MD, Pave GA, Foxton CH, Carr JL, Mistry NS; 2007. Amino-Ethyl-Amino-Aryl (AEAA) Compounds and Their Use.

Reiland J, Furcht LT, McCarthy JB. 1999. CXC-chemokines stimulate invasion and chemotaxis in prostate carcinoma cells through the CXCR2 receptor. Prostate 41(2):78-88.

Rennecke J, Johannes FJ, Richter KH, Kittstein W, Marks F, Gschwendt M. 1996. Immunological demonstration of protein kinase C mu in murine tissues and various cell lines. Differential recognition of phosphorylated forms and lack of down-regulation upon 12-O-tetradecanoylphorphol-13-acetate treatment of cells. Eur J Biochem 242(2):428-32.

Rennecke J, Rehberger PA, Furstenberger G, Johannes FJ, Stohr M, Marks F, Richter KH. 1999. Protein-kinase-Cmu expression correlates with enhanced keratinocyte proliferation in normal and neoplastic mouse epidermis and in cell culture. Int J Cancer 80(1):98-103.

Rescigno M, Avogadri F, Curigliano G. 2007. Challenges and prospects of immunotherapy as cancer treatment. Biochim Biophys Acta 1776(1):108-23.

Rey O, Sinnett-Smith J, Zhukova E, Rozengurt E. 2001. Regulated nucleocytoplasmic transport of protein kinase D in response to G protein-coupled receptor activation. J Biol Chem 276(52):49228-35.

Rey O, Yuan J, Young SH, Rozengurt E. 2003. Protein kinase C nu/protein kinase D3 nuclear localization, catalytic activation, and intracellular redistribution in response to G protein-coupled receptor agonists. J Biol Chem 278(26):23773-85.

Ristich VL, Bowman PH, Dodd ME, Bollag WB. 2006. Protein kinase D distribution in normal human epidermis, basal cell carcinoma and psoriasis. Br J Dermatol 154(4):586-93.

Roy R, Yang J, Moses MA. 2009. Matrix metalloproteinases as novel biomarkers and potential therapeutic targets in human cancer. J Clin Oncol 27(31):5287-97.

Rozengurt E, Rey O, Waldron RT. 2005. Protein kinase D signaling. J Biol Chem 280(14):13205-8.

Rozengurt E, Sinnett-Smith J, Zugaza JL. 1997. Protein kinase D: a novel target for diacylglycerol and phorbol esters. Biochem Soc Trans 25(2):565-71.

Ruegg UT, Burgess GM. 1989. Staurosporine, K-252 and UCN-01: potent but nonspecific inhibitors of protein kinases. Trends Pharmacol Sci 10(6):218-20.

Ruggeri B, Singh J, Gingrich D, Angeles T, Albom M, Yang S, Chang H, Robinson C, Hunter K, Dobrzanski P et al. 2003. CEP-7055: a novel, orally active pan inhibitor of vascular endothelial growth factor receptor tyrosine kinases with potent antiangiogenic activity and antitumor efficacy in preclinical models. Cancer Res 63(18):5978-91.

Saar M, Korbel C, Jung V, Suttmann H, Grobholz R, Stockle M, Unteregger G, Menger MD, Kamradt J. 2010. Experimental orthotopic prostate tumor in nude mice: Techniques for local cell inoculation and three-dimensional ultrasound monitoring. Urol Oncol.

Sano D, Myers JN. 2009. Xenograft models of head and neck cancers. Head Neck Oncol 1:32.

Sarker D, Reid AH, Yap TA, de Bono JS. 2009. Targeting the PI3K/AKT pathway for the treatment of prostate cancer. Clin Cancer Res 15(15):4799-805.

Satyanarayana A, Kaldis P. 2009. Mammalian cell-cycle regulation: several Cdks, numerous cyclins and diverse compensatory mechanisms. Oncogene 28(33):2925-39.

Sciume G, Santoni A, Bernardini G. 2010. Chemokines and glioma: invasion and more. J Neuroimmunol 224(1-2):8-12.

Seaton A, Scullin P, Maxwell PJ, Wilson C, Pettigrew J, Gallagher R, O'Sullivan JM, Johnston PG, Waugh DJ. 2008. Interleukin-8 signaling promotes androgen-independent proliferation of prostate cancer cells via induction of androgen receptor expression and activation. Carcinogenesis 29(6):1148-56.

Shapiro BA, Ray S, Jung E, Allred WT, Bollag WB. 2002. Putative conventional protein kinase C inhibitor Godecke 6976 [12-(2-cyanoethyl)-6,7,12,13-tetrahydro-13-methyl-5-oxo-5H-indolo(2,3-a)py rrolo(3,4-c)-carbazole] stimulates transglutaminase activity in primary mouse epidermal keratinocytes. J Pharmacol Exp Ther 302(1):352-8.

Sharlow ER, Giridhar KV, LaValle CR, Chen J, Leimgruber S, Barrett R, Bravo-Altamirano K, Wipf P, Lazo JS, Wang QJ. 2008. Potent and selective disruption of protein kinase D functionality by a benzoxoloazepinolone. J Biol Chem 283(48):33516-26.

Shaw A, Gipp J, Bushman W. 2010. Exploration of Shh and BMP paracrine signaling in a prostate cancer xenograft. Differentiation 79(1):41-7.

Shirai T. 2008. Significance of chemoprevention for prostate cancer development: experimental in vivo approaches to chemoprevention. Pathol Int 58(1):1-16.

Singh R, Li H, Zhao H, Payan DG, Kolluri R, Tso K, Ramphal J, Gu S; 2009. Cyclic Amine Substituted Pyrimidinediamines as PKC Inhibitors.

Sinnett-Smith J, Jacamo R, Kui R, Wang YM, Young SH, Rey O, Waldron RT, Rozengurt E. 2009. Protein kinase D mediates mitogenic signaling by Gq-coupled receptors through protein kinase C-independent regulation of activation loop Ser744 and Ser748 phosphorylation. J Biol Chem 284(20):13434-45.

Sinnett-Smith J, Zhukova E, Hsieh N, Jiang X, Rozengurt E. 2004. Protein kinase D potentiates DNA synthesis induced by Gq-coupled receptors by increasing the duration of ERK signaling in swiss 3T3 cells. J Biol Chem 279(16):16883-93.

Sinnett-Smith J, Zhukova E, Rey O, Rozengurt E. 2007. Protein kinase D2 potentiates MEK/ERK/RSK signaling, c-Fos accumulation and DNA synthesis induced by bombesin in Swiss 3T3 cells. J Cell Physiol 211(3):781-90.

Steiner TS, Ivison SM, Yao Y, Kifayet A. 2010. Protein kinase D1 and D2 are involved in chemokine release induced by toll-like receptors 2, 4, and 5. Cell Immunol 264(2):135-42.

Stewart JR, Christman KL, O'Brian CA. 2000. Effects of resveratrol on the autophosphorylation of phorbol ester-responsive protein kinases: inhibition of protein kinase D but not protein kinase C isozyme autophosphorylation. Biochem Pharmacol 60(9):1355-9.

Stock CC, Clarke DA, Philips FS, Barclay RK. 1960. Cancer chemotherapy screening data. V. Sarcoma 180 screening data. Cancer Res 20(3)Pt 2:1-192.

Stolz A, Vogel C, Schneider V, Ertych N, Kienitz A, Yu H, Bastians H. 2009. Pharmacologic abrogation of the mitotic spindle checkpoint by an indolocarbazole discovered by cellular screening efficiently kills cancer cells. Cancer Res 69(9):3874-83.

Storz P. 2007. Mitochondrial ROS--radical detoxification, mediated by protein kinase D. Trends Cell Biol 17(1):13-8.

Storz P, Doppler H, Johannes FJ, Toker A. 2003. Tyrosine phosphorylation of protein kinase D in the pleckstrin homology domain leads to activation. J Biol Chem 278(20):17969-76.

Storz P, Doppler H, Toker A. 2004. Protein kinase Cdelta selectively regulates protein kinase D-dependent activation of NF-kappaB in oxidative stress signaling. Mol Cell Biol 24(7):2614-26.

Storz P, Doppler H, Toker A. 2005. Protein kinase D mediates mitochondrion-to-nucleus signaling and detoxification from mitochondrial reactive oxygen species. Mol Cell Biol 25(19):8520-30.

Sturany S, Van Lint J, Muller F, Wilda M, Hameister H, Hocker M, Brey A, Gern U, Vandenheede J, Gress T et al. 2001. Molecular cloning and characterization of the human protein kinase D2. A novel member of the protein kinase D family of serine threonine kinases. J Biol Chem 276(5):3310-8.

Stylli SS, Kaye AH, Lock P. 2008. Invadopodia: at the cutting edge of tumour invasion. J Clin Neurosci 15(7):725-37.

Suggitt M, Bibby MC. 2005. 50 years of preclinical anticancer drug screening: empirical to target-driven approaches. Clin Cancer Res 11(3):971-81.

Sumara G, Formentini I, Collins S, Sumara I, Windak R, Bodenmiller B, Ramracheya R, Caille D, Jiang H, Platt KA et al. 2009. Regulation of PKD by the MAPK p38delta in insulin secretion and glucose homeostasis. Cell 136(2):235-48.

Syed V, Mak P, Du C, Balaji KC. 2008. Beta-catenin mediates alteration in cell proliferation, motility and invasion of prostate cancer cells by differential expression of E-cadherin and protein kinase D1. J Cell Biochem 104(1):82-95.

Takahashi-Yanaga F, Sasaguri T. 2008. GSK-3beta regulates cyclin D1 expression: a new target for chemotherapy. Cell Signal 20(4):581-9.

Tamaoki T, Nomoto H, Takahashi I, Kato Y, Morimoto M, Tomita F. 1986. Staurosporine, a potent inhibitor of phospholipid/Ca++dependent protein kinase. Biochem Biophys Res Commun 135(2):397-402.

Thudi NK, Martin CK, Murahari S, Shu ST, Lanigan LG, Werbeck JL, Keller ET, McCauley LK, Pinzone JJ, Rosol TJ. 2011. Dickkopf-1 (DKK-1) stimulated prostate cancer growth and metastasis and inhibited bone formation in osteoblastic bone metastases. Prostate 71(6):615-25.

Torres-Marquez E, Sinnett-Smith J, Guha S, Kui R, Waldron RT, Rey O, Rozengurt E. 2010. CID755673 enhances mitogenic signaling by phorbol esters, bombesin and EGF through a protein kinase D-independent pathway. Biochem Biophys Res Commun 391(1):63-8.

Toullec D, Pianetti P, Coste H, Bellevergue P, Grand-Perret T, Ajakane M, Baudet V, Boissin P, Boursier E, Loriolle F et al. 1991. The bisindolylmaleimide GF 109203X is a potent and selective inhibitor of protein kinase C. J Biol Chem 266(24):15771-81.

Trauzold A, Schmiedel S, Sipos B, Wermann H, Westphal S, Roder C, Klapper W, Arlt A, Lehnert L, Ungefroren H et al. 2003. PKCmu prevents CD95-mediated apoptosis and enhances proliferation in pancreatic tumour cells. Oncogene 22(55):8939-47.

Troeberg L, Nagase H. 2004. Zymography of metalloproteinases. Curr Protoc Protein Sci Chapter 21:Unit 21 15.

Valverde AM, Sinnett-Smith J, Van Lint J, Rozengurt E. 1994. Molecular cloning and characterization of protein kinase D: a target for diacylglycerol and phorbol esters with a distinctive catalytic domain. Proc Natl Acad Sci U S A 91(18):8572-6.

Van Lint J, Rykx A, Maeda Y, Vantus T, Sturany S, Malhotra V, Vandenheede JR, Seufferlein T. 2002. Protein kinase D: an intracellular traffic regulator on the move. Trends Cell Biol 12(4):193-200.

van Montfort RL, Workman P. 2009. Structure-based design of molecular cancer therapeutics. Trends Biotechnol 27(5):315-28.

Vantus T, Vertommen D, Saelens X, Rykx A, De Kimpe L, Vancauwenbergh S, Mikhalap S, Waelkens E, Keri G, Seufferlein T et al. 2004. Doxorubicin-induced activation of protein kinase D1 through caspase-mediated proteolytic cleavage: identification of two cleavage sites by microsequencing. Cell Signal 16(6):703-9.

Vega RB, Harrison BC, Meadows E, Roberts CR, Papst PJ, Olson EN, McKinsey TA. 2004. Protein kinases C and D mediate agonist-dependent cardiac hypertrophy through nuclear export of histone deacetylase 5. Mol Cell Biol 24(19):8374-85.

Vindrieux D, Escobar P, Lazennec G. 2009. Emerging roles of chemokines in prostate cancer. Endocr Relat Cancer 16(3):663-73.

von Blume J, Knippschild U, Dequiedt F, Giamas G, Beck A, Auer A, Van Lint J, Adler G, Seufferlein T. 2007. Phosphorylation at Ser244 by CK1 determines nuclear localization and substrate targeting of PKD2. Embo J 26(22):4619-33.

Waldron RT, Iglesias T, Rozengurt E. 1999. Phosphorylation-dependent protein kinase D activation. Electrophoresis 20(2):382-90.

Waldron RT, Rey O, Iglesias T, Tugal T, Cantrell D, Rozengurt E. 2001. Activation loop Ser744 and Ser748 in protein kinase D are transphosphorylated in vivo. J Biol Chem 276(35):32606-15.

Waldron RT, Rozengurt E. 2000. Oxidative stress induces protein kinase D activation in intact cells. Involvement of Src and dependence on protein kinase C. J Biol Chem 275(22):17114-21.

Waldron RT, Rozengurt E. 2003. Protein kinase C phosphorylates protein kinase D activation loop Ser744 and Ser748 and releases autoinhibition by the pleckstrin homology domain. J Biol Chem 278(1):154-63.

Wang QJ. 2006. PKD at the crossroads of DAG and PKC signaling. Trends Pharmacol Sci 27(6):317-23.

Wang S, Li X, Parra M, Verdin E, Bassel-Duby R, Olson EN. 2008. Control of endothelial cell proliferation and migration by VEGF signaling to histone deacetylase 7. Proc Natl Acad Sci U S A 105(22):7738-43.

Wang X, Gorospe M, Huang Y, Holbrook NJ. 1997. p27Kip1 overexpression causes apoptotic death of mammalian cells. Oncogene 15(24):2991-7.

Wang Y, Waldron RT, Dhaka A, Patel A, Riley MM, Rozengurt E, Colicelli J. 2002. The RAS effector RIN1 directly competes with RAF and is regulated by 14-3-3 proteins. Mol Cell Biol 22(3):916-26.

Watkins JL, Lewandowski KT, Meek SE, Storz P, Toker A, Piwnica-Worms H. 2008. Phosphorylation of the Par-1 polarity kinase by protein kinase D regulates 14-3-3 binding and membrane association. Proc Natl Acad Sci U S A 105(47):18378-83.

Waugh DJ, Wilson C. 2008. The interleukin-8 pathway in cancer. Clin Cancer Res 14(21):6735-41.

Wei YQ, Zhao X, Kariya Y, Fukata H, Teshigawara K, Uchida A. 1994. Induction of apoptosis by quercetin: involvement of heat shock protein. Cancer Res 54(18):4952-7.

Wen Y, Giardina SF, Hamming D, Greenman J, Zachariah E, Bacolod MD, Liu H, Shia J, Amenta PS, Barany F et al. 2006. GROalpha is highly expressed in adenocarcinoma of the colon and down-regulates fibulin-1. Clin Cancer Res 12(20 Pt 1):5951-9.

Wilczynski JR, Duechler M. 2010. How do tumors actively escape from host immunosurveillance? Arch Immunol Ther Exp (Warsz) 58(6):435-48.

Wong C, Jin ZG. 2005. Protein kinase C-dependent protein kinase D activation modulates ERK signal pathway and endothelial cell proliferation by vascular endothelial growth factor. J Biol Chem 280(39):33262-9.

Woods AJ, White DP, Caswell PT, Norman JC. 2004. PKD1/PKCmu promotes alphavbeta3 integrin recycling and delivery to nascent focal adhesions. Embo J 23(13):2531-43.

Yanagihara N, Tachikawa E, Izumi F, Yasugawa S, Yamamoto H, Miyamoto E. 1991. Staurosporine: an effective inhibitor for Ca2+/calmodulin-dependent protein kinase II. J Neurochem 56(1):294-8.

Yang F, Tuxhorn JA, Ressler SJ, McAlhany SJ, Dang TD, Rowley DR. 2005. Stromal expression of connective tissue growth factor promotes angiogenesis and prostate cancer tumorigenesis. Cancer Res 65(19):8887-95.

Yeaman C, Ayala MI, Wright JR, Bard F, Bossard C, Ang A, Maeda Y, Seufferlein T, Mellman I, Nelson WJ et al. 2004. Protein kinase D regulates basolateral membrane protein exit from trans-Golgi network. Nat Cell Biol 6(2):106-12.

Zaviacic M. 1997. Prostate-specific antigen and history of its discovery. Bratisl Lek Listy 98(12):659-62.

Zhang W, Zheng S, Storz P, Min W. 2005. Protein kinase D specifically mediates apoptosis signal-regulating kinase 1-JNK signaling induced by H2O2 but not tumor necrosis factor. J Biol Chem 280(19):19036-44.

Zhou JR, Yu L, Zerbini LF, Libermann TA, Blackburn GL. 2004. Progression to androgen-independent LNCaP human prostate tumors: cellular and molecular alterations. Int J Cancer 110(6):800-6.

Zhukova E, Sinnett-Smith J, Rozengurt E. 2001. Protein kinase D potentiates DNA synthesis and cell proliferation induced by bombesin, vasopressin, or phorbol esters in Swiss 3T3 cells. J Biol Chem 276(43):40298-305.

Zugaza JL, Sinnett-Smith J, Van Lint J, Rozengurt E. 1996. Protein kinase D (PKD) activation in intact cells through a protein kinase C-dependent signal transduction pathway. Embo J 15(22):6220-30.

Zugaza JL, Waldron RT, Sinnett-Smith J, Rozengurt E. 1997. Bombesin, vasopressin, endothelin, bradykinin, and platelet-derived growth factor rapidly activate protein kinase D through a protein kinase C-dependent signal transduction pathway. J Biol Chem 272(38):23952-60.